Wearable Energy Harvesting for Charging Portable Electronic Devices by Walking

Submitted by **David Pritchard** to the University of Exeter

As a thesis for the degree of

Doctor of Philosophy in Engineering

In January 2020

I certify that all material in this thesis which is not my own work has been identified and that no material has previously been submitted and approved for the award of a degree by this or any other University.

Signature: 

Blank Page

Abstract

Wearable energy harvesting technologies will become an everyday part of future portable electronic devices. By generating the energy where the energy is needed and not relying on a main power source to recharge the portable devices battery, wearable energy harvesters will enable future generations to have even more freedoms, travel further, and never run low on battery again. This will reduce the energy consumption of the mains grid and thus in turn reduce CO^2 emissions generated by this traditional power source making this research important for the whole plant.

This research project aims to take another step towards in helping the development of future technologies by investigating novel wearable energy harvesting designs and showing ability to charge current portable electronic devices such as smart phones and tables. This required research into a broad range of topics including, energies from humans, energy conversion mechanisms, the movement of people and the power demands for charging current portable electronic devices.

Background research in the human energy levels and how research to date had gone about exacting different energy sources in different ways was the starting point for this research. This leads on to a more detailed look into the exaction methods and optimization of footfall energy harvester designs. Looking into the human gait cycle gave the information required to replicate human footfall motion for use in scientific experiments.

From this background research, two bespoke designs of wearable energy harvester have been created. The first novel design showed a promising way of extracting footfall energy and converting it into useable

electrical energy producing Watt-Level of power. The second design is an evolution of the first design but expands the extraction method to both feet and relocated the main harvester unit into a backpack worn by the user. The improved design incorporates a novel approach to energy conversion method by introducing a mechanical energy storage system before transduction into electrical energy. This is shown to increased electrical power output from footfall energy, reduced energy consumption of the wearer and is shown to truly be able to charge current portable electronics. The improved design is shown to produce 2.6 Watts average power from normal walking.

The experimental set ups, procedures, and their results are shown throughout this thesis. These experimental results are confirmed by using the wearable energy harvesters on a treadmill at the three main walking speeds showing their real-world capabilities. To demonstrate the wearable energy harvester deigns shown in this research project were truly able to charge current portable technologies, endurance testing was also performed. This confirms the harvesters were able to work for longer periods of time. This longer time frame is needed for the charging times of the current portable devices.

After researching into wearable energy harvesting from over the last 20 years it was a struggle to compare all the different forms, designs, types and power outputs. It became clear that the existing methods were unable to provide a clear picture of harvester's scalability, changeability and useability for future design ideas. This is why a new form of comparison was created and is shown to have strong benefits over the existing methods.

Acknowledgments

First, I would like to thank my family for putting up with me throughout this process. The stress and pressures of research got to me at times and without their love and support I would never of made it this far. My mother has helped me over come fears and worries about completing this on time and my wife has been nothing but understanding for the many late nights and long weekends working away on this research project.

Without the EPSRC funding, this PhD would never have happened. My thanks go to Professor M. Zhu and the EPSRC council for making this an opportunity.

Special thanks to Professor Gavin Tabor for providing me support within the university. Always making the time for chats and meetings, and always having a positive look on things.

Lastly, I thank the energy harvesting research group at Exeter for showing me the way at times and Professor Meiling Zhu has been supportive, understanding, and an inspirational role model. Without Professor Zhu guidance experience and expertise, I have no doubt I would not have been able to complete this thesis.

Thank you to you all.

Contents

List of Figure

List of Tables

Chapter 1 Introduction

In this chapter, an introduction to this research project, the motivations behind the research, the aims and objectives, and the layout of the thesis will be explained. Wearable energy harvesting has been and still is an important area to research with researchers continuously creating new innovations to solving existing problems with portable power sources.

1.1 Motivation

Wearable energy harvesting uses the waste or spare energy sources found in, on, or around humans and their activities. It converts the energy source into useable power, usually in the form of electricity. The power outputs vary dramatically depending on the energy source and transducer type.

Current portable electronic devices use built-in batteries to power the device. These batteries are depleted by the device, but charged from an external power source. This is most commonly a main power source from a wall socket or a computer USB port. Having to charge the portable electronic device from a mains power source limits the range and endurance of the portable device. This is where wearable energy harvesting technologies can help. If the portable electronic devices battery was charged via a wearable energy harvester this would have two key benefits; one is a reduction on the use of mains power stations running on fossil fuels and the second the length of time the portable electronic device could be used, before needing to find a traditional power source for charging.

Wearable energy harvesters come in all shapes and sizes, some fitted into existing wearable items such as shoes or jackets being very small, lightweight and in some cases flexible. These harvesters tend to have low power outputs, generally below 0.5 Watt [1]–[7]. Other harvesters are externally attached or carried by the wearer, for example; these can be in the form of a harvester that straps to the leg or is carried in a backpack. These harvesters tend to be bigger, heavier, and more rigid, but are also shown to produce higher power outputs. These are called “watt-Level” harvesters [8]–[12].

Portable electronic devices range from sensors, which monitor the wearer and report back data used in the internet of things, to modern communication devices and portable computers which are deemed as small lightweight technologies. All of which help the user achieve a goal without the need to stay in a fixed location.

All wearable energy harvesters aim to do one thing, reduce the need to charge or replace batteries used in a portable electronic device. Wearable body sensors that monitor health conditions powered from wearable energy harvesters have had a strong growth in the past decade. Furthermore, the idea of not having to charge your smart phone because it is being charged in your pocket during your normal day, is something that appeals to those that use one. The military currently use big heavy batteries in order to provide their ground troops with a portable power source. Research has already shown that a wearable energy harvester could be used to reduce the capacity of such a battery by recharging a smaller, lighter battery from human movement [13].

Footfall forces seen during walking, jogging or running show an abundance of available power ready for harvesting. 67 Watts has been calculated as an available power level from an example case found in research [14], [15]. This figure seems extreme, but the theory stands. However, this theory does not take into account the effects on the wearer if harvesting at this level. From research found, no Watt-Level energy harvester, harvesting from footfall forces has been able to show the energy sources true potential, and as a result no footfall harvesters have been shown to charge portable technologies, only the suggestion that they could.

This research project aims to show research, methods, designs, and the results from novel wearable energy harvesters for charging portable electronics harvesting from footfall. The contribution will be in the form of two bespoke harvester design which have not been seen before. This is supported by rigorous testing of the designs to confirm their higher power output compared to previous footfall harvesters research. A new comparison method for comparing wearable energy harvesters is also explored. This will assist the energy harvesting research community's by making it clearer which design is more suitable for a wearable application.

1.2 Research Aims and Objectives

The overall research area is; *Energy Harvesting*

This can be narrowed down to; *Wearable Energy Harvesting Technologies*

This research project needed an end goal set to help concentrate the future aims. From early investigations into the area, setting a target of charging modern portable devices such as current smart phones and tablets seemed a demanding challenge.

This led to the following question;

Can a wearable energy harvester charge current portable devices such as smart phones and tablets?

Only 3 harvester approaches have published data that show designs to produce high enough average power to be able to say yes to this question [12], [13], [16]. These harvesters are cited countlessly in papers and presentations as examples of the future possibilities of wearable energy harvesting being one day part of our everyday lives. Since these papers have been published, other researches have continued to develop these harvesters' basic concepts and have shown to improve the harvester's efficiency or power output.

1.2.1 **Research Aim**

Looking further into this research area it was found that no footfall harvesters had proven their abilities to charge modern portable devices. This led to the final research question being set.

Can a footfall wearable energy harvester be shown to generate enough power to charge a smart phone currently available on the domestic market?

After setting this as the research project's question, a hypothesis was formulated.

If a wearable energy harvester is designed correctly, it should be able to produce a high enough average power from human footfall to charge a smart phone or tablet without affecting the users walking style and have as little effect on the wearers metabolic energy consumption as possible.

This led to the aim being to design, manufacture and test a bespoke novel wearable energy harvester. It will harvest from human footfall forces and produce enough electrical energy to charge a current portable electronic device.

1.2.2 **Research Objectives**

Now the question is clear, and the aim of the project has been set, the objectives of the project are presented in the list below.

- Research into available energy from humans for harvesting applications
- Research current wearable harvesting approaches, designs and testing methods
- Research into modern portable technologies and their charging requirements

- Design and develop a footfall wearable energy harvester for charging modern portable devices
- Investigate improving comparison methods of wearable energy harvesters, to aid design decisions of new innovations of harvester approaches or extraction methods
- Document findings and confirm the hypothesis.

Each of these objectives will be used as steps throughout this research project, and will be used as a way of ensuring the research question is answered.

1.3 Research Contribution, Justification, and Novelty

Wearable energy harvesting has been researched intensively in the past 2 decades. With an ever increasing demand towards green energy supplies, this research area could not be more relevant in today's "*on-the-go*", modern world. The domestic market for portable technologies increases year on year, with new innovations not only in hardware, but also in the interface, interaction method and even location for the device to be used. The current trend of power source for portable technologies are batteries. These batteries are routinely re-charged from fixed power source, such as a mains connection. Although battery capacity technologies are increasing at a fantastic rate, batteries have a limitation on the power capabilities. Batteries are electrical storage vessels and once the vessel is empty, it needs to be refilled. This is where energy harvesters come in. Imagine a smart phone that charged itself. Here, batteries might be replaced with a capacitor, but an electrical storage medium will still exist in some form. This vessel is continuously topped up by a wearable energy harvester, ultimately meaning never needing to charge your smart phone at home again.

This is not a new idea, and researchers have already shown the potential of this in multiple different ways. As of yet, no research into footfall wearable harvesters can be shown to charge a modern portable device from walking. The two novel designs of wearable energy harvester presented here show the ability to produce high enough average power to charge current portable electronic devices. This is a strong contribution to the energy harvesting research community by showing it connection to the real world. The improved design of wearable energy harvester shown later, introduces a new approach to the harvesting process by incorporating a mechanical storage mechanism before the transducer. This concept has not been seen before making the research novel, but also could be adapted for use in future research making a strong contribution to the research community.

Research published by N. Terry in 2016 presents research conducted by *Owon* [17]. Here they researched into energy use in domestic households and the charging of smart phones. They concluded that individual phones use less than 5 kWh/year on average. This small energy demand could by generated by wearable energy harvesting technologies. If mass adoption of wearable energy harvesters were to be implemented, a reduction on the mains power grid from not charging portable device would be seen. This will in turn reduce the emissions produced by the mains power supply which is paramount for the future of our planet.

1.4 Thesis Structure

This thesis is structured in such a way that it aims to lead the reader through the scientific processes followed throughout this research project. The start of the thesis intends to set a research question based on the

research topic and continue on to identify, explore and explain any relative research in the area of wearable energy harvesting published in the last decade, or any research published earlier that shows strong connections to this field.

Chapter 2 with a literature review into published research in the field of wearable energy harvesting, and expands into the biomechanics of humans in order to confirm energy use, expenditure rates and where waste or spare energy might be available for harvesting applications. This will determine where the harvester is harvesting from to produce high enough power level to be Watt-level energy harvester. , and the impact the harvester will have on the wearer.

Chapter 3 will look into more details surrounding footfall movements, the power levels needed for charging portable technologies and how they could be converted into electrical power. The how, where and why the wearable harvester designs needs to be constructed in a particular way, will be explained and will continue on to explain how the experimental test procedures were created and controlled. This chapter will justify why things were done the way they were and how consistency in testing was achieved.

Chapter 4 lays out how the initial harvester design works, how it was made (including materials and manufacturing processes used), how it was tested and finishes with a detailed examination of the results obtained. The chapter will end with a conclusion on the harvester's design, power outputs and feasibility for use in the real world shown by a 5.4 km walk on a treadmill for the period of 1 hour.

Chapter 5 shows the improved design of harvester and how it evolved from the initial design. The improved design will be explained and how the

negative factors found from the testing and results of the initial design have been addressed. Due to the complexity of the improved design, the results from testing will be examined in detail and evidence that achievements of the research aims have been met will be presented. The harvester will again be tested via a 5.4 km walk on a treadmill using the harvesters to charge a smart phone currently available. This will confirm and proofing the real world potential of these designs.

Chapter 6 aims to present a new way of comparing wearable energy harvesters to each other and is called “User-Impact-Factor”. Here, the existing ways of comparison will be explained and why it was felt that a new comparator method would benefit the research community. The chapter will use existing methods and the new method mentioned, to compare wearable energy harvesters to each other and provide evidence showing the advantages in the new method. This chapter will finish by showing how the two new designs of wearable energy harvester have performed against previous designs and why they would be more beneficial over other current design approaches.

Chapter 8 is a discussion and conclusion chapter and should bring the thesis and research project to a close. First a look into potential markets, and improvements to designs necessary for commercialisation to fit these markets is explained. It also explores the idea behind developing the improved harvester design for military use. The chapter continues with the research project being summarized, goals met or missed and why the research project has been a worthwhile investment in time and money. The chapter will finish showing how the thesis and research project benefits the

research community, and how others could continue this research in the topic of energy harvesting.

By the end of this thesis, the reader will have seen evidence that this research project demonstrates the understanding of scientific methods, benefits the scientific community, and that all research goals have been achieved.

To summaries:

- Understand the aims and objectives of the research project
- See a detailed background research and literature review was performed
- Understand the two new bespoke wearable energy harvester designs
- Agree with the experimental methods used for testing and concur the results to be honest, true, and scientifically accurate.
- Understand the new comparator method and why it is a new useful tool
- Feel the research presented throughout is to a standard worthy of a PhD.

Chapter 2 Literature Review

In this chapter, wearable energy harvesting technologies and research within this area are explored. Before any wearable energy harvesting applications are investigated, the available energy from humans is researched. This leads on to looking at how researchers have previously approached extracting this energy for wearable energy harvesting designs and applications. Previous methods for comparing wearable energy harvesters to each other and to portable power supplies are compared and examined. The chapter will conclude with a more detailed look into Watt-level wearable harvesters with regards to their designs, transducer styles and output powers.

2.1 Human Energy Sources and Harvested Power Levels

Here the areas available for energy harvesting from around the human body is investigated. It is shown in terms of research performed, looking at body movements or forces seen in activities, as well as results from energy harvester publications and their reported power outputs.

The average male human is recommended to consume 2500 Calories of a mixed health diet every day. Females are recommended slightly less at 2000 Calories per day. This is equivalent to 10.5 MJ of energy for males and 8.4 MJ for females per day [15], [18]. This might seem a fantastic opportunity for harvesting, but unfortunately the human body is always consuming this energy even when at rest or sleeping. In general, average humans consume around 70 Calories an hour even when sleeping. At rest is defined by the human sitting or lying, not performing any exercises, or moving with too much effort.

This can be converted into Watts and an average of 81 Wh of energy is consumed by the body when at rest or sleeping [15]. These figures indicate that humans are always using their energy reserves. Wearable energy harvesters need to ensure they are not designed to use to much of a human's energy reserves or a detrimental effect on the wearer could result. Humans are burning through this energy in forms of body heat, muscle movement or even brain activity. So, the question that every wearable energy harvesting researcher needs to ask is;

Can any of the energy held within or dissipated by a human be harvested without resulting in the human requiring the intake of more energy?

In 1996 T. Starner published a paper called "Human-powered wearable computing" [15]. In this, he hypothesise' different energy levels available from humans and suggests these energies could be used to power a rapidly expanding new trend of portable electronics at the time. The paper created the illustration shown in Figure 2-1. This started to give the idea that there are lots of opportunities where spare or wasted energy could be available for harvesting applications. The values shown in the parentheses are the total or maximum power figures for each area. Figure 2-1 shows that from even simple activities there is energy available and different areas have different energy levels. Here, Starner calculates 67 Watts of power could come from footfall when walking.

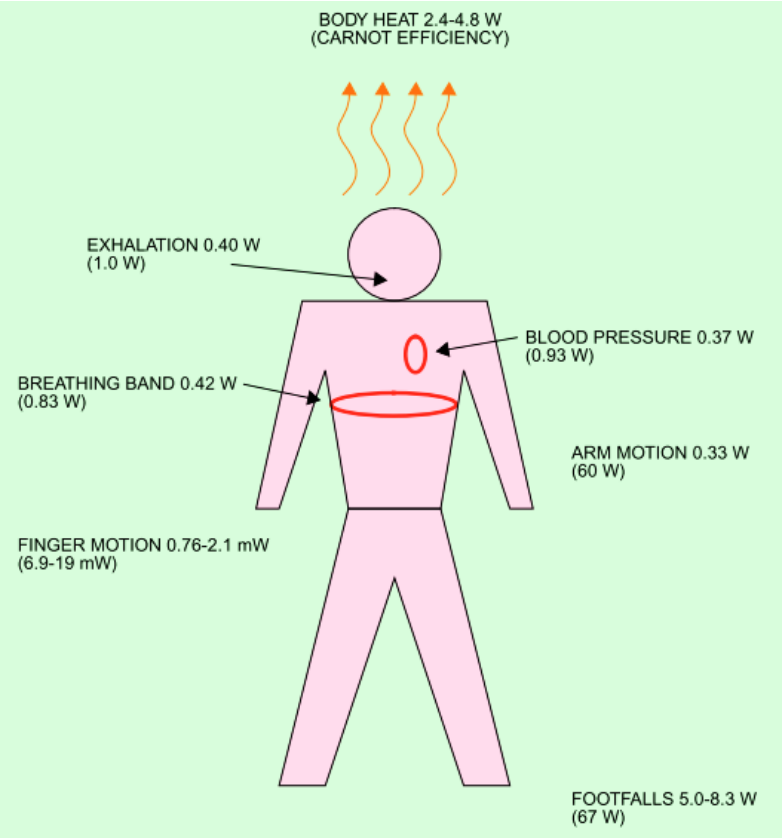

Figure 2-1 Illustration of power sources from the human body by T. Starner's [15]

Since this work, over 24 years ago, researchers have looked into more detail at the energy expenditure of humans,[18]–[21] and how the energy harvesting research community can use some of the energy.

Work published by R. Riemer in 2011, looks into more accurate ways of calculating energy available from humans with the aim of using it for energy harvesting applications [22]. Here the author researches into energy in the form of heat emission and shows that the human body radiates up to 100 W of heat energy when simply sitting at rest. Here the research calculates a harvester energy transfer efficiency of 2.15%. This is based on their research into this area resulting in a maximum power output of 2 W from the heat emissions of a human.

This output is low but is similar to the predictions by T. Starner. The paper also looks at energy sources from leg and arm motion along with centre

of gravity movements and footfall forces. From their findings a table of available energies was produced and is shown in Table 2-1.

Table 2-1 Available energy from different human based sources or movements [22]

Source	Energy Available (J)
Body Heat	2
Leg Movements	
Knee Joint	16.7 *
Ankle Joint	9.7 *
Arm Movement	
Elbow Joint	0.4*
Shoulder Joint	0.65*
Centre of Gravity Movements	20 **
Footfall Forces	2 ***

* per Joint Per normal swing
** using a 20 kg mass in backpack
*** per foot @ 1Hz

Riemer, used existing energy harvester's experimental method to improve the prediction figures of actual power from harvesting, rather than only looking at what might be available [22]. The footfall power is calculated from one foot only and uses a more realistic displacement figure of 4 mm. This reduction comes from research into the gait cycle and the defection seen in the insole of shoes.

One of the areas that looks promising for providing high power levels from around a human body is the movement of the centre of gravity. 20 W of power is calculated to be available from this source according to research presented in Table 2-1. This figure does come with a massive drawback of having to carry a 20 kg load in a backpack. The backpack is designed to harvest the motion of the mass moving up and down as the wearer is walking and of course most of us carrying a backpack to work or for day trips would never reach a backpack weight of 20 kg. Regardless it would also involve a

huge increase in metabolic energy consumption of the wearer from carrying this added mass needed to generate the power from the harvester.

Multiple researchers have worked on energy harvester designs that work from the heat dissipation of humans or the Carnot effect and have shown the possibility of this using thermal-electric generators to do this [2], [23]–[26]. The main problem seen with using thermal generators was presented at the 2017 Energy-Harvesting-Network Event (EHN), by S. Beeby [27]. Here the presenter explained that the limitation to using humans as a heat source, is the human itself. The human body is very clever, and if the skin temperature starts to drop in a particular area, then the body reduces the blood flow and in turn heat supplied to that area. The larger the area used for heat harvesting, the better the power outputs will be, but also the larger the risk of reducing the wearer's body temperature too much. Harvesting too much of this energy will increase the metabolic energy consumption of the wearer and could lead to a risk to health if not controlled or limited in the correct fashion. More details on thermal generators will be looked at later in this chapter.

2.1.1 **Foot Energy**

In the next section a more detailed look into a number of different energy sources is investigated. Here, each area will be looked at to see where the energy is coming from and how this could be useful; with an aim to charge or run portable electrics.

In this area the forces seen when walking or jogging are reviewed and how these forces can be converted into theoretical available power figures are also explained.

The first part is to understand how humans walk and at what point in the gait cycle is there free energy to harvest.

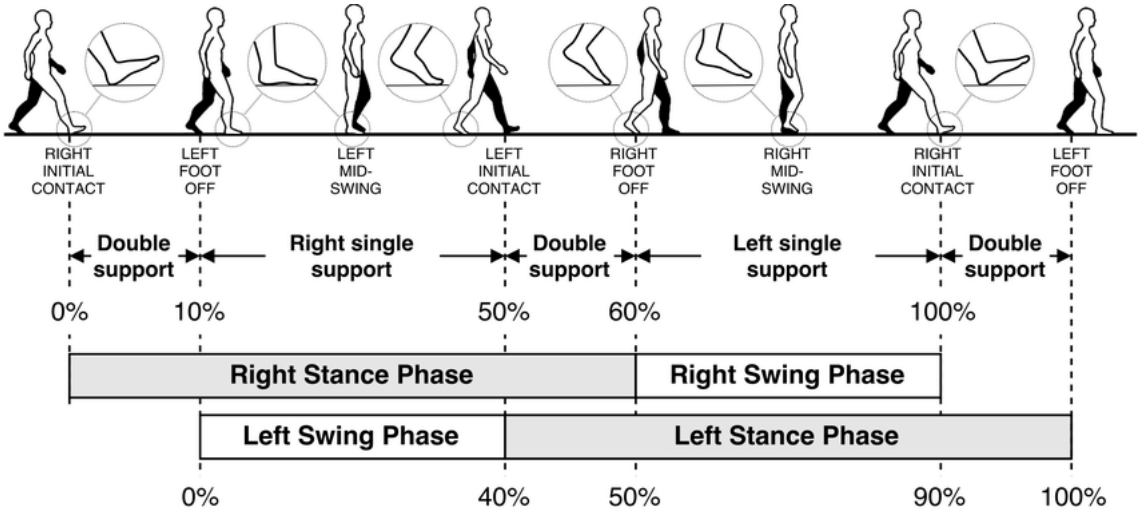

Figure 2-2 Standard human gait cycle layout by C. Tunca [28]

Figure 2-2 taken from work by C. Tunca 2017, shows a standard human gait cycle [28]. This is a good illustration of the different foot positions during normal walking. The standard gait cycle starts with the right foot just touching the ground. This is also called heel strike and the gait cycle ends when this point reoccurs.

As most footfall energy harvesters are aiming to harvest the forces seen during the heel strike stage, starting at this point in the gait cycle can make it hard or confusing to analyses.

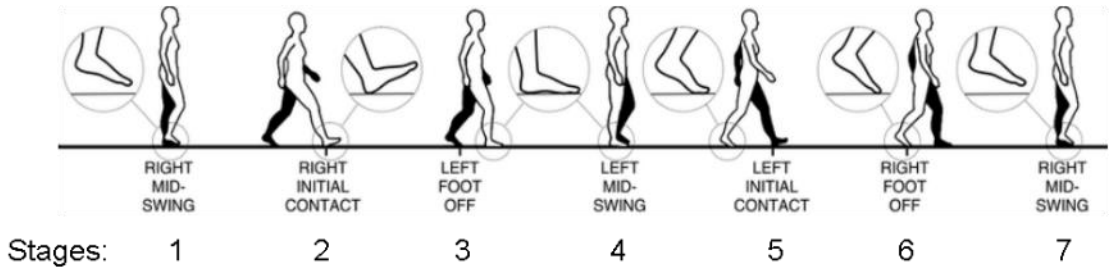

Figure 2-3 Re-ordered human gait cycle layout with numbers identifing the key points

Figure 2-3 shows a modified gait cycle illustration modified for this research project. Here the cycle starts at the mid-swing of the right leg. The

right foot heel contact now occurs in stage 2. T. Starner calculated 67 W of power could come from stage 2, the heel strike stage when walking [15] and how this figure was calculated is shown in equation 2-1.

$$Power = mass\ x\ gravity\ x\ displacement\ x\ step\ rate \qquad (2\text{-}1)$$

The author's calculations are based on a 68 kg person, walking at 2 steps per second, using an input displacement of 5cm. By having such a large displacement input, the suggested available power is very high, and it also assumes that all of the force from the footfall is converted into the output power.

T. Starner uses the maximum ground clearance of the heel to ground when walking as the input displacement of the harvester. If a harvester was created to capture all of this displacement, the wearer would struggle to walk in a normal manner and would be forever catching and snagging the input mechanism, making this available power figure unrealistic. Whereas, the power output seen by Riemer research in 2011, uses a more realistic displacement that is already seen in shoes worn today [22].

Using the stage numbers added into figure 2-3, from stage 2 to stage 6 the right foot is in contact with the floor. This is as the left foot is swung through to take the next step.

Researchers have looked into how the weight of the human is transferred from the heel in stage 2, to the toes in stage 6 and this has led to energy harvesters being designed to extract this energy. In 2001, N. S. Shenck published a paper with two piezoelectric harvesters mounted within the sole of a shoe [29]. One harvester is towards the back, designed to harvest the impact from the heel strike in stage 2, then the second is towards the front of the shoe to harvest the weight moving onto the toes in stage 6.

The illustration shown in Figure 2-4 is from this paper and shows the two piezoelectric harvesters. It can be seen that the heel strike harvester is designed to withstand the shock loading of the foot hitting the ground during stage 2. Whereas the PVDF stave is far thinner and designed to harvest the gradual weight transfer occurring from stage 2 to stage 6.

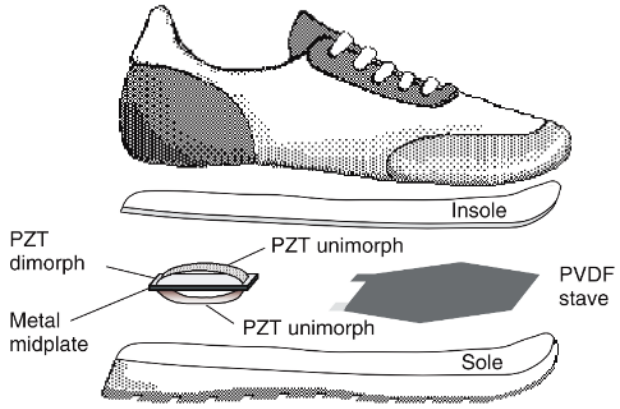

Figure 2-4 Piezoelectric shoe harvesters concept by N. S. Shenck [29]

This in-shoe harvester produced 9.7 mW of power on average from normal walking, but 8.4 mW came from the heel strike PZT, and only 1.3 mW from the PVDF stave. This shows there is a lot more power in the heel strike stage compared to the weight transfer during stage 3, 4, and 5.

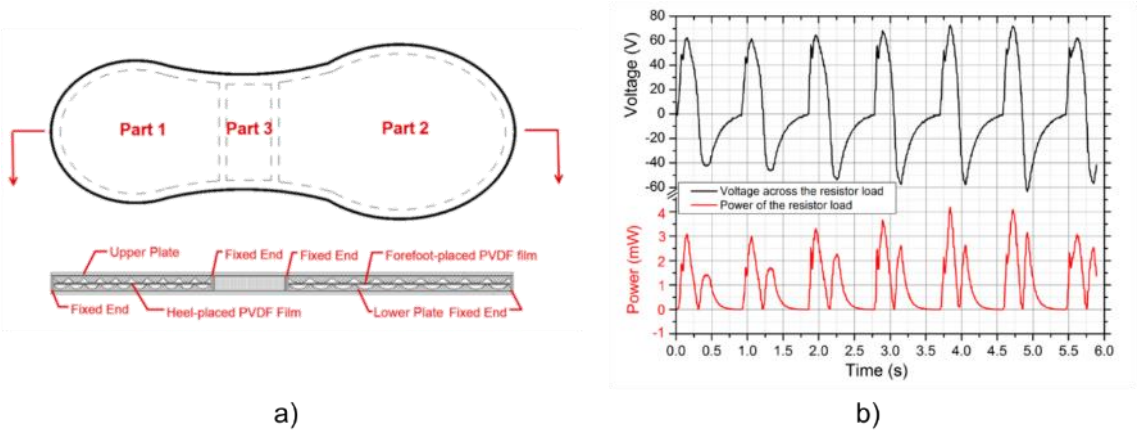

Figure 2-5 Shoe-embedded energy harvester by J. Zhao [6]: a) Design layout, and b) Output results [6]

Figure 2-5 shows a similar design by J. Zhao published in 2014, [6]. Here the author reports an average power output of only 1 mW, but the recorded results shown in Figure 2-5 b), clearly there is more power in stage

2 of the gait cycle, over the power gained during stage 3, 4, and 5. The graph seen in Figure 2-5b shows over 60 V are generated as the heel strike occurs and generates 3 mW of power during this time. It also shows how sharp and sudden this inrush of power is. The voltage generated during the weight transfer is not only lower, but also at a slower rising rate. This results in a lot less power from the weight transfer compared to the heel strike.

A clever design by J. Y. Hayashida in 2000, aimed to harvest more of the heel strike energy [30]. This design is shown in Figure 2-6. Here this harvester design produced an average power of 58.1 mW from stage 2. When the foot comes into contact with the ground, the input bar (labelled with the single red arrow) is forced up and this turns two small electric motors (labelled with the two green arrows).

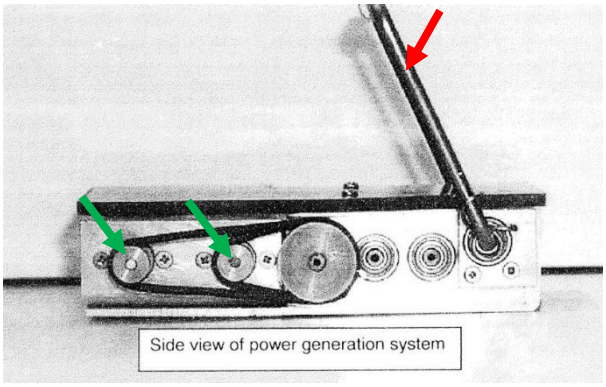

Figure 2-6 Heel strike wearable energy harvester by J. Y. Hayashidas [30]

A number of footfall harvester designs have been created and researched into during the past decade[14] [16]–[20], and it is clear to see, that by utilizing the force of the foot moving towards the ground, a harvester could be designed to produce high power outputs (Watt levels of power). This is a gap in current research that will be explored further. Using the forces seen in heel strike is a clever idea, but the forces seen in this stage of gait are very high.

Figure 2-7 shows a graph recorded by researcher Rod Cross, published in 1999, where the forces seen from footfall are recorded by a force plate [36].

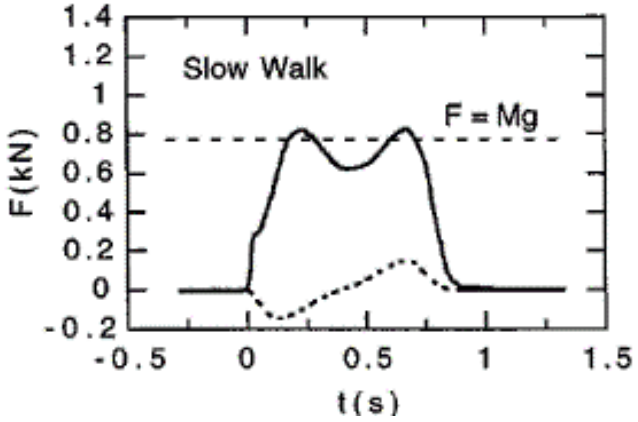

Figure 2-7 Results from walking on a force plate by R. Cross [36]

R. Cross measures over 800 N of force from normal walking on, and off, the force plate. These load figures only increase when the subject runs or jumps on the force plate. This denotes that any footfall harvester design will need to be able to withstand very high shock loads at low frequencies.

It also shows that the time frame in which stage 2 of the gait cycle occurs is only 0.1 s. This time frame is from the first point that force is seen on the force plate (Start of stage 2, Heel strike), up until the maximum force is seen (End of stage 2, entering stage 3, flat foot). This results in the fact that even though there might be a lot of power available from heel strikes, it only happens for a short period of time. This will have a dramatic effect on the average power generated by a footfall energy harvester by having a small active duty cycle time.

Footfall energies indicate the potential to provide the power needed to charge modern portable electronics, but they also show the sudden high force loading needing to be withstood and complex integration methods to be overcome.

2.1.2 **Legs and Leg Joint Energy**

Here the key research is referenced to the work done by Q. Li in 2009 [37]. Here, Li and their research group developed a wearable energy harvester that worked off the movement of the knee joint.

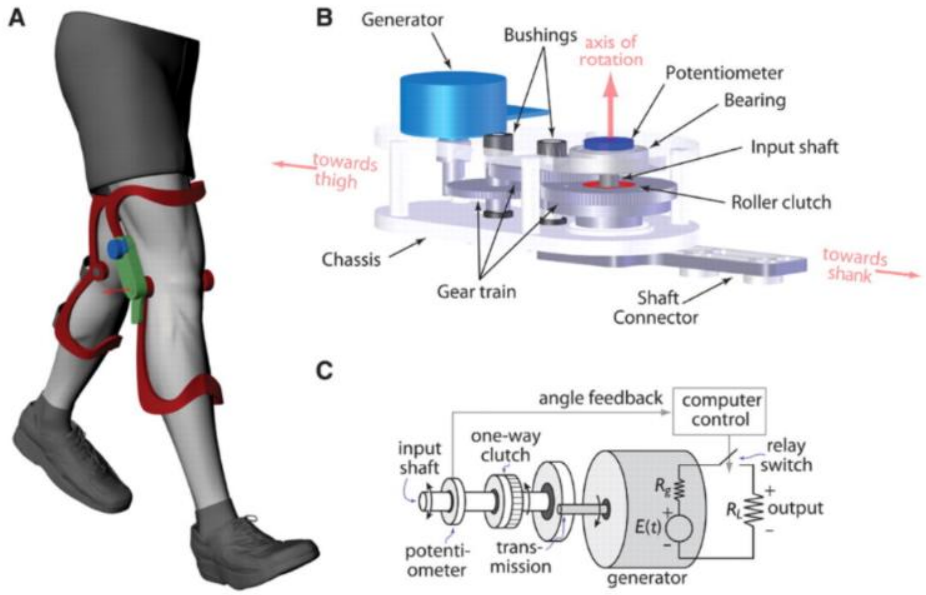

Figure 2-8 Bio Walk, knee-joint energy harvester illustration by Q. Li [37]

This harvester has been named Bio-Walk and can be seen pictured in Figure 2-8. This was not the first wearable energy harvester to look into harvesting from the knee joint but is by far the highest power found in research from the knee joint to date. The research found here goes into a good level of detail surrounding the movement of the knee joint and how much energy could be generated by the knee movement. Of course, if this harvester was designed to generate power throughout the whole of the knee joint movement in both directions, then the wearer would have to exert more effort and in turn, use more energy to drive the harvester. This is where this design is very clever. The harvester is designed to only engage and generate power at the final stage of the leg swing. This means the harvester is harvesting at the point a muscle would normally be being used to slow the

leg. Their research showed there is over 20 W of power available from the knee joint movement and their harvester design produced just over 4 W of electrical power due to inefficiencies in the design. Another wearable energy harvester that works on the knee joint rotation was designed and created by Y Kuang [38]. The design illustration and test rig is shown in Figure 2-9.

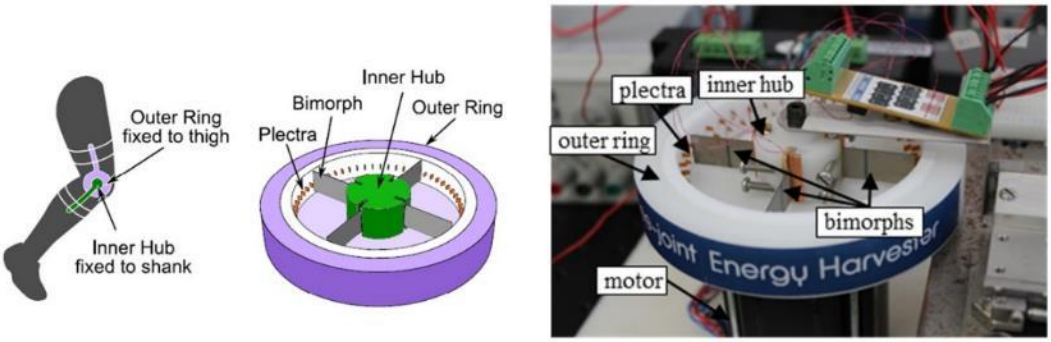

Figure 2-9 Knee-joint energy harvester by Y Kuang: a) illistration of harvester to wear on the external side of the knee and (b) prototype mounted on a stepper motor

Here the design only produces 1.76 mW but shows a novel way of extracting the energy from the knee joint rotation without impacting the wear walking style.

A number of researchers have looked into exploiting the free energy from the leg swing itself, [35], [39]–[41]. Here, these harvester designs are strapped to the ankle area and include a small internal mass. When the leg is swung from walking or moving, the mass moves. The energy they are harvesting is from the velocity of the leg and the acceleration of the internal mass. It was found in research that the leg velocity is directly linked to walking speed and step rate [28], with the ankle of healthy males being the highest speed seen during normal walking, with an average being 0.8 m/s.

The speed and acceleration of the ankle might seem a useful area for harvesting, but the power output will always be limited by the maximum internal mass the researcher is willing to apply or the subject is willing to

wear. The heavier the internal mass, the higher the power output, but in turn the heavier the mass the bigger the energy consumption of the wearer.

An intelligent design was published in 2015 by M. Shepertycky, called "*lower limb-driven energy harvester*" [12]. Their design is shown in Figure 2-10. The device uses an AC motor to generate the electrical power output and is driven from the leg swing during walking.

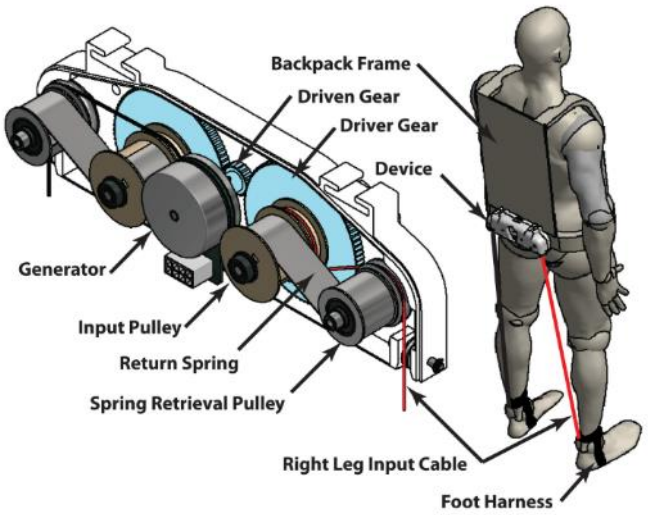

Figure 2-10 Wearable energy harvester design by M. Shepertycky [12]

The author shows the harvester produces 5.2 W of power, but also says that at this power generation level the harvester affected the wearers walking and heavily increased their metabolic energy rate. When the harvester was set up to generate 3 W of power (by reducing the connection resistive load on the harvester), the author reports better results in terms of metabolic energy consumption of the wearer.

From the author showing how the resistive load connected to the harvester affected the walking of the wearer of the energy harvester, this showed that there will be a trade-off between matching the optimal resistive load for optimum energy transfer from the transducer, and the maximum load acceptable for the harvester not to impact on the wearer above a set point.

Unfortunately, that set point will be an individual preference. What one person might not notice, another might find unbearable.

2.1.3 **Torso, Respiratory, and Centre of Gravity Movements**

In this section the main part of the body (torso) will be examined to determine what level of energy is available for wearable energy harvesting applications. The torso area includes looking at the respiratory system and whole-body movements with respect to the movement of the centre of gravity of the subject.

Referring back to the work by T. Starner [15], here the author looks at the flow rate and the work performed by the heart to pump blood around the body under pressure. They calculated 0.9 W of power per beat but harvesting this would be detrimental to the wearer and add strain on the heart. Because of this, T. Starner states no more than 2% of this energy source should be extracted. Why the author states 2% is not explained. A published report by J. Wand in 2014 presented a design that harvests energy from breathing via the waistband and managed to produce 290 μW of power from normal breathing [42]

There has been much research published on energy harvesting from the heartbeat, even though there are risks to the wearer[43], [43]–[50]. None the less an energy harvester that could be used to power, run, or charge a pacemaker is vitally needed by the medical community, and could ultimately save unnecessary surgery just to replace the battery years down the line. It can be said here that the energy found from the heart beating is not going to provide a high enough power level to charge any portable electronics, so will not be investigated further here.

The second area to look at here, is the energy available from breathing or the respiratory system. This can be seen in two areas. One being from the air flowing in and out of the lungs via the mouth, and the second being the movement of the diaphragm, including the expansion and contraction of the lungs and rib cage. Estimation of the power available from breathing and the waist band movements are 1 W and 0.8 W respectively [15]. The energy from breathing will be explored and from research found, the power levels harvested or predicted from this action are low. Work by J. K. Gupta published in 2010 investigated the air flow from breathing and talking. Here they found peak flow rates of 0.7 and 1.6 l/s from breathing and talking respectively [51]. This instantly showed there was not going to be a large power level available from this action. Research performed by H. Xue published in 2017 presented a wearable energy harvester designed to harvest energy from breathing [52]. Their work confirms the low power availability as their harvester only produced 8.3 μW on average from normal breathing. Combine this with other research into harvesting from the air flow from breathing which also produced very low power output [52]–[56], it would confirm that there will not be enough spare energy from breathing to charge a portable electronic device therefore it will not be investigated further here.

The second area of waist band movements from breathing was also researched. Published research in this area is sparse, and from reading papers looking into stretchable bands measuring this area, the power available will be again very low. Work by J. Wang published in 2014 showed an energy harvester design using the movement of the diaphragm [42]. Here the researchers were working on a stretchable piezoelectric band and harvesting from changes in the band's diameter, perfect for harvesting from

breathing muscle movements. However potential power is hard to determine due to the researchers' work concentrating on fabrication and feasibility of the idea, rather than power generated. It does state that from a single breath, the band is deformed by 2.5 cm and generates an electric charge of 0.2 μC. This shows there is not going to be enough power available from this area and will not be looked at any further here.

However, the movement of the centre of gravity does show promise for generating Watt levels of power, confirmed and proved by a number of backpack harvester designs working from this movement [8]–[10], [13], [22], [57], [58]. The idea behind these harvesters is, that when the wearer is walking, a large internal mass held with in the backpack is moved up and down. This movement is then transferred into a controlled output, an electro-magnetic transducer which generates the useable electric power. Referring back to the work published by R. Riemer in 2011, here the research predicts 20 W of power from the centre of gravity movements [22]. However this figure is based on carrying a 20 kg load in the backpack.

A better way of interpreting the power available from the centre of gravity is summarized towards the end of R. Riemers work. 1 W of power from every 1 kg mass carried. This shows there is a direct connection between additional mass added to the harvester and the amount of power that said harvester will generate.

In order for a wearable energy harvester design to work off the centre of gravity movements and to generate Watt levels of power, the wearer would have to carry additional mass. This seems a little redundant when the wearer could simply carry more batteries to fulfil their energy demand. Saying that, if the wearer of the backpack was already carrying a large battery for the

power needs, then this could be used as the harvester's internal mass, and the harvester could keep topping up the battery ready for use.

This was the idea behind the work of L. C. Rome [13]. This research was for the U.S Military and aimed to reduce the mass of the personals' backpacks by reducing the battery size and adding an energy harvester. This proved to work and generated up to 7.4 W of power but required a 38 kg mass to be carried in order to produce this power figure.

The centre of gravity movement shows the potential of high enough power to charge portable electronics but comes with the drawback of having to carry an additional load. As this thesis is aiming to charge portable electronics in the domestic market, simply adding more weight to the wearer will be unacceptable and the public would not be interested. The second drawback is the limited space for scientific contribution. This area has been investigated intensively and could make it hard to show clear technological progress over previous designs. Because of this, creating a wearable energy harvester working off the centre of gravity of the wearer, will not be looked into further here.

2.1.4 **Arms, Arm Joints and Hands Energy**

Finger motion has been looked into by a number of different researchers over the past ten years and most are simply looking to how much power they can generate, rather than the energy available [59]–[61].

The work mentioned earlier by T Starner did some calculations on how much energy might be available when using different keyboards for typing. The equation shown in equation 2-2, shows how they calculates the available energy.

$$finger\ energy = finger\ force\ x\ gravity\ x\ displacement \quad (2\text{-}2)$$

Here the author uses the force required to depress a key on a keyboard and the displacement needed for the key pressed to be registered by the computer. They use 130 grams of pressure as the input force and a displacement of 1 mm. They concluded that this motion of typing on a keyboard could produce 1.3 mJ of energy per key pressed. This started to show that although there would be energy available from finger motion, the power outputs would be in the milliwatt range and not produce enough power to charge portable devices such as smart phones and tablets

In 2013, Ya Yang published an article introducing a small lightweight energy harvester that could work on finger electrostatic induction [62]. They performed experiments attaching small energy harvesters to the top of keys on a computer keyboard and measured the power generated over a 100 MΩ resistive load. When the keys were depressed by a human finger the energy harvester produced 4 μW of power. The author does not state the pressure, force or the velocity of the finger required to generate this power. This makes it hard to establish the energy entered into the harvester to generate this power but does confirm that the power generated by finger movement is too low for the needs of current portable devices, (smartphones and tables).

Hand movement is very complex with over 34 muscles used to move the hand and fingers. Harvesting from this seems another area of opportunity. An estimation of 7.7 mWh could be available from hand movement during a normal day according to research by N. B. Amor in 2008, [63]. The author measured the hand displacement about all three axes to find which direction had the most dominant movement. With the power available, the author proposes charging a super capacitor to aid in the battery life of a

hearing aid. Hearing aids have a small power requirements compared to smart phones, but the power available from hand movement is again too small for the charging aims of this research.

Moving up the arm to the elbow, larger displacements are seen. The elbow joint is a complex joint and has a maximum angle change of up to 135° [64], [65]. The torque around the elbow joint suggests that this might be a good area of available energy. Research performed by V. Linnamo in 2006 produced the graph shown Figure 2-11.

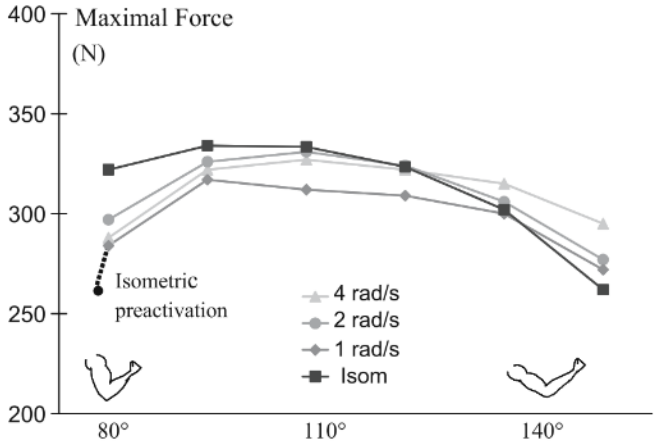

Figure 2-11 Avaliable force relative to the angle of the elbow joint by V. Linnamos [66]

Looking at Figure 2-11 confirms the amount of force the elbow joint experiences, but doesn't help with how much energy might be available to be harvested. If a harvester creates too much resistance to the elbow joint, then the wearer would need to use more energy to move their arm. T Starner's work also had this thought and from their calculations predict a maximum of 1.5 W of power to be generated from the elbow joint [15]. Any more than this and the wearer would need to use more energy moving their arm. T. Starner goes to say how complex the mechanism would need to be, in order for it to be able to harvest the elbow movement directly. He suggests the use of piezoelectric materials to help extract this energy.

Another area that might have energy availability, is the arm swing during walking or general movements. Old wind up wrist watches used the arm swing to extend intervals between manual wind ups and battery replacements. During normal walking the arm is swung at the same frequency as the legs and varies between 0.8 – 1.1 Hz, [67]. Harvesting this movement would mean using an internal mass held within a wearable harvester. As the arm is swung the internal mass moves and inputs into the transducer in lots of different ways, [68]–[71]. The larger the mass used the larger the input into the harvester. Research by P. Pillatsch, published in 2014 uses a 4.8 g internal mass and records a harvested power of 43 μW [72]. This is used as an example of the available energy record from arm swing. This is very low and does not so the potential of scaling to the Watt-levels needed for charging portable electronics.

2.1.5 **Head and Heat Energy**

The head has a number of devices that would benefit from being powered or charged by a wearable energy harvester, such as hearing aids or smart glasses, but as of yet no wearable energy harvesters have been commercialized to fill this need.

The head does however have a few areas where a wearable energy harvester could harvest energy from the wearer. Work performed by E. Goll and published in 2011 went into detail about the energy available from the head area. This led the researchers to be able to set "*Upper Bounds for Energy Harvesting in the Region of the Human Head*" as the title of their paper, [73]. By setting different scenarios for the different areas of available energy, the author was able to predict available energy more accurately. The

author also researched into environmental conditions that a wearable energy harvester might be able to harvest, such as light and radio waves. From the ambient conditions the author predicts between 4 μW to 40 nW of power, both of which are too low to be able to charge or run a portable device. Regarding movements to the head, the author splits these movements into two groups:

One, for sporadic, nonlinear movements, such as nodding or shaking of the head. These movements tend to occur at random intervals throughout a normal day. The author calls these movements "*Transient movements*" and predicts an average of 0.35 J of energy from a 15 minute conversation.

The second head movement the author investigates are categorized as "*Periodic Movements*". These are rhythmic movements with a sustained period of predicable frequency and displacement. These movements come from the head bobbing up and down during walking or running. From this type of movement, the author predicts 2 mW of power from running half an hour, 4 days a week. From either type of head movement there is not enough power to charge or run a smart phone. Another area E. Goll investigates is that of energy available from chewing or jaw movements. The author refers to another paper [74] and uses data from their research into biting force seen from different foods. E. Goll predicts an average power of 7 mW from chewing. The way this figure is predicted assumes a certain chewing rate and also sets what food is being eaten making it hard to say for sure, whether this is the available power.

Work done by A. Delnavaz published in 2014 presented their investigations into a wearable energy harvester that extracted energy from jaw movement [5]. Here they proved their harvester design produced 7 μW

of power from normal chewing. This figure is low, and the author explains the limitations of their design. The author does not want to impact the wearer or increase the user's effort during chewing. This limits the harvestable power and is the reason the power is so low. If a jaw harvester design was designed to harvest energy from chewing to produce a higher power output, it would simply mean a higher energy input from the wearer.

The research into harvesting from chewing or jaw movement clearly shows there will not be a large enough power available for charging portable devices such as smart phones, so will not be investigated further.

The last area that a wearable energy harvester might be able to harvest energy from around the head is in the form of heat dissipation into the environment. Work by V. Leonov, designed a wearable energy harvester that could harvest from the heat loss from the head [75]. Figure 2-12 shows their published photos of the harvester.

Figure 2-12 Thermal energy generator for harvesting the heat from a human's head by V. Leonov [75]

This harvester design produced 2.5 mW of power at 22 ˚C. The researchers show how it can power body sensors, but again this energy source is too low for the power needs of charging smart phones. The author here reports that when power levels of 3.7 mW were seen at 19 ˚C, the

wearable energy harvester became uncomfortable and gave the feeling of being “*cold*”.

This confirms the thought by S. Beeby mentioned earlier, i.e. harvesting heat from humans can lead to discomfort [27].

2.1.6 **Summary**

After researching into energy available for wearable energy harvesting applications, it has become clear that certain areas of energy available from around the human body are not going to be able to provide a large enough power output to charge portable technologies such as smart phones or tablets.

Referring back to Table 2-1 shown earlier, only four areas show potential for producing high enough powers to charge smart phones. These areas are Knee joint movement, ankle joint movement, centre of gravity movements and footfall forces. The centre of gravity energy extraction needs added mass for the harvesters to generate electrical power and the size of the mass is directly related to the power produced. Because of this drawback and the fact that lots of research has been done into this area before [9], [13], [57], [58], [76], this area will not be investigated in this thesis.

The knee joint harvesters have varying power outputs from 1.76 mW, seen in work done by Y. Kuang [38], to 4 W produce by Q. Li [11]. This shows there is enough power available from the knee joint movement to charge portable technologies but would need to be designed with these power outputs in mind. The harvester would also have to ensure it did not increase load to the wearer’s muscles to power the harvester. This would be detrimental to the wearer and cost the wearer energy via an increased

metabolic energy consumption rate. This would also apply to ankle joint wearable energy harvesters. If the harvesters are designed to harvest as much from the joints movement as possible, then this would lead to the wearer having to apply more energy to their muscles to move their joints at the same rate. Because knee and ankle joints both have the drawback of using extra muscle force to generate their electrical power, they will not be investigated in this work. This leaves footfall energy harvesting as an open area for future energy harvesting research. From research into available energies in this area, predictions of up to 67 W were found. This was ultimately reduced down to a level of 8 W after implementation considerations were added. It will also mean no direct muscle energy goes into the harvester, footfall energy harvesters utilize the mass of the wearer and the ground reaction to generate the power.

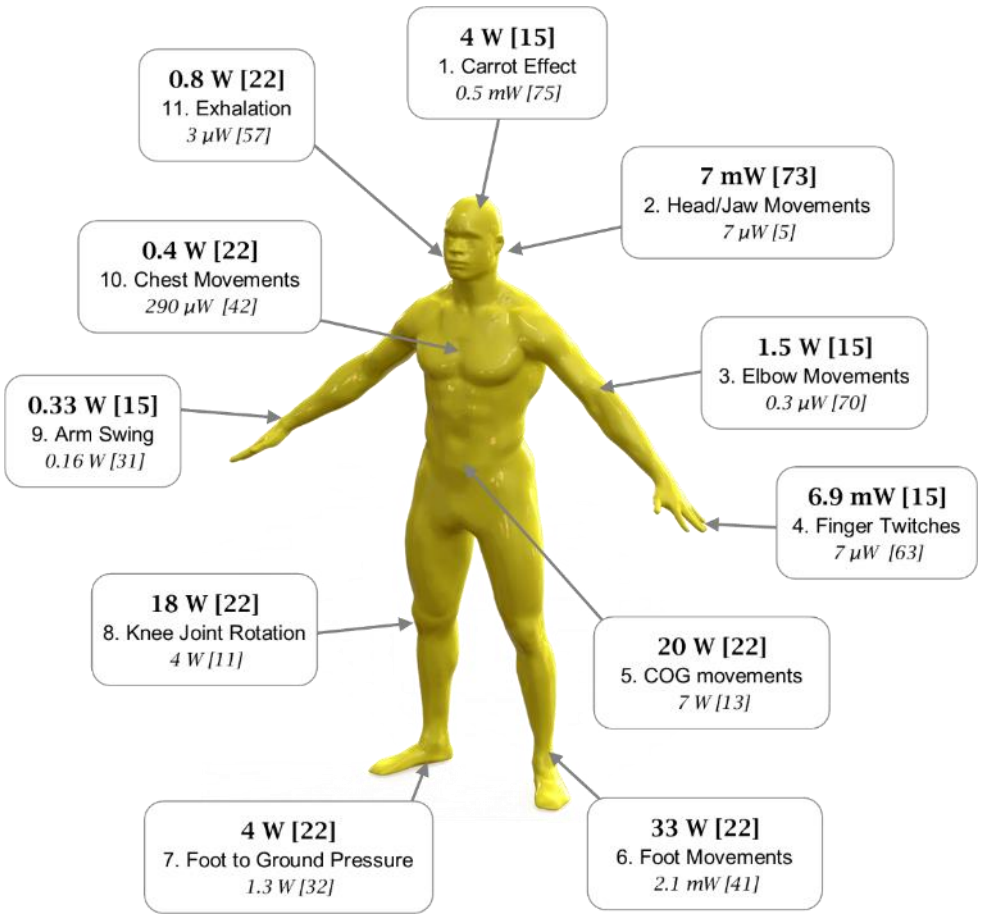

Figure 2-13 Current predictions on harvesting energy levels available from humans and published wearable energy harvester designs electrical power generated. Predictions above in bold, proven results in italic below.

Figure 2-13 shows a more detailed view on the predicted energy levels available from around the human body found in research and presented in the previous sections. This can be used to show what areas are no good for watt level wearable energy harvester applications.

2.2 Wearable Energy Harvesting Transducer Mechanisms

In this section the different transduction methods for transferring energy sources from around the human body into a useable electrical output will be examined. When the energy is changed or “transferred” it must have gone through some design of “transducer”. Here the different styles of transducer will be reviewed along with recently published research on new approaches or designs.

2.2.1 Piezoelectric Transducers

Piezoelectric transducers have been used in wearable technologies for decades. Seiko in December 1969, released a watch with a Quartz crystal, the Seiko-Quartz-Astron 35SQ [77]. Here the piezoelectric transducer was in the form of a quartz crystal. This was used as a frequency controller, not being used as an energy harvester. This does indicate how long the piezo-electric effect has been understood and used in a wearable form.

Piezoelectric materials shows promising signs for use in wearable energy harvesting due to what these materials can accomplish. The piezoelectric effect is a process from transferring energy from a physical to electrical energy and vice-versa. When a piezoelectric material receives a physical input from its surrounding it generates an electrical charge and if an electrical charge is applied to a piezoelectric material it will physically change shape, size, or position. Piezoelectric materials can be used as wearable energy harvesters in which the material will receive a physical input and convert this into an electrical output. There are many piezoelectric material used for different applications, these include, but are not limited to; PZT,

PVDF and composites. Research is continuing into the development of these materials and new formulas in order to improve the materials efficiency in the transfer of energy, [78]–[81]. Wearable energy harvester researchers have used piezoelectric materials in multiple applications from in-shoe harvester [29], [82], [83], Knee joint harvesters [84], Finger movement harvesters [59], [85], and even jaw movement harvesters [5]. Researchers in wearable energy harvesting see potential in piezoelectric materials for its power density. Piezoelectric harvesters are small light weight units which can be worn or even incorporated into existing clothing with very little impact to the wearer. They can harvest very small amounts of energy, but in turn only produce small amounts of electrical energy, and this is why improving the energy transfer through the piezoelectric transducer is critical for piezoelectric wearable energy harvesters.

An early paper using piezoelectric material as a transducer for power generation in a wearable form was by J. Kymissis and was published in 1998 [82]. Here the researcher used two types of piezoelectric transducers. One being a PZT (Lead zirconate titanate) unimorph shown in Figure 2-14 a) and the second being PDVF (Polyvinylidene fluoride) bimorph shown in Figure 2-14 b).

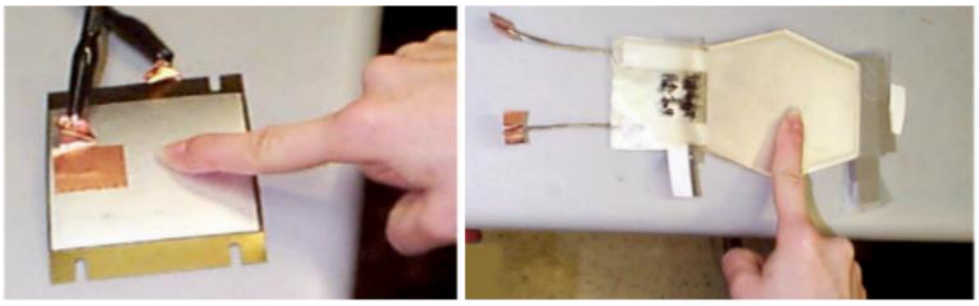

Figure 2-14 Piezoelectric transducers by J. Kymissis [77]: a) PZT Unimorph, and b) PVDF Bimorph

This research was published in 1998 and at this time was a revolutionary idea into generating power from a wearable energy harvester. This design of harvester produced 1 mW per step from the PVDF bimorph and 2 mW from the PZT unimorph. This work confirms that different types of piezoelectric material produce different power levels and confirms the fact that when working with these two types of piezoelectric material and structures, each had their advantages and disadvantages that need to be considered. For example, the author confirms that working with the PVDF was far easier, as it was possible to cut it into a more complex shape. However, the drawback here is that it is not as power dense as the PZT. PZT is a hard-brittle ceramic. This results in very high-power density, but limitations in usability. PZT being a ceramic also has a tendency to crack if shown a sudden shock load slightly over its maximum plasticity. Once the PZT has broken or cracked the power output drops dramatically.

This research and others that have investigated using piezoelectric materials for footfall harvesting [1], [1], [6], [29], [43], [83], [86], [87] have all produced power from footsteps, a maximum of 20 mW being generated by the design created by F. Qian and published in 2018 [1]. This is a 10-fold increase over the early work by J. Kymissis in 20 years.

This shows that piezoelectric material can be used as the transducer for wearable energy harvesters, but the power outputs required for charging a smart phone are far higher than what PZT or any of the piezoelectric materials can produce currently. There might be a design that could produce watt level powers, but any research would need heavy investment of funding into large volumes of this material. As a result, these piezoelectric transducers will not be considered for the research project.

2.2.2 **Triboelectric Transducers**

We have all had a nice electric shock reaching for a door handle or someone's hand at some point. This is called a static shock. This comes from the triboelectric effect that generates an electrical charge from friction. Researchers have investigated ways of creating energy harvesters that generate electricity by using the triboelectric effect, [4], [62], [85], [88]–[90]. The researchers are investigating new materials and manufacturing processes to improve the power generated by these types of harvesters. Work published by P. Bai in 2013 showed a wearable triboelectric energy harvester that contained two materials that when moved towards and away from each other, they build an electric charge that can be extracted. When the plates are forced together under pressure, say from pressure under the foot, the highest power outputs are recorded. Their device is shown in Figure 2-15 and they have a recorded a maximum power output of 4.2 mW.

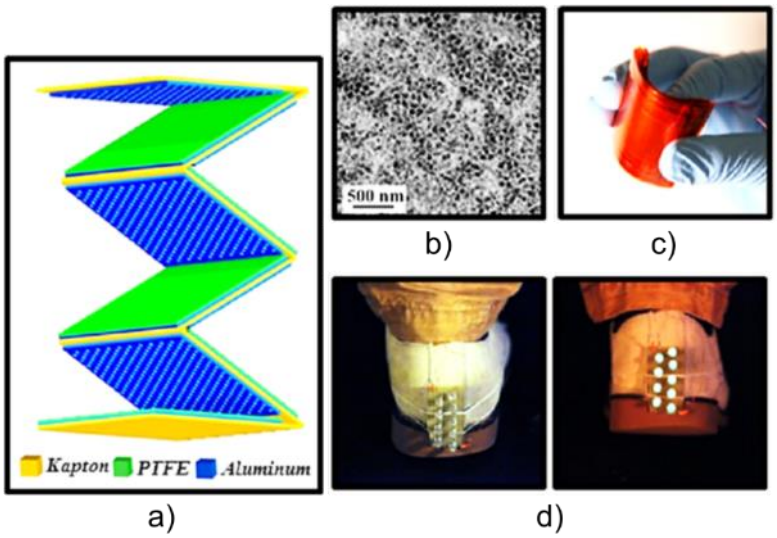

Figure 2-15 Triboelectric energy harvester design and applications by P. Bia [88]***:***
a) structure of triboelectric generator plates, b) SEM image ofnanopores on aluminum foils, c) Photograph of a fabricated flexible multilayered design and d) Photographs of the self-lighting shoe during normal walking

The power level out of this harvester is impressive, but this is only the maximum power seen and not an average. This means that power output will be reduce dramatically once an average is calculated.

Recent work by K. Dong published in 2017 demonstrates a flexible thread triboelectric generator that can be woven into fabrics. The researchers decided not to state a power output of the harvester, instead stating the power density of the device. This means it is very hard to compare to other research. What is good in this publication though is the figure shown in Figure 2-16 taken from their paper.

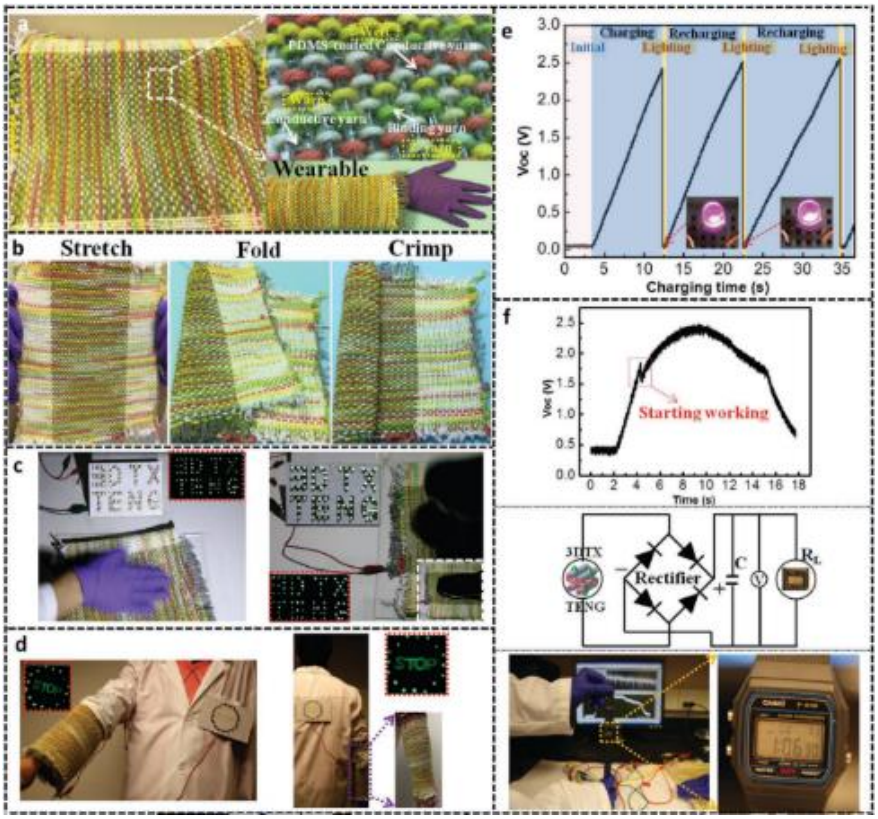

Figure 2-16 Examples of woven triboelectric energy harvester by K. Dong [91]***:***
a) photographs of large-area wearable textile, b) photographs showing the harvester in various mechanical deformations, c) photograph demonstrating that the harvester can light up 71 LEDs, d) photograph demonstrating the harvester, e) charging capability by practical hand tapping, and f) demonstration of continuously driving a smart watch by hand tapping

It is good to see real work examples of the wearable harvester being worn and producing useable power. It helps identify the real useable powers being generated by this design. Unfortunately from research found, wearable triboelectric energy harvesters are unlikely to deliver high enough power outputs to charge smart phones or tablets, so will not be considered for this research project.

2.2.3 **Thermoelectric Transducers**

Thermo-electric transducers or generators work with special materials such as Bismuth telluride (Bi_2Te_3) and antimony telluride (Sb_2Te_3) [23]. These materials generate an electrical charge when they have a temperature difference across the material. Multiple researchers have developed wearable energy harvesters that generate electrical power from human body heat and the temperature difference to the environment [2], [23]–[26]. Research released in 2015 by Z Lu [24], and published in the journal Applied Energy showed a thermo-electric harvester generating power from human body heat emissions. They report a power output of 15 nW from a small-scale prototype that the researchers built and tested during their research. The researcher tested the 4 x 8 cm generator at a ΔT of 5 – 35 K during 100 cycles of bending and twisting. In this paper, it is clear where the harvester was tested on humans by the photos included in the paper, shown in Figure 2-17. The scale of the device is also shown along with the voltage output of 6 mV in use.

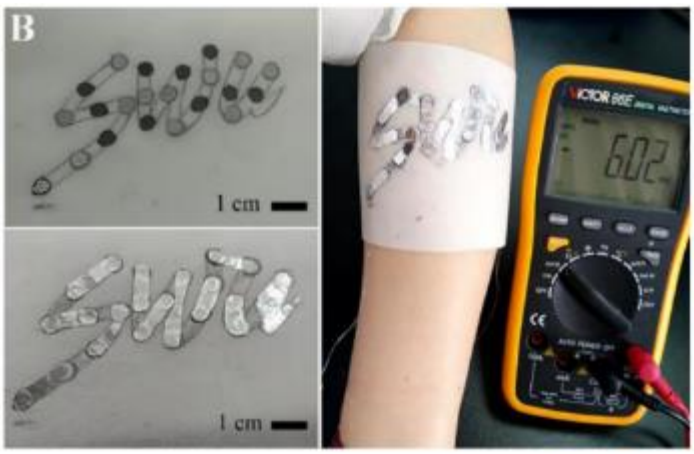

Figure 2-17 Wearable thermo-electric energy harvester by Z. Lu [24]

A review document by S. Mahmud published in 2017 goes over multiple researchers' work in the arena of wearable thermo-electrical energy

harvesting from the past decade [2]. Here the author looks at how thermo-electrical wearable energy harvesting has changed and developed in the last ten years. It reports that wearable thermal-electric energy harvesters have increased their power outputs from 21 μW generated by M. Takashiria in 2007, up to 100 μW by Z Lu in 2015. This shows good development regarding power output from thermo-electric energy harvesters, but the power outputs are still very low and will not produce enough useable energy to charge smart phones or tablets. Because of this, thermo-electrical generators will not be considered as an option for this harvester's aims.

2.2.4 **Vibrational-Electro-Magnetic**

A number of researchers have looked into using magnets passing coils to generate electrical power that work off of vibrations or movements found around the human body. Magnet-Vibration harvesters suspend a permanent magnet that is free to move when an energy input is seen by the harvester. The magnet can be suspended on a spring as seen in work by D. Zhu published in 2013 [92]. Here the author continues their work surrounding the movement of magnets from a spring force. Figure 2-18 shows their prototype energy harvester design.

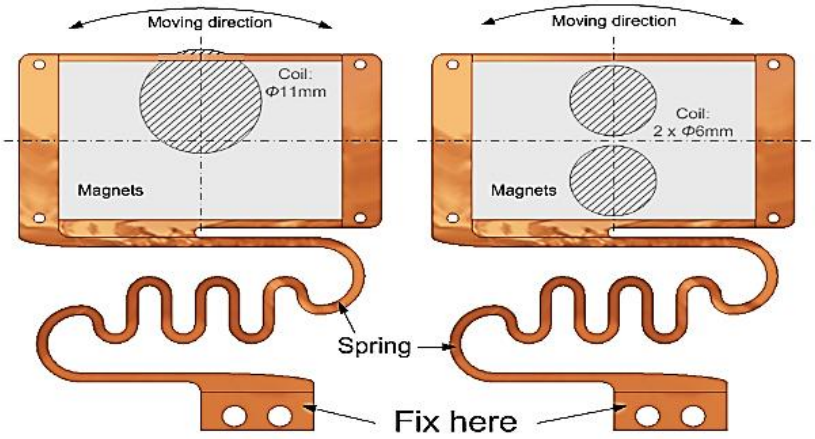

Figure 2-18 Vibrational energy harvester design by D. Zhu [92]

As the whole harvester moves, the internal mass moves according to the force and spring rate of the spring. In this work, D. Zhu shows the power outputs from the harvester in the form of a graph and does not state the maximum or average power output from their design in the test. This can be seen as an effective way of portraying grouped data, but makes it harder for fellow researchers to use their results to compare to others.

Work by C.R. Saha published in 2008 reported a power output of up to 2.5 mW from their design shown in Figure 2-19 [41].

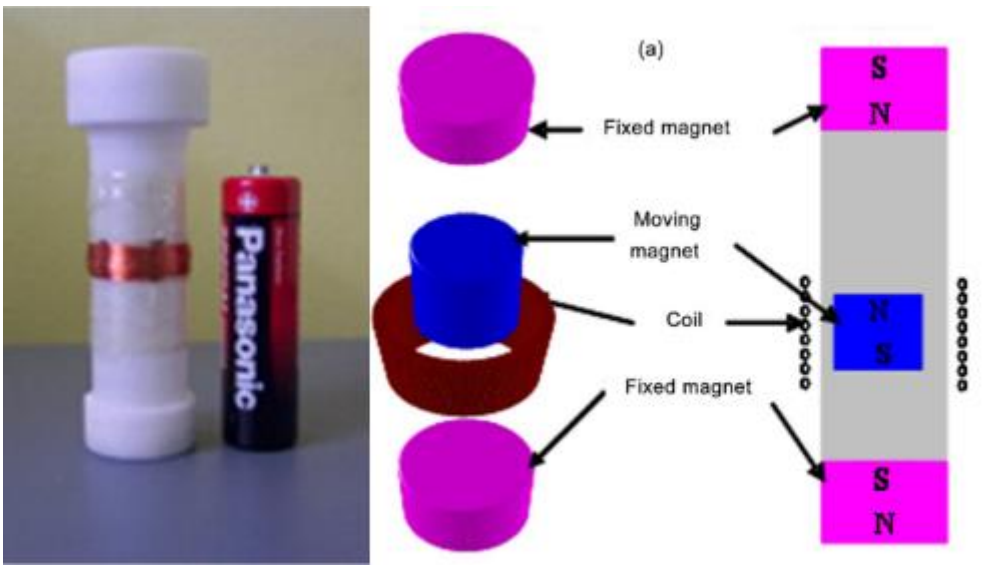

Figure 2-19 Magnetic Vibration Harvester by C. R. Saha [39]

This photo and illustration makes it easy to understand the size of the harvester and how it is intended to work. This harvester was placed in a

backpack and tests were performed under conditions of the wearer walking and slow running.

This work also confirms that the energy extractable from a magnetic vibration harvester is going to be low. Magnetic vibration harvesters suffer from the same drawback as the backpack harvester design shown in section 2.1.3. The harvester will produce more power indirect relation to internal mass used within the harvester. This is a problem for wearable energy harvester designs as they aim to be as lightweight as possible, thus limiting their maximum power outputs.

This leads to the conclusion that magnetic vibration transducers are not going to be able to generate the power levels needed for charging a smart phone or portable electronic device.

2.2.5 **Mechanical-Electro-Magnetic**

Mechanical-Electro-magnetic conversion is a very old form of energy transducer. These systems typically convert the input energy into a rotational form and higher velocity's. The magnets are moved past a set electrically conductive windings. When the magnet passes the windings, it generates an electric current inside the winding. Seen in a number of energy harvester designs this transducer is an electric motor [10]–[13], [32], [37].

This style of transducer was used in the backpack harvester design by L. C. Rome[13] mentioned in section 2.1.3 and produced over 7 Watts of power by using an electric motor as the transducer.

Work done by Y. Yuan published in 2018, showed a design improvement to the backpack harvester design. They add in a mechanical motion rectifier (MMR) into the design. This converted the up and down

movements of the harvester's internal mass, into a unidirectional rotational output which transferred to an electro-magnetic transducer. Their design and layouts from their publication are shown in Figure 2-20.

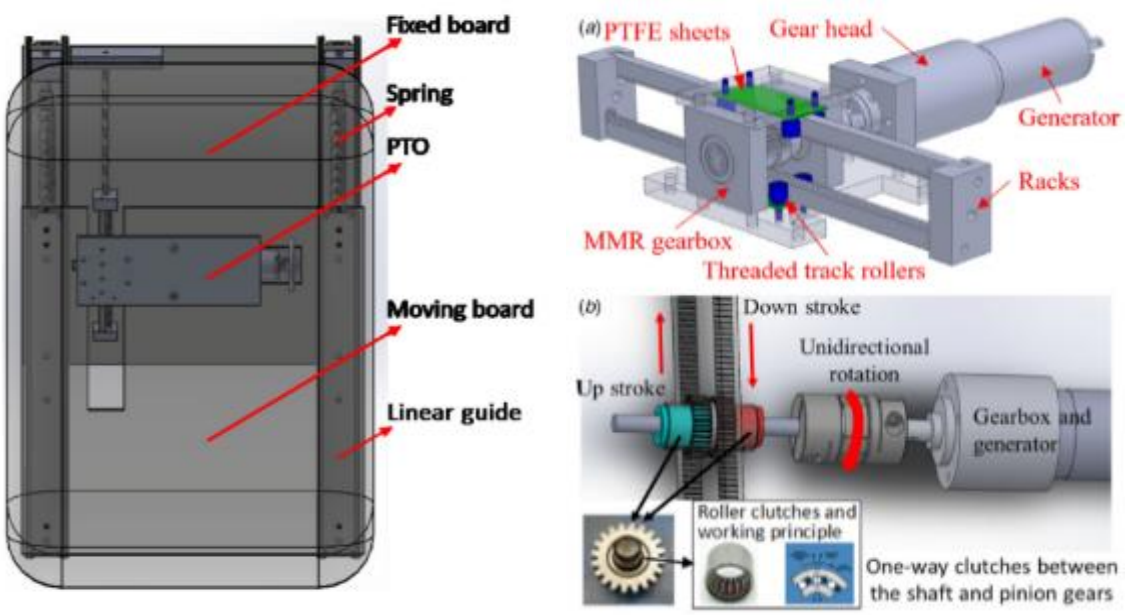

Figure 2-20 Wearable energy harvester design by Y. Yuan [9]

This improved the power outputted of a backpack energy harvester by reducing the internal mass needed by the harvester, in order to rotate the mechanical electro-magnetic transducer. Here the researchers reduced the mass to 13.6 kg and produced 3.3 W of electrical power. This shows that mechanical-electro-magnetic transducers have the potential to produce Watt levels of power from a wearable energy harvester but do require large forces on the input side to generate these power levels.

The lower limb harvester mentioned in section *2.1.2,* also used a mechanical-electro-magnetic transducer to generate their recorded power levels of 3 W. Here the leg movement was captured by pull cords strapped to the feet which rotated an input gear. This rotated the transducer at a higher velocity by using an up-ratio gear train at the ratio of 1:5.

Mechanical-electro-magnetic transducers produce a higher voltage output, with a higher velocity of the magnets passing the windings. This was

confirmed by researchers that used mechanical-electro-magnetic transducer for energy harvesting. Most were from to use an up ratio gear train before entering the transducer, [11]–[13], [93].

The adverse effect of using an up-ratio gear train before the transducer is the increased torque required to rotate the transducer. Increasing the velocity into the transducer, also increases the torque needed by the transducer in order to start rotation and sustain momentum.

The backpack design by Y. Yuan used a 1:33 ratio gearbox to increase the velocity into the transducer and the work by Q. Li, on their Knee joint harvester used 1:113 ratio gear train to increase the knee angle change velocity into larger angular velocities for the mechanical-electro-magnetic transducer.

2.2.6 **Summary**

After researching into different types of transducers that could be used for wearable energy harvester applications, it has been confirmed that a number of the transducers mentioned will not be able to generate a high enough power output to charge a smart phone or tablet.

For example, piezoelectric and thermoelectric generators are producing mW levels of power. They have the advantage of being lightweight, small and in some cases flexible, but are not able to produce the power needed for this research project there by making them redundant. The same can be said for triboelectric and vibrational-electro-magnetic harvester designs to date. Some novel designs were seen aiming to improve the energy transformation from waste energies from the human body into useable electric power.

The mechanical-electro-magnetic transducers have the largest power outputs of wearable energy harvesters, in some papers it was shown to be hundreds of times greater than other transducer styles. They have also been proven to produce Watt levels of electrical power from a few wearable energy harvester designs.

It is clear from this section of research, that mechanical-electro-magnetic transducers could charge portable technologies such as smart phones and tablets and will be the transducer of choice going forward investigating wearable harvester's designs for harvesting from humans.

2.3 Wearable Energy Harvester's Comparison Methods

From research performed so far a clearer idea of energy available and transducer method have been explored. It also came clear there are a number of different approaches to comparing ones work to fellow researches. In this section explaining the different ways researchers have gone about comparing wearable energy harvesters to each other's work will be presented.

2.3.1 Power to Weight Ratio

The power to weight ratio (PTW) is used as a comparator in the automotive and transportation industries [94]–[96]. It is an important figure for these industries as it will determine how much of the power is used in moving the weight of the power unit and its assembly. The ideal figure here is a high power to weight ratio. This will mean that the power source is capable of doing one of two things; increase capacity or load (lorries, trucks, trains, and planes) or increase acceleration (cars, bikes, and rockets). This is shown in equation 2-3.

$$PTW = \frac{Power\ Generated}{Final\ Assembled\ Weight} \qquad (2\text{-}3)$$

This ratio could be used as a useful comparator for wearable energy harvesting. Comparing different harvesters by their power to weight ratio would aid in seeing how a heavy but powerful harvester compares to a lightweight and low power harvester design.

For example:

- Harvester 1 has a weight of 2.3 kg and a power output of 1.5 W.
- Harvester 2 has a weight of 0.03 kg and a power output of 0.025 W.

Looking at these figures, it is hard to see which would be more effective as a wearable energy harvester. If a design was needed where a wearable energy harvester needed to produce an output power of 1 W, which harvester design would be better to develop?

- Harvester 1 has a power to weight ratio of 0.65 W/kg
- Harvester 2 has a power to weight ratio of 0.83 W/kg.

By taking the target power (1 W) and dividing it by the power to weight ratios, the weight of the developed harvester's design when generating this power would be known.

- Harvester 1 generating 1 W would weigh 1.5 kg and
- Harvester 2 generating 1 W would weigh 1.2 kg.

For this example, harvester 2 shows a better ability at producing this power level for a lower weight. This confirms this as a useful way of predicting a harvester's weight, when aiming for a higher, or set power outputs.

The drawback to this comparison is that it does not take into account size, energy input method/ increased human energy consumption, and harvester location for use in a wearable design. If harvester 2 was originally inside a shoe, enlarging the harvester to produce this degree of higher power will ultimately result in the harvester no longer being able to be placed in its original position. One could assume it would also be very uncomfortable.

2.3.2 **Normalized Power and Normalized Power Density**

Normalized power was an early way of comparing energy harvesters to each other. This was first found in research by P. D. Mitcheson published

in 2006 [97]. The research here calculates the normalized power from a number of devices by normalizing the frequency in this case and comparing them to each other in terms of frequency input. Figure 2-21 shows the graph the researchers produced using this method.

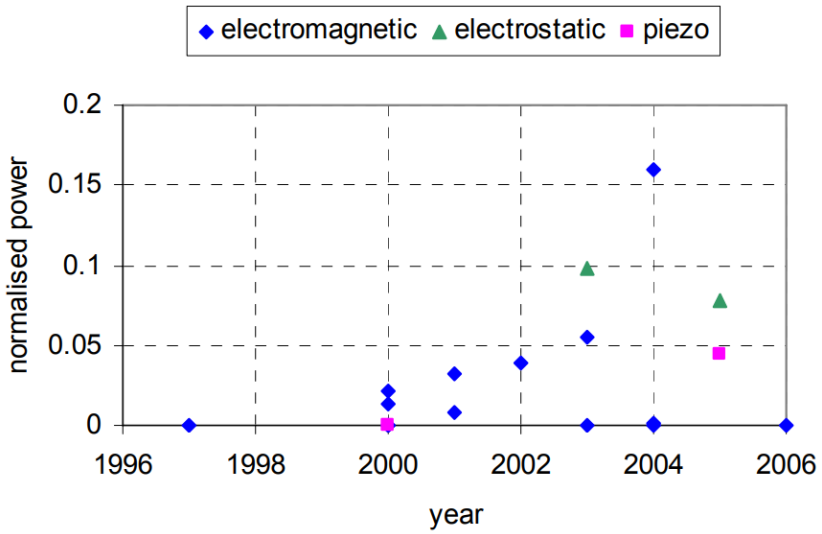

Figure 2-21 Normalized power vs year of publication by P. D. Mitcheson [97]

This graph is useful as it shows a trend of power increasing year on year, which might not have been evident if normalized power wasn't calculated first. The research continues to compare the same group of devices in terms of volumes, this was the first reference found referring to a normalized power density. In 2007 S. Beeby released a paper looking into an electromagnetic generator for vibration energy harvesting [71]. Here the researcher compares another group of harvesters with their normalized power density over volume of the devices. The author chooses to normalize the harvester by acceleration input and by doing so give a different picture of what might be the best harvester.

Normalized power density as a comparator works well for vibration harvesters and provides a way of comparing them in a number of different ways. One of the reasons this is not suitable for wearable energy harvesters as the inputs are from a human and not a consistent or known input. When

harvesting from a living being, one must be careful not to harvest so much energy so that it effects or depletes the energy levels of the subject. This was found and presented earlier in section 2.1. From research found normalized power density does not provide a clear value of harvester's performance or versatility so will not be used as a comparator for this research.

2.3.3 **Cost of Harvesting**

Cost of harvesting (COH) was first found in research by Q. Li published in 2008, [37], but doesn't go into too much detail. Their later work published in 2009, creates an equation corresponding to the one seen in equation 2-4.

$$Cost\ of\ Harvesting\ = \frac{\Delta MET}{Electrical\ Power\ Generated} \qquad (2\text{-}4)$$

This takes the increased metabolic energy consumption (ΔMET) of the wearer and divides it by the power generated.

The cost of harvesting is the most commonly found way of comparing wearable energy harvesters [11], [10], [13] and [98]. It shows a good indication of how energy is going to be consumed by the wearer for carrying and using a wearable energy harvester. It will also show whether the wearer would need to carry more food supplies in order to overcome the increased metabolic rate. This is an important way of looking at wearable energy harvesters, if the harvester uses muscles to input the energy into the harvester. This is the case for the Knee-Joint harvesters where their energy input is taken from the knee joint rotation, which is powered by the leg muscles.

Footfall energy harvesters working from footfall forces and the ground reaction, do not use any direct input from muscles specifically. The input

energy comes from the foot to ground forces seen during walking or running. This means the increased metabolic energy consumption of the wearer is only due to carrying the device.

The obvious drawback to using the cost of harvesting comparison method here, is the fact it does not show how heavy the harvester is, or where the harvester is located, for the harvester to generate the power.

It has become apparent that a new way of comparing wearable energy harvesters to each other could be developed. The new formula will need to take all of the previous figures used and combine them into a new comparable figure. The important data to include in the new formula is as follows:

- Power generated
- Mass of harvester
- Increased metabolic energy consumption

2.3.4 **Summary**

Currently no one formula takes all of these factors into account. Each formula found in research has its strengths, but also have their drawbacks. In Chapter 6 - *Comparing Wearable Energy Harvesters,* an investigation into a new comparator for wearable energy harvesting research is presented.

2.4 High Power Wearable and Footfall Energy Harvesters

Here the most powerful wearable energy harvesters that have been found that involve walking movements or footfall forces are presented. This should help with conceptualizing the forces, velocities, and powers, which were found during previous research projects and how it can be used here to help develop a new wearable energy harvester design.

2.4.1 Watt-Level Wearable Energy Harvesters

The backpack harvester designs have the highest power outputs of any wearable energy harvester to date, with the maximum power level from a wearable energy harvesting being from L. C. Rome's work in 2005 where the researcher's published 7.4 W of power from walking [13]. To get this power level the wearer does need to carry a 38 kg load in the backpack, not very useful for everyday life. Next, the bio-walk harvester for harvesting knee joint angle change by Q. Li in 2008 published a power level of 4 W [37]. This harvester requires having two large leg braces strapped tightly around the legs, with a pivot at the knee joint. This harvester weighs 2 kg, 1 kg per side. This would feel heavy when picked up, but once strapped on to the legs, the weight would be distributed and would be not be as noticeable. The final harvester that is worth mentioning due to having a high power output, is the lower limb harvester design by M. Shepertycky in 2015 [12]. Shepertycky published a power output of 5.6 W. This figure is later reduced in the paper to say under normal walking conditions and not increasing the load on the wearer significantly, the actual power output is 3 W. Still a very high output for a wearable energy harvester.

Though these energy harvesters do need the wearer to be walking for them to produce energy, they do not get their energy from footfall. One uses the centre of gravity movement of the wearer (backpack designs), another uses the knee joint rotation (Bio-Walk) and the final one uses the leg swing of the wearer (lower limb harvester). All of these designs stand out. They have paved the way in wearable energy harvesting technologies, and all have the potential to charge a portable electronic device, yet none of them demonstrate the harvester doing this.

2.4.2 **Footfall Transducers and Harvesting Approaches**

The forces seen in footfall show a clear area as a potential for providing high enough energy extraction levels required for charging portable electronic devices such as smart phones. Therefore a more detailed look into this area will be presented here. This section was used to show areas where researchers had not looked at harvesting footfall or the drawbacks they found in their designs.

The highest power found from a wearable footfall energy harvester is by L Xie published in 2015 and reports a power output of 0.8 to 1.35 W depending on walking speed. They continue on to state, when connected to charge a phone the harvester produced 5 V at 100 -150 mA, this being lower than the power output from the harvester at 0.5 - 0.75 W. Plus the author doesn't say what walking speed this is tested under. Unlike the three harvesters mentioned in the previous section, this design is fitted into a shoe and cannot be swapped to a different wearer unless the users are willing to share shoes, which is not advised. Being fitted in a shoe will also reduce the comfort of the shoe. The next highest footfall harvester found that shows strong research

methodology was by J. Hayashida, and published in 2000 [30]. The author reports the design of a small lightweight wearable energy harvester that produces 59 mW. Again, this harvester design was designed to fit inside a modified shoe (sports trainer). This restricts the potential energy extraction due to the limited space available, and in turn reduces the size of the mechanical components. This means the components will have a maximum power transfer before failing.

Looking at the three designs that produced multiple Watts of power, it is clear that for a prototype wearable energy harvester, the weight of the device will be in the kilogram range.

Part of this will be down to needing reliable results and an energy harvesting design that can consistently be used to test and confirm proof of concept. Adding in a high factor of safety for reliability will in turn increase the weight of the harvester. Future developments of the wearable energy harvester design, that concentrate on reduce weight could be looked into after the research stage has confirmed energy extraction approach.

2.5 Conclusions

From the research performed for this chapter, a number of key points can now be made to support the next step of the research methodology.

Not all areas of available energy will be suitable for charging portable devices such as smart phones as their available power will be too low for the requirements of charging smart phones and tablets. An area that shows promise for having spare energy is that of human footfall. An energy harvester designed to harvest the movement of the foot moving towards the

ground could produce enough power to charge today's modern portable electronic devices such as smart phones and tablets.

From research found it can be seen that a design of a retrofit wearable energy harvester that can be removed if not needed or given to someone else for their charging needs would be a novel contribution to the energy harvesting community. This is another point that has not yet been explored in research, along with the aim of Watt-level electrical power output from a footfall energy harvester. Current designs of footfall harvesters generating Watt-level power found were few, and none were retro-fit designs. Alongside this, a one-size-fits-all seems to have not been researched; the designs found are aimed at being fitted in a shoe of a particular size, or using the force input of a particular mass of subject. This means there is a research opportunity for testing a design that could be used by anyone, no matter their size or weight, and removed when not needed.

Current methods of comparison between wearable energy harvesters don't give a clear indication as to what makes a good, useful, or feasible energy harvester. From the research found, the methods used by researchers are useful for their own research project and helps them promote their device or design. This however does not give a fair comparison between any type of wearable energy harvester, no matter what the size, location, input method, power target, or research objective. This will be investigated and explored later in this work.

This list of bullet points was created after completing the background research, with the intention to set the final research aims and objectives, in a more detailed fashion under the broader title of wearable energy harvesting.

- Design new method of extracting footfall forces
- Must be wearable and real
- Produce a Watt-level of power for charging modern technologies
- Must be easily removable (retrofit)
- Can be used by anyone (one-size-fits-all)
- Output power via a USB port
- Examine a new method for comparing wearable energy harvester

From the others research presented in this chapter and the list bullet points above, a clear path for this research to take has now been establish in order to create a novel wearable footfall energy harvester.

Chapter 3 Design Requirements and Parameters for Footfall Energy Harvester

In this chapter, how the energy can be extracted from footfall will be explored, along with the thought procedures used to optimize the design of a watt-level wearable footfall energy harvester.

Firstly, there is a detailed look into the human gait cycle and when the energy is available, followed by an investigation into ideas of how to maximize the extraction and conversion of this energy into electrical power. This chapter will also present the data collected from modern portable electronic devices and the charging requirement as well as current forms of portable power sources. This will aid in the understanding of the power requirements the wearable energy harvester will need to produce. This chapter will finish with how the gait cycle of a human was replicated for use in the experiment.

3.1 Human Gait Cycle Analysis

Here a more detailed look into the movements of the foot during a single gait cycle will be explained. Figure 3-1, shows one complete gait cycle and the right foot will be the main focus. It can be seen from this figure that the foot to ground force is only available for part of the cycle. This is from right initial contact to right foot off, (stage 2 – 6).

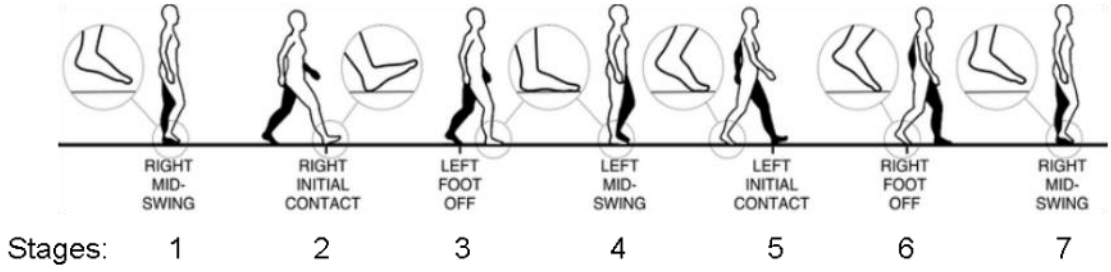

Figure 3-1 Re-ordered human gait cycle layout with numbers identifing the key points

What this figure doesn't show well, is the position of the foot relative to the ground. To help clarify the key points at which the cycle needed to be investigated in more detail, an illustration was created to aid in this analysis and is shown in Figure 3-2. From research, it was found that one cycle occurs once per second, per foot, for normal walking. Fast walking was reported to be up to double normal frequency and slow walking as low as half a normal rate. This means the upper value used as an input frequency will be 4 Hz, (2 Hz per foot, using both feet as input) and the lowest will be 0.5 Hz (0.5 Hz, one foot input only) [15], [99], [100].

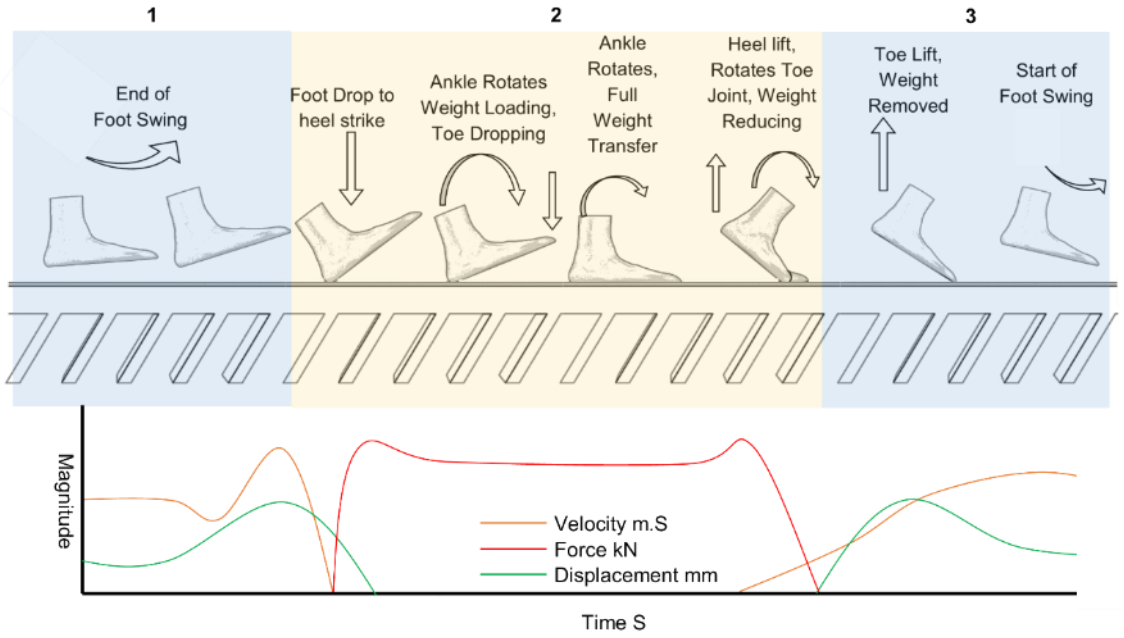

Figure 3-2 Foot movements during a standard gait cycle

Figure 3-2 shows one complete cycle for the right foot of a human. This helps show the distances and angles of the foot sees relative to the ground. Section 2, the yellow area, is where the majority footfall energy harvesters target. At the start of section 2 the foot comes into contact with the ground and this point is called heel strike. From the research found, it is at this point where maximum vertical velocity differences are seen and is also where the foot to ground force starts.

The foot has been in swing, and at the end of this swing the foot is moved quickly towards the ground. The foot stops moving vertically suddenly at the heel strike. Research found a vertical foot velocity of 0.1 to 0.4 m/s is seen at the end of the mid swing up to heel strike but is dependent on walking style. This figure appears to change most depending on terrain. Humans move their foot towards the ground at a slower velocity if they are uncertain about the ground reaction, e.g. when walking on sand, foot velocities are slower than when on solid flooring or a hard pavement. This is also true about displacement. The foot displacement from the ground varies hugely depending on terrain and environment. For example, if the floor is slippery, humans tend to lift their foot as little as possible, whereas on grass or sand, humans over-compensate by lifting their floor higher than needed. This under and over lifting results in a foot to ground clearance of between 0 mm when dragging along a slippery floor to over 50 mm when on grass or on soft sand.

In Figure 3-2, the conditions that the foot undergoes during one gait cycle are shown. The vertical foot velocity shown in orange, and the foot to ground displacement shown in green both turn to zero during section 2. This is due to the foot being in contact with the ground. Due to the heel being in contact with the ground, the dropping of the toes in section 2 is seen as the foot applying more pressure to the ground, rather than foot to ground movement.

The foot force is a measurement of the ground reaction force seen by a human placing their foot on the ground during normal walking on a hard surface. The biggest factor affecting this value is the mass of the human subject. The heavier the subject, the higher the maximum value seen. As this wearable energy harvesting research project is aiming for a “one-size-fits-

all”, the harvester must be designed so that any weight of human can use it. No upper limit will be set, but a lower one might be needed to ensure safety of the wearer using it.

3.2 Key Parameters for Harvesting Energy from Human Footfall

After studying the human gait cycle and the foot movements, it is clear there are four parameters that will affect how much energy is available and it turn how much power a wearable energy harvester could produce.

The four main factors that will affect the design and the maximum energy harvested have been identified. These are as follows;

- Footstep frequency
- Foot to ground clearance
- Foot vertical velocity
- Foot force

3.2.1 Foot Frequency

Footfall frequency is the most influential condition on the average power generated by the harvester. The more inputs the harvester sees in a given period of time, the higher the average power will be. It was found in research from a number of different areas, that an average person walking at a normal walking speed of 5.4 km/h has an average step frequency or cadence of 2 Hz. This means one step per foot, per second. This will be set as the normal frequency condition for the first harvester design. The velocity the humans walks or moves at affects the step frequency recorded. When walking fast at 7.8 km/h, a cadence of 2 Hz is seen per foot [15], [99], [100].

Table 3-1 was created showing the different frequencies and the input conditions used.

Table 3-1 walking speed relitive to footfall frequency

Walking Speed km/h	Step Rate (both feet) Hz	Input condition per foot Hz	Walking Speed and Harvesting From
3.6	1	0.5	1 foot, slow walking
5.4	2	1	1 foot, normal walking
5.4	2	2	2 feet, normal walking
7.8	4	4	2 feet, fast walking

3.2.2 **Foot Displacement**

The foot displacement needs to be considered in order to be sure that the harvester design will not trip the wearer when walking. The maximum input displacement that the harvester design could incorporate to maximize power extraction, was found here. The foot clearance to the ground changes during the gait cycle. When the foot is swung though the mid-swing of the gait cycle, an average maximum ground clearance of 50 mm for the heel is seen and 100 mm clearance for the toe [15], [99]–[102]. In Figure 3-3 an average foot displacement curve is shown relating to a single gait cycle.

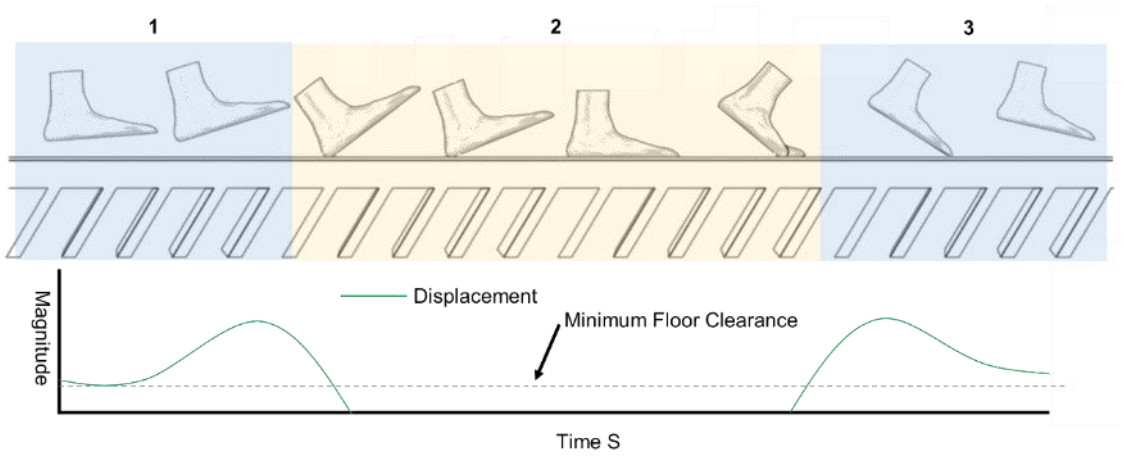

Figure 3-3 Maximum foot displacement during a normal walking gait cycle

It was found that the heel gives the lowest clearance during the mid-swing whereas the toes have the largest clearance just before section 2. What is important here is the minimum floor clearance seen. The minimum

floor clearance will denote the maximum input displacement that the harvester design could protrude below the shoe line before intruding on the wearer's walking style.

As the minimum floor clearance depends on walking style, shoe type and terrain, researchers have studied this in different ways depending on their research goals. It is hard to suggest a minimum foot to ground clearance, as ultimately this is always moving towards zero when the foot is in contact with the ground.

Research into trip hazards conducted by the biomedical research community found that a minimum foot to ground clearance is measured during the mid-swing and is reported to be 50 mm [15], [99]–[102]. If the average minimum floor clearance is 50 mm, a maximum input displacement of 40 mm will be set to ensure the harvester design does not affect the wearer, or cause a trip hazard to the wearer by snagging the floor during the mid-swing.

After the initial footfall research, an optimal area for the harvester input mechanism was found. The Figure 3-4 shows the optimal input location for a footfall harvester where the input mechanism is located below the sole of the shoe.

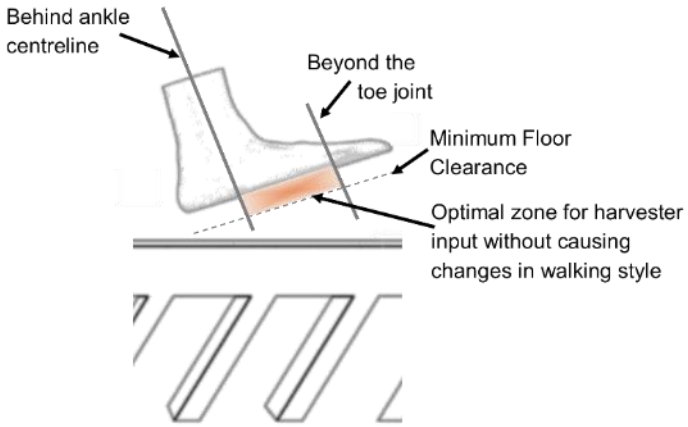

Figure 3-4 Optimal extraction zone under a humans foot

3.2.3 **Foot Force**

The maximum foot force seen during walking starts at heel strike and ends when the foot is almost flat on the floor. The accrual figure is simply dependent on the maximum weight of the subject. The heavier the subject the higher the maximum force seen. As this is a retro-fit, one-size-fits-all harvester, the design needs to ensure that lighter wearers will be able to use the harvester and the resistance generated by the harvester is never greater than the minimum force the lightest wearer could input.

Setting a minimum user weight will be helpful in the design of the harvester. It was found in research that a 12 year boy should weigh 40 kg [103]. Using the data found in research it can be predicted that the maximum foot force seen during normal walking would be 432 N. Setting this as a minimum input required would still mean that a wearer weighing 40 kg would struggle to wearer a footfall harvester requiring this force input and would most definitely affect their walking style. This means setting a factor of safety on this figure to ensure that any wearer above the age of 12 years of average weight would be able to use the harvester.

A figure of 300 N will be set as an acceptable maximum input force for using any footfall harvester. By using 300 N as a lower limit a factor of safety of 1.44 is calculated. This is to ensure the wear is safe at all times using the harvester, even if they are at the lower end of the advised age and weight. This will also mean that any adult wearer will be able to use the harvester, and the design will not impact their walking style by restricting their foot movements.

When testing the harvesters in laboratory conditions, a load cell will be used to measure the force seen from the harvester receiving an input. This will ensure the device does not go over the 300 N limit.

The input force will not be a controlled, it will be recorded by the load cell installed in the laboratory equipment being used. As long as the harvester does not record over 300 N, the harvester will be deemed as fit for all adult wearers.

3.2.4 **Foot Velocity**

From research published by C. Kai-Jung in 2005 [20], and work published P. R. Cavanagh in 1989 [104], when humans change their walking speed, they also change their footfall frequency. This means that the horizontal foot velocity must increase with the increase of frequency. Horizontal foot speed is not important for the research project only the velocity of the foot moving towards the ground, vertical foot velocity.

From research it is shown that humans don't vary their vertical foot velocities greatly during different walking speeds. The biggest change occurs when humans start to run. At this point both feet are off the floor and the velocity is from gravity. As this research project is looking into harvesting from walking, the running footfall velocities will be ignored.

Vertical footfall velocities range from 0.2 to 0.4 m/s, [19]–[21], [104]–[106]. The lower 0.2 m/s foot velocity is seen during slow walking at 3.6 m/s, whereas the 0.4 m/s is seen during high speed walking at 7.8 m/s. This shows that there is going to be different amounts of energy available from footfall depending on the foot vertical velocity.

This means that the harvester needs to be able to harvest at slow input velocities as well as high velocities. This also shows that the design will need to withstand rapid acceleration of components under high speed walking, but then not restrict the footfall when walking at slow speeds.

3.3 The Displacement and Torque Relationship

From the previous chapter, it was decided that an Electro-Magnetic transducer is going to be used for this wearable energy harvester's research project. This will be in the form of a small lightweight electric motor. In order for the motor to transfer the mechanical energy into electricity, the motor will need to receive an input torque and angular displacement of the motor shaft. When converting from a linear displacement to a rotation movement, a number of variables will affect the transfer properties and the resultant outputs. One of the most common methods to conversion from linear to rotational movements is the rack and pinon system. The dimensions of the rack and pinon gears will denote the transfer properties. The torque generated and angular displacement are directly linked. Increased torque will decrease angular displacement and vice-versa. Shown in Figure 3-5 a) is an example of a rack and pinon system with the key parameters labelled.

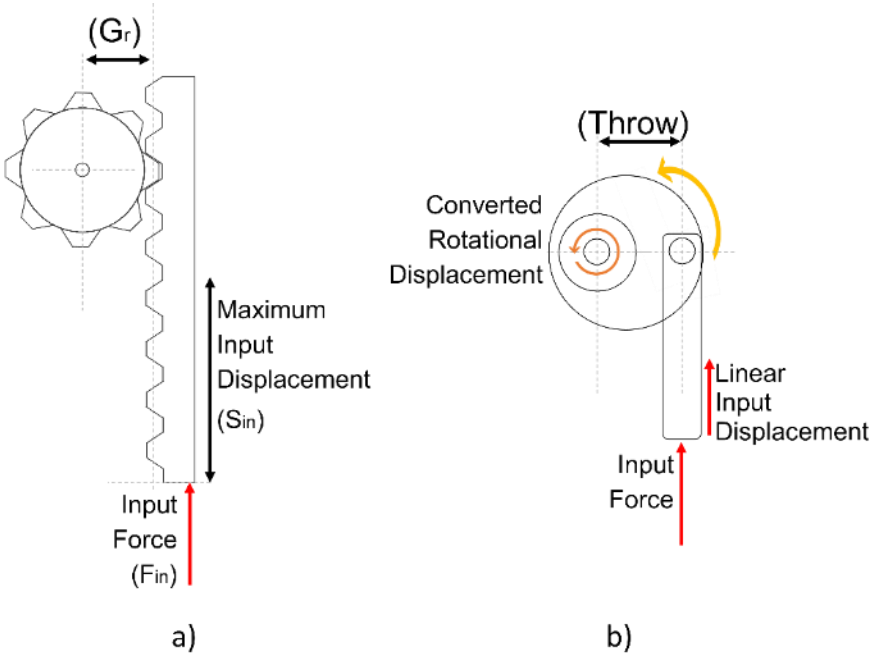

Figure 3-5 Linear to rotational examples: a) Rack and pinon system, b) Crank and connecting rod system.

The torque to displacement relationship is also seen in the "crank" design of movement conversion, Figure 3-5 b). The longer the throw on the crank the larger the torque, but the lower and slower the angular displacement. Crank designs also are limited to a maximum rotation of the crank before the input needs to reverse direction. The torque generated on the pinon or crank shaft is equal to equation 3-1.

$$T = G_r \cdot F_{in} \quad (3\text{-}1)$$

And the angular displacement is equal to equation 3-2.

$$\theta = S_{in}/G_r \quad (3\text{-}2)$$

It can be seen increasing Gr will increase torque but lower the angular displacement. This relationship can be used to control the maximums of both parameters transferred into the harvester. By simplifying the crank design to a direct drive system, the angle change from a linear displacement could be controlled.

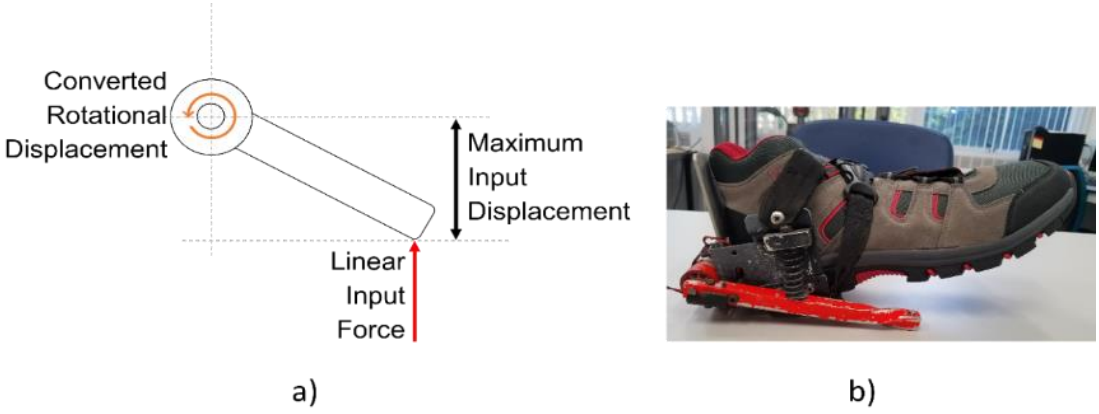

Figure 3-6 Final energy extraction method: a) Technical illustration, and b) First prototype proofing concept

Figure 3-6 shows the final input design and quick rough prototype to confirm proof of concept. The prototype confirmed that the input mechanism was going to work in an optimal way without impacting the wearer's walking style and proved to be a reliable way of converting the linear force seen from footfall into a rational movement needed to drive an up ratio-gear train.

Torque and angular displacement are in a trade-off. Increases one decreases the other. As shown earlier the maximum input displacement (linearly) is set at 0.04 m and the maximum input force is set to 300 N. By changing the length of the input bar both torque and angular displacement are effected.

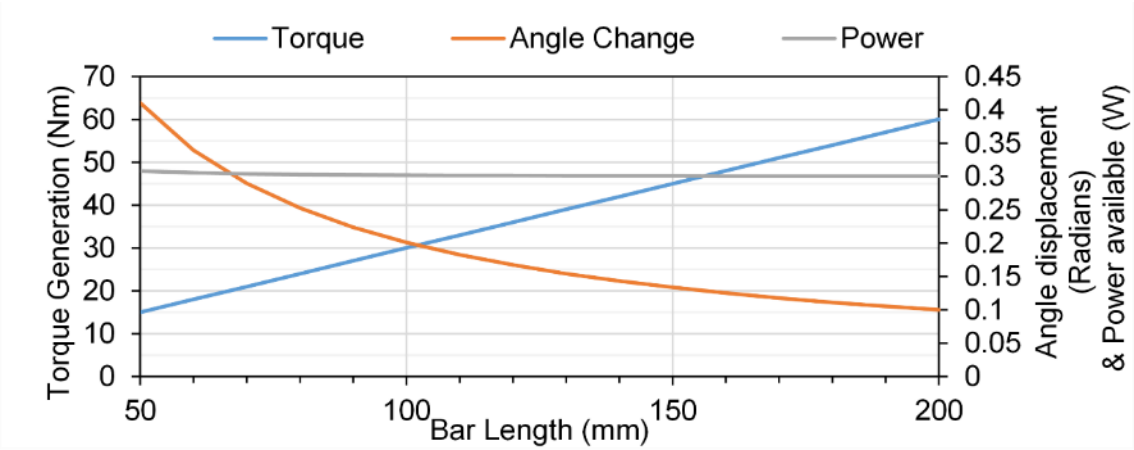

Figure 3-7 Torque Vs angular displacement and available power

Figure 3-7 shows this relationship clearly. With a 100 mm input bar length, the greatest torque and angular displacement are seen. It will be this length of input bar that will be used as a starting point for the design stage.

However even though these appear to be in a trade off and changing one might decrease the other. The input power into the system is the same. If the input bar is moving at 0.4 m/s (high footfall velocity), the power available can be calculated and is also shown in Figure 3-7.

As the torque generation increase the angular displacement decreases, and this results in only a very small change in available power inputted into the harvester. This can be seen to be true in Figure 3-7 where a change of 150 mm in bar length only changes the power available by 0.00757 W.

Using a 100 mm long input bar, 40 mm foot displacement, and a 300 N input force, this will give 30 Nm torque and 11.5 degrees in angular displacement when the foot is placed on to a hard surface. These figures can now be used to start specifying components in the following chapters.

3.4 Portable Electronics and their Charging Requirements

In this section portable electronics will be explored. This commences with an investigation into what the most common devices in use in today's modern world are (2017). It continues to look at the requirements these devices have with regards to charging, and the energy storage capacities held within them. This should result in a minimum power needed to be harvested from a wearable energy harvester in order to charge a modern portable electronic device such as a smart phone or tablet.

3.4.1 **10 Portable Technologies Sold and Used In 2017**

After searching online and looking at hundreds of websites surrounding portable electronic devices a simple list was created and is shown in Table 3-2.

Table 3-2 Modern portable devices list compiled in January 2017.

Type	Device Name & Manufacture	Energy Stored (mAh)	Available Power (Wh)	Charge Time 0-100%	Charging power (W)
Tablets	Google pixel C	9000	34.2	4h	10.4
	Samsung galaxy tab S2 10.5	7900	30.2	4h40m	10
	Apple iPad pro 9.7	7306	27.0	3h50m	12
	Sony Xperia Z4 Tablet	6000	22.2	4h	10.4
	Apple iPad mini 4	5124	19.0	3h10m	18
Smart-phones	Samsung galaxy s7	3600	13.7	1h40m	10
	Google pixel phone	3450	13.1	1h15m	5
	Motorola moto G4	3000	11.4	1h50m	5
	Apple iPhone 7 plus	2900	11.1	3h15m	10
	Apple iPhone 7	1960	7.6	2h10m	10

A number of trends can be seen in Table 3-2 which can help confirm the power output needs of a wearable energy harvester. It is clear to see that tablets have larger battery capacities than smart phones which in turn gives them a higher available power.

With a larger battery, a longer charge time will be needed, and this is also confirmed by the data in Table 3-2. Table 3-2 shows what the manufacturers' state as maximum charging limits. This limit is down to the battery construction within the device, rather than capacity. It can be said that most current lithium batteries are limited by a maximum charging power limit. This means that they will have a minimum time within which they can be charged in and any attempt to hasten this, will result in the battery becoming unstable, if not dangerous. If the charging limit is ignored and the portable battery is charged at a higher power, it will mean that the battery will

not last as long as the manufacturers expect and will require more frequent charging, as the battery's health deteriorates.

Most modern portable devices are designed to be charged from a USB port and all of the technology listed in table 2 charges from a USB cable. The photo in Figure 3-8 shows a multi-charger or universal USB charging lead. These are designed to connect to any USB port capable of charging and then connect to a range of portable devices. This shows how many different types of charging connections there are. The only consistence connection is the USB. Because of this a USB port will provide the power output from the harvester designs.

Figure 3-8 USB universal charging cable

A USB port is regulated to output 5 V and depending on its power supply, 0.02 – 2 A. This results in a maximum power output of 10 W. This in lines with the maximum charging rates of some of the technologies listed in Table 3-2.

A standard computer found in the office or home will have multiple USB ports and in most cases they output at 5 V and 0.5 A. This is a power delivery of 2.5 W.

As an example, the Motorola moto G4 has a battery capacity of 3000 mAh and if this smartphone battery was to be charged from a standard computer USB, it would take 6 hours to charge from flat to full.

Whereas the Google pixel C has a capacity far larger than the Moto G4, and would take 18 hours to charge from a computer USB port supplying the same 2.5 W.

This shows that the time it takes to charge batteries or portable technologies changes depending on the size of the storage (battery capacity) as well as power supplied.

Batteries are however very complex things and what might take 6 hours to charge from flat to full one day, might take 7 hours the next or even 5 hours the following day. These variations in time come from a number of factors such as, battery temperature, battery age, or previous charging cycles and of course power supplied to the battery. This makes it very hard to state how long a battery will take to charge.

The second contributor to battery energy confusion, is trying to understand when a battery is “flat” or empty? This would depend on the battery and its intended use. An AA battery (LR6) used in a remote control will stop working generally when the battery voltage drops below 0.8 V. Considering that the battery’s full voltage is only 1.5 V at best, the battery is still over half full, yet is no longer able to perform. This means that simply measuring a batteries voltage should provide enough information to be able to state whether the battery was at 50% or 75% full.

Modern lithium-ion batteries state a battery voltage of 3.7 V and this is standard across most lithium batteries seen from the research found. It was also found that most of these batteries are deemed as flat when their battery voltage drops below 3.1 V. At this point the device will turn off indicating a flat or empty battery in need of charge.

Because of the complications surrounding battery energy levels and the time taken to charge a battery changes can depend on a large range of factors; this work will only refer to power delivered to a portable device rather than energy stored or battery energy levels. Once a harvester design has shown a continuous power delivery at a high enough level to charge like a USB port power supply, basic tests will be done to prove the harvester's ability to charge portable technologies in terms of the device's storage level indicator.

Power delivery to charge portable devices changes depends on multiple factors. All of the modern portable electronic devices found could be charged from a USB port. A USB voltage is set to 5 V and this will need to be the output voltage of any harvester design, be it via a voltage regulator control circuit or the average transducer output voltage.

The power supplied to charge a portable device varies. The minimum power seen from USB charging ports is 0.1 W at 5 V and the maximum allowed by the portable electronic device is 10 W at 5 V. The higher the power from a wearable harvester, the shorter the period of time required for charging any device. A minimum target of 1 W average power generated will be set. This will provide a figure to start aiming for in the design stage.

3.4.2 **Portable Batteries as Power Supplies for Charging**

The most common form of portable power source is in the form of batteries. These can be small, lightweight and hold a large amount of energy, but once this energy source is depleted, the battery is no longer of any use. Battery technologies have been improving year on year, with storage levels increasing at the same time as the weight and size of the battery are

decreasing [107]. Today, a typical AA battery (E91 or LR6) holds around 2400 to 2900 mAh at best. This in energy, can be calculated by equation 3-3.

$$E = V \times I \times t \qquad (3\text{-}3)$$

Where, E is the energy stored, V and I are the batteries specified voltage and current and t is 3600 s to convert the hours into seconds.

This shows that a single AA battery with an average storage level of 2750 mAh has a maximum of 14,850 J of electrical energy available. From this, if the battery was used for a 1-hour period it would have an average power level of 4.1 W. After this point the battery is useless and, if being carried, is now dead weight. This is not a very accurate way of calculating energy within a battery as the voltage changes as it is used, but this is sufficient to be able to make comparisons here.

To keep recharging portable technologies such as a smart phone or tablet from AA batteries would result in having to carry copious amounts of batteries. This would cause the wearer to consume more metabolic energy from carrying the additional mass of the batteries. This means that using batteries to top up your portable technologies is acceptable, as long as you don't need to carry an unrealistic amount to sustain this.

Any situation where a user of portable technologies wants to charge their devices from flat to full, or maybe daily, for days at a time due to being away from a mains power source, would need to carry far too many batteries to be able to do this. This is where energy harvesters can take over.

For example the battery in a Samsung galaxy S7 has the following battery specifications:

Voltage: 3.7 V
Energy Stored: 3.6 Ah

To charge this battery using AA batteries would firstly require three batteries to be connected in series to produce a voltage greater than the smartphone battery in order for it to be charged. The amp-hours would stay the same. This results in using 10 AA batteries for each charge. Most smartphones and tablets need charging daily (broadly speaking), this would mean using 10 AA batteries per day to keep your portable technology going.

One common AA battery (Alkaline based) has a mass of 23 g, ten of these is of course 230 g. If the person needing to charge their portable technologies was going off grid for 10 days, this would mean carrying 2.3 kg of batteries. Imagine if the user was off grid for a few months, this would mean carrying somewhere in the region of 20.7 kg of batteries alone, not mentioning the extra food the user would have to carry to refresh their energy levels from carrying extra batteries.

From these basic calculations, it shows that using batteries for a few days is fine, but no good for longer periods away from normal or standard charging systems running from mains power (the grid). It is very hard to compare batteries to energy harvesters as a battery has a set amount of energy held within, whereas the energy harvester could produce power indefinitely. For the purpose of this research, investigation into batteries and usability for portable power will not be investigated any further as this research is concentrating on wearable energy harvesters.

3.4.3 **Wearable Energy Harvesters & Portable Power Generators**

Here the differences between wearable energy harvesters and a portable power generator will be explained.

Portable power generators have been available for many decades. They have been used for running communication and location systems from very basic old telephone systems to powering lights that aid search and rescue efforts. They are still around today and are now being used for charging portable electronics such as smart phones and GPS units. Figure 3-9 shows commercially available power generators. Here, the portable generators need a deliberate input of energy from the user, winding it by hand, and because of this are not deemed to be energy harvesters.

a) b)

Figure 3-9 Examples of portable power generators: a) Wind up torch by iGadgitz, and b) Wind up phone charger by ChinkyBoo

Research into these modern style portable power generators for charging portable electronic devices, has revealed that they are inefficient. From research, the power outputs from “off the shelf” portable power generators vary dramatically, and the data presented on websites is designed to promote sales, rather than scientific results or figures.

Due to not being able to find data on energy expenditure of the user of these devices, comparing them to energy harvesters is redundant and this type of portable power generators will not be investigated any further.

Wearable Energy Harvester Technologies are portable power generators that the user or wearer of the harvester does not need to change their normal activities or purposely expand energy in order to generate power. They work by transforming waste or spare energy from around a human's body into usable electric power.

To prove the advantages of one wearable energy harvester design over another, researchers have come up with a couple of different ways of comparing their work to previous designs and others power outputs. In the following sections, the meaning of these terms will be explained, alongside why considerations of a new format might be needed.

3.5 Experimental Set Up

In this section input data used for the experimental setup will be explained and how this was used to ensure the experimental set up matched the data surrounding human footfall movements. The input frequency for normal walking has been found to be 1 Hz. This means the Instron will need to displace the harvester once per second for normal walking harvesting from one foot. Under normal walking a displacement of 40 mm is used and is moved at a velocity of 0.4 m/s. With these variables set, an input wave pattern was generated and is shown in Figure 3-10.

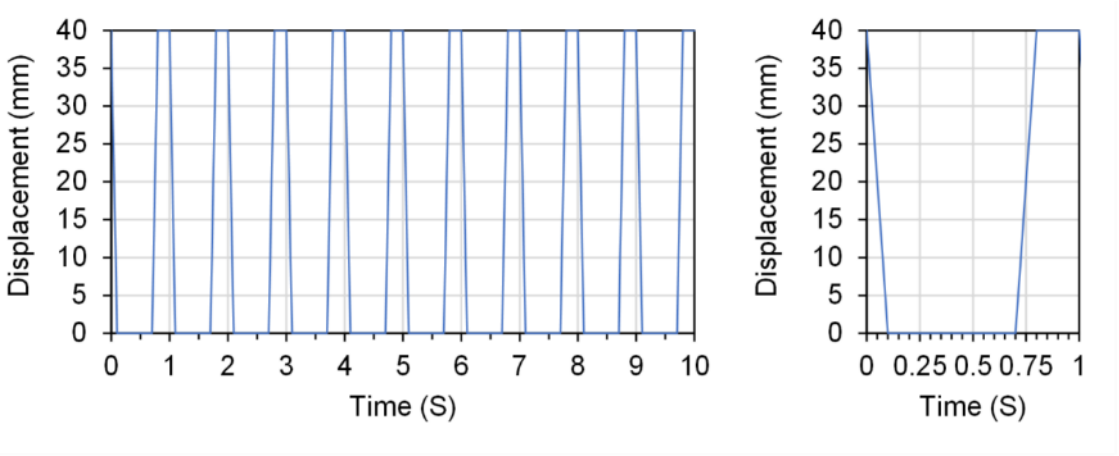

Figure 3-10 Normal walking wave function used to control the Instron machine in experimental testing at 40 mm displacement, 0.4 m/s vertical foot velocity and 1 Hz step frequency

The displacement, velocity, and frequency will be controlled and changed depending on the walking style being tested.

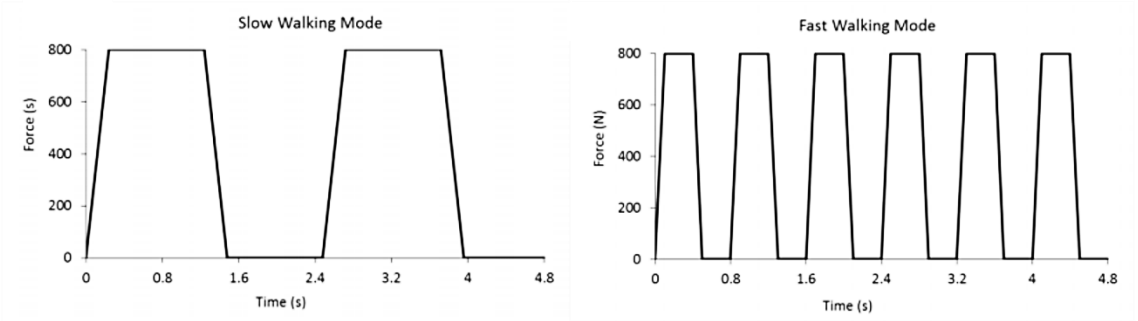

Figure 3-11 Force graphs used for testing a footfall energy harvester by Z. Luo [108]

Figure 3-11 shows the wave functions used by Z. Luo published in 2015, [108]. Here the experiment is controlled using force as the input condition for different walking speeds. The force input stays the same, but the frequency changes and is seen in Figure 3-11 showing slow and fast walking frequencies.

Foot force will change dramatically depending on the wearers mass, and as the research project is intending on creating a One-Size-Fits-All harvester, force will not be used as the controlled condition. Instead the force reaction will be recorded on the Instron. These results will then be checked to insure the harvester does not create a greater reaction force than 300 N set in section 3.2.3.

The intron is set up to hold the harvester just above the ground plate as if the wearer was about to make contact with the ground, heel strike. When the wave function is started, the harvester is moved vertically down making contact with the ground plate as if the wearer was taking a step.

The velocity at which the harvester moves will changed from slow footfall velocity at 0.2 m.s to 0.4 m.s for normal and fast walking.

The displacement in which the harvester is moved will be set to 40 mm. The average maximum heel displacement seen during walking is 0.05 m (50 mm), and to ensure the harvesters input mechanism doesn't stag the ground or floor when walking a 10mm reduction will be applied to the maximum input displacement of the harvester.

The frequency of the foot step is a focus of this study and tests are performed at low frequencies seen during slow walking at 0.5 Hz, normal walking at 1 Hz, fast walking at 2 Hz. 4 Hz tests are to represent if a harvester was worn on both feet and the wearer was on a fast walk this will prove the maximum output from harvesting from both feet.

The final tests will be performed on a treadmill at the three main walking speeds and the power generated recorded. This should result in similar power generation as the Instron testing validating the Instron set up and the wave function.

The electrical connections from the harvester were connected to a variable resistor that could be set to different resistances depending on the electrical load required. A National Instruments data acquirer 9229 unit was connected to the resistor in parallel to measure the voltage across the resistor. LabVIEW was used to write a program that interpreted the voltage signal from the data acquirer log the voltage generation over time. The same

LabVIEW program was used to record all the data from all of the tests. By knowing the Voltage and the time, energy generation can be calculated via equation 3-4.

$$E = \sum_{i=1}^{n} \frac{V^2(t_i)}{R} \cdot \Delta t \qquad (3\text{-}4)$$

Where, E is the total energy generated, T is the time, V is the voltage generated by the harvester and R is the resistive load connected to the harvester The energy generated data can be used to calculate average power outputs(P_a) from the harvester via equation 3-5.

$$P_a = {}^{E}/_{T} \qquad (3\text{-}5)$$

The current generation (I) from the harvester can also be calculated by knowing the connected resistive load and the voltage generation from the harvester via equation 3-6.

$$I\,(t_i) = \frac{V\,(t_i)}{R} \qquad (3\text{-}6)$$

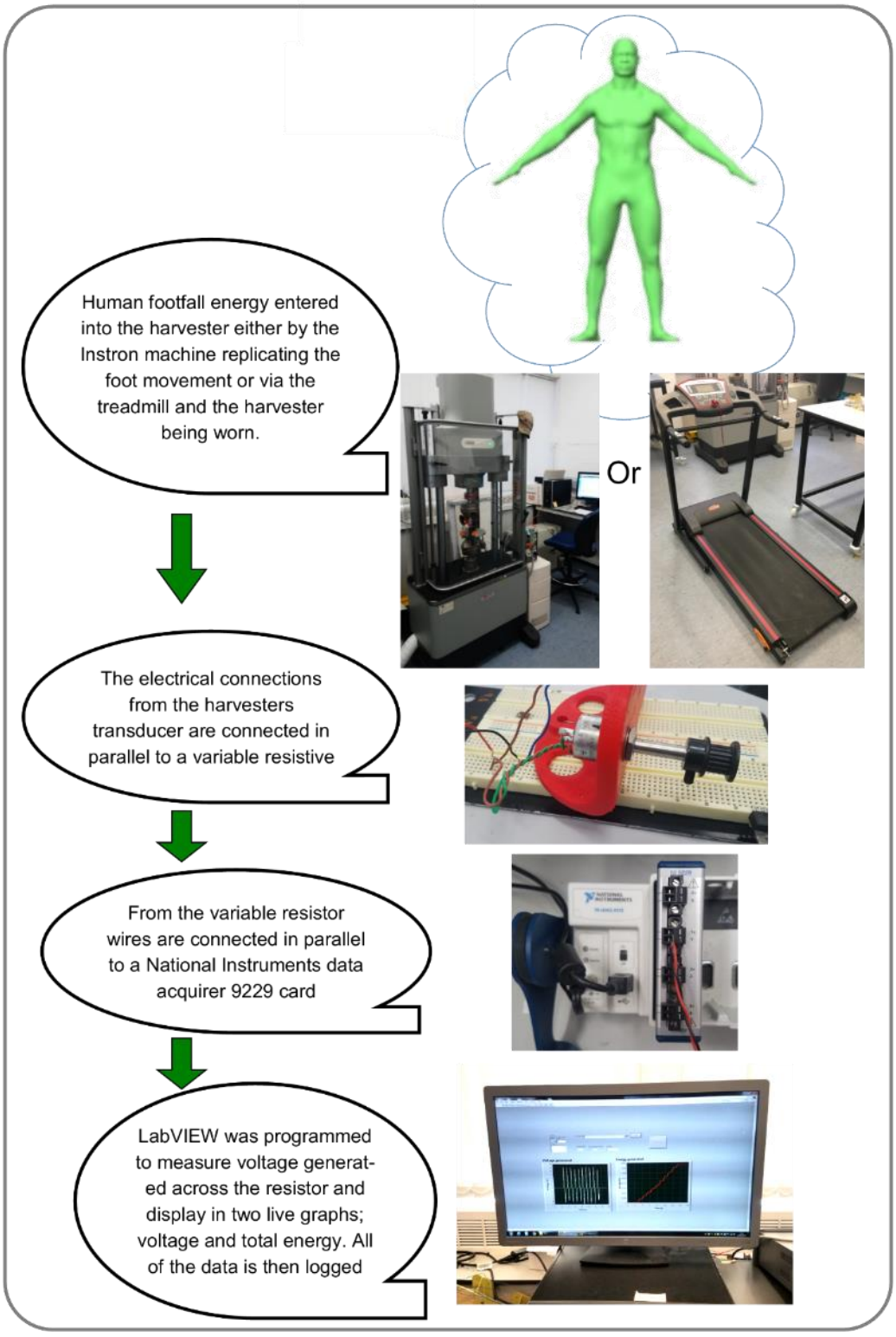

Figure 3-12 Testing set up flow diagram between harvester and data logging system

The flow diagram shown in Figure 3-12 represents the connections between harvester and the measurement system used to measure, record and analyse the harvester's electrical outputs.

A treadmill was used for the real world testing. The treadmill was programmed to move at the 3 main walking speeds via the on board computer. The speeds were set at 3.6, 5.4, and 7.9 km/h to represent slow, normal, and fast walking patterns respectively. The harvester prototypes were worn as intended whilst testing on the treadmill and data was recorded in the same method as shown in Figure 3-12.

3.6 Conclusion

Humans are all very different from one another and what might be little effort for one, might be unbearable by another. This means the harvester designs need to harvester the footfall force from the optimum input displacement zone. This will ensure the maximum input force and displacement are seen without impacting the wearer. From this, it can be said, foot force is dependent on the wearer's mass. This is not to be controlled due to all humans being different, only recorded and a limit of up to 300 N has been set. The harvester is designed not to require any more than this figure. The input frequencies or foot frequency affects the average power the most, but the harvester needs to work for any frequency. testing at multiple different frequencies will need to be performed. Foot displacement is limited by the minimum foot to ground clearance during the mid-swing, and an input limit is set to 40 mm to ensure there is no snagging of the input mechanism during normal walking as found in research. Foot velocities vary depending on walking style, speed and terrain. This means testing the harvester at different velocities to ensure the harvester works with them all.

All of the examples of portable devices shown in Table 3-2, had lithium-ion batteries installed, rated at 3.7 V and varied in charge times depending

on energy storage volume of the battery as well as power supplied. From research, a computer USB ports output 5 V at 500 mA which equates to 2.5 W of electrical power. This will be the target power to produce from a wearable energy harvester, though achieving a watt-level wearable harvester working from footfall forces will be a strong development in the field of energy harvesting. A USB port will be used as the outputting power connection from the harvester to ensure its use to as many portable devices as possible.

The experiments need to include a force reaction measurement to ensure the harvester designs are not going to impede on the wearer. This will be done using the Instron machines data logging system.

An input wave form replicating the vertical footfall of a human has been created and is used throughout the experimental work with the Instron machine. This wave function can be changed to match the walking criteria being tested at the time. A treadmill will be used for real world testing to confirm the harvester's electrical power output at different gait speeds. Along with providing evidences the Instron and wave functions are accurate.

After investigating optimization of energy availability from footfall here in chapter 3, a design list can be created. These designs must include;

- Extract footfall energy from the optimal input zone.
- Pivot/rotation point close to the ankle joint
- Produce voltage above 4 V to charge modern device, (5 V optimum)
- Average power above 0.5 Watts to charge at a reasonable rate

Chapter 4 Initial Design of Foot Mounted Energy Harvester

From the research found in the previous two chapters, a clear path is formed to now design and test the initial design of energy harvester. This chapter presents the initial wearable energy harvester design. The design is explained and laid out in phases of harvesting. As the user of the wearable energy harvester walks, the harvester will generate electrical energy that could be used for running or charging a number of portable electronic devices, such as sensors or GPS systems. The chapter will continue to explain the design, parameters and the equipment used in order for the harvester to tested and examined in our energy harvesting lab. The chapter will conclude with real life tests and how the harvester is optimized for use as an exchangeable wearable energy harvesting.

To help design thoughts, a table showing priorities of different aspects of the design was produced and is shown in Table 4-2. The aspects are listed in top priority order.

Table 4-1 Wearable energy harvester design priorities

Aspect	Priority
Produce enough electrical power to charge modern portable tech	1
Not affect the walking pattern of the wearer	2
Lightweight design	3
Ergonomic fitting	4
Be adjustable	5
Push wearable energy harvester expectations	6

4.1 Early stage concepts

From a couple of early stage prototypes investigating energy extraction methods from footfall forces, it was found that having an input mechanism towards the heel of the shoe, meant the input mechanism dragged along the floor during the mid-swing. These prototypes are shown in Figure 4-1.

Figure 4-1 Early stage prototypes experimenting with heel extraction area and methods

This showed that not only is the maximum input displacement important, but also the exact point under the foot at which this was captured.

The toes see the maximum displacement at the end of the mid-swing, but harvesting this is limited by the minimum floor clearance. When early design ideas were experimented with, it was also found that having an input mechanism towards the toes, resulted in a number of problems. One of these designs are shown in Figure 4-2.

Figure 4-2 Early stage prototype experimenting with toe extraction area and method

It was found in these early design prototypes that if the harvester input mechanism touches the ground before the heel, the wearer feels this, and it leads to an “unstable feeling”. To ensure the wearer of a footfall energy harvester doesn’t feel unnerved using the harvester, the input mechanism must make contact just after first heel contact.

4.2 Initial Harvester Design and Parameters

The harvester is designed to be exchangeable from wearer to wearer. This means the harvester will sit on the outside of the wearer’s shoe. For this research project the harvester is strapped to the back and side of the wearer’s right shoe. A wearable energy harvester that would be able to be used by most humans, has a large design scope. This meant a simple table was created to set some conditions to help start the design process. This is shown in Table 4-2.

Table 4-2 Design Considerations and Boundary Conditions

Scope	Problem	Solution	How
One size fits all	Must fit shoe sizes from 5-12	Large shoe cup with adjustable strap	Manufacture Carbon fibre shoe cup with adjustable strap
High shock loading	Cracking and snapping of parts	Make chassis from a tough and malleable material.	Use aluminium 6063 for the chassis and bolt tight to shoe cup.
Rapid acceleration of components	Shearing of rotation components (gear teeth, shaft connectors and input part)	Use high strength materials. Use a gearbox with a high torque loading factor	Use steel components and a heavy duty gearbox.
Extract as much energy from footfall as possible	Short time frame of landing. Varies in frequency and velocities	Use a light weight, high efficiency transducer for mechanical to electrical transfer	Specify a DC motor with low rotor inertia, low stall torque, yet with high efficiency.
Must be ready to harvest from each step	Input components need to protrude back below the shoe before each step, ready for next input	Use an input bar that is returned to its start position each time the foot is lifted	Add a return spring to reverse the bar back down (harvest from this movement as well)

The harvester's design needed to work and withstand worst case scenarios; jump landings, heavy wearers, fast walkers and large shoes to fit around, but also needed to be as light-weight and as user-friendly as possible. After compiling multiple designs for harvesting footfall a final concept was designed using SolidWorks, the 3D modelling software.

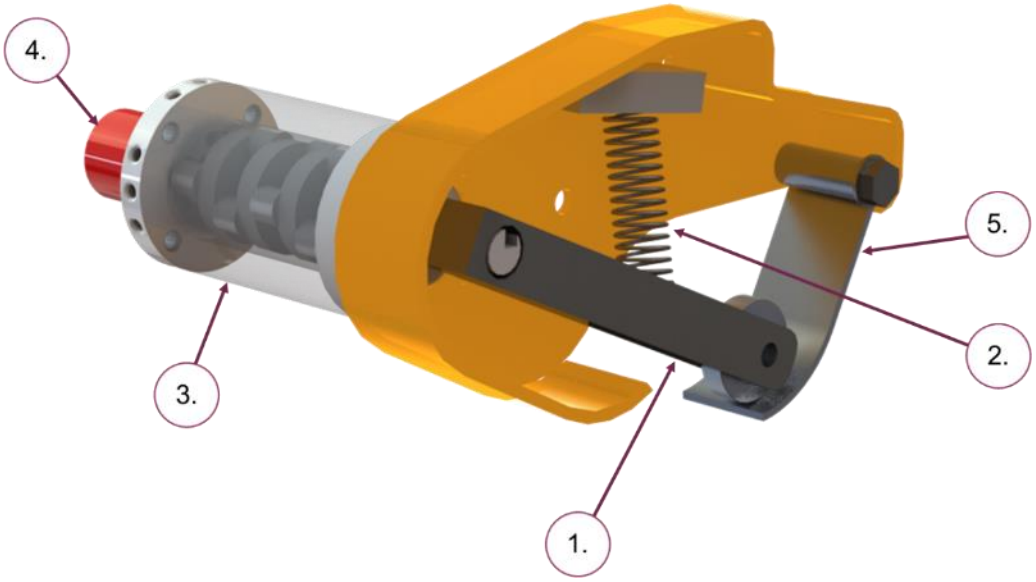

Figure 4-3 Illustration of initial harvester design shown without fitting connections to the shoe.

Figure 4-3 shows the final design render of the mechanical system used for the initial wearable energy harvester design.

4.3 Initial Harvesters Operation

The harvester is designed so that the input bar (1) protrudes below the sole of the wearer's shoe. As the wearer walks and places their foot onto the ground the input bar is forced upwards by the ground reaction force. This compresses the return spring (2) and starts the rotation of the up ratio planetary gearbox (3), and in turn starts rotating the transducer (4) at a greater angular velocity when compared to the input bar's angular velocity. From feedback regarding safety of the design an additional Anti-Snagging-Plate has been introduced (5). This will ensure the input bar is not able to catch or snag on protruding object on the ground or surface the wearer is walking on which might have led to a trip or a fall. With this plate (5) position here the input bar can still receive full input from the wearer's foot force, but any trip hazards will now be deflected. When the transducer is rotating from this input, it will be generating electrical energy and this is deemed as active

harvesting time. When the wearer then lifts their foot again to take the next step, the return spring pushes the input bar back down to its starting position, projecting the input bar back below the sole of the wearer's shoe. This is a direct drive design, meaning that when the spring returns the input bar, it also drives the gearbox and transducer, thus also generating electrical energy. This increases the generating duty cycle of the harvester. This is the second point of active harvesting.

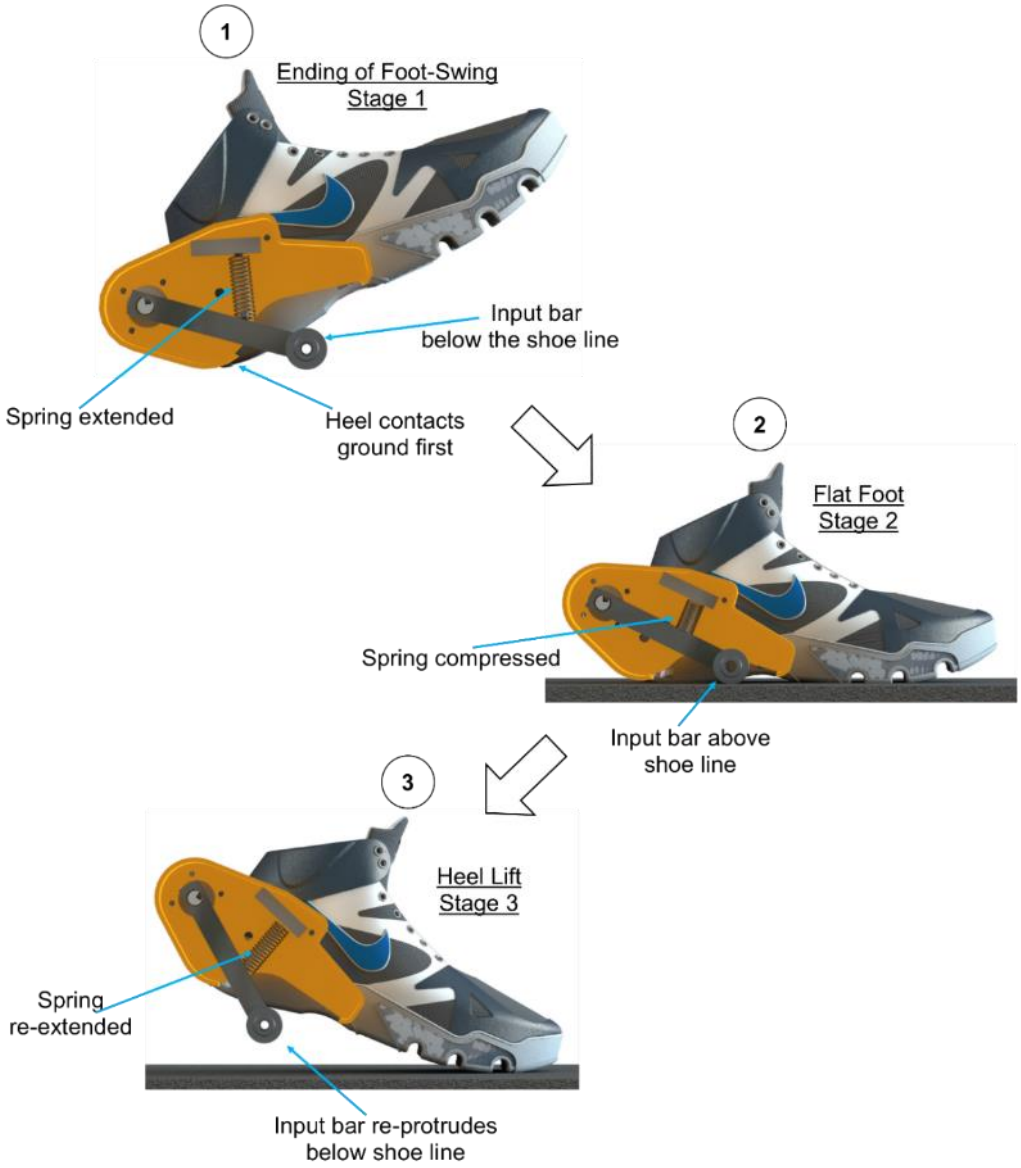

Figure 4-4 Harvester input bar movements relative to the gait cycle stages when attached to the wearers shoe and walking at a normal rate.

It can be seen in Figure 4-4 that the input bar is forced upwards each time the wearer places their foot on to the ground and the return spring

restores the input bar to its starting position when the foot is lifted for the next step. The gearbox and motor are positioned behind the foot in line with the leg. From research, this was found to be a more comfortable position for the heavy components as they are lifted by the leg muscles and not the foot muscles. A strap is used across the top of the foot to hold the harvester to the wearer's shoe.

4.4 Initial Design Theoretical Analysis

Wearable energy harvesting is different from other areas of energy harvesting because it is harvesting energy from a human. Other areas of energy harvesting aim to be harvester as much energy from the source as possible, but if the harvesting from a wearable energy harvester was to become too excessive, it would have a detrimental effect on the wearer. This means that care must be taken when designing any wearable energy harvesters, to ensure the harvested energy is advantageous over the energy consumption of wearer wearing and using the harvester. If the energy consumption of the harvester increases beyond a realistic and useable point, the wearer would need to either consume more energy (food) or have a rest (sleep) in order to continue using the harvester. This energy exchange or trade-off is called the *cost of harvesting*. This gives a comparable figure that can be used to compare other harvesters and batteries to each other. This will be shown in more detail later in Chapter 6 Comparing Wearable Energy Harvesters.

Table 4-3 Harvester conditions and parameters

Symbol	Environment Condition	Unit	Value
m	Wearer Mass	kg	75
Freq	Step Frequency	Hz	1
v	Footfall Velocity	m/s	0.4
g	Gravity	g	9.81
	Harvester Conditions		
r	Input Bar Length	m	0.1
y	Input Displacement	m	0.04
Gb rat	Gearbox Ratio	1:	188
Gb eff	Gearbox Efficiency	%	40
K e	Motor Speed Constant	V/RPM	1.1
K m	Torque Constant	mNm/A	15.7
R_m	Motor Terminal Resistance	Ω	4
R_l	Connected Resistive Load	Ω	10 - 40

By using the conditions and design dimensions shown in Table 4-3, calculations were performed to determine the energy and power throughout the system. This needed to be done to ensure the gearbox and motor pinon gear were going to be able to withstand the shock-loads of the wearer's weight each and every step against the back torque generated by the harvesters transducer. Along with ensuring the harvester's design was able to generate enough power to charge or run portable electronics devices without harvesting too much energy from the wearer.

The first calculation is to find the average angular velocity entering the transducer. To find this, the angle change of the harvesters input bar was found via equation 4-1.

$$\theta_{in} = Sin^{-1}\frac{y}{r} \qquad (4\text{-}1)$$

Where, y is the maximum linear input displacement of the bar and again r is the radius from the gearbox's centre line and the input bar's tip.

This is calculated by knowing the set input displacement of the input bar (0.04 m) and the length of the input bar, (0.1 m). The angle change (θ_{in}) seen by the gearbox input shaft is 23 degrees, or 0.4 Radians. By knowing the average footfall velocity (0.4m/s) and the set displacement of the input bar (0.04 m), the time frame the active input occurs can be calculated. This was found to be 0.1 s. By knowing the angle change and the time frame in which it occurs, the average angular velocity can be calculated and was found to be 4.1 Rad/s.

The transducer has an efficiency of 88% when running at its optimum speed, 6800 RPM, but this design means the motor will be offset from its optimum speed due to the limited availability of gearbox ratios. The average angular velocity entering the transducer is 772.1 Rads/s, (7374 RPM) and is calculated using equation 4-2.

$$Gb_{out}\omega = \frac{(((\frac{\theta_{in}}{t}) \cdot 60 \cdot) Gb_{Rat})}{360} \quad (4\text{-}2)$$

Where, $Gb_{out}\omega$ is the average input velocity from the gearbox into the motor, t is the active input time, and Gb_{Rat} is the planetary gearbox ratio.

Knowing the input velocity into the transducer and the motor specification from the manufactures data sheet, the open circuit voltage from the transducer was calculated using equation 4-3.

$$V = ((\omega \cdot K_e)/1000) \quad (4\text{-}3)$$

Where, V is the voltage generated at the motor terminals, ω is average angular velocity into the motor, K_e is back EMF constant of the motor. Calculating this give a theoretical voltage output of 12.1 V.

Once the open circuit voltage was found, then the back torque generated by the motor was calculated using equation 4-4.

$$T_{gen} = \frac{V}{R_m + R_l} \cdot Km \qquad (4\text{-}4)$$

Where, T_{gen} is the back torque generated by the motor when generating the maximum voltage, V. R_m is the motors terminal resistance, R_l is the connected resistive load, and Km is the torque constant from the motor data sheet.

Using equation 4-4, it was found that this transducer would produce 13.7 mNm of back torque from the given input velocity and the voltage generated. This may seem small, but this is at the transducer end of the gear box. To know the torque required by the wearer, this torque figure needs to be multiplied by the gearbox ratio (188:1) and the gearbox efficiency (40%). This results in a minimum torque input requirement of 3.6 Nm from the wearer.

By knowing the maximum voltage generated and the resistance of the electrical circuit, the electrical power generated from the harvester can be calculated. This is done via the simple electrical equation shown in equation 4-5.

$$P = \left(\frac{V^2}{(R_m + R_l)} \right) \qquad (4\text{-}5)$$

Using this equation, it shows the harvester could produce 8.4 W. But this is assuming the harvester would see a continuous input of energy for the whole second. As seen in research, an average vertical footfall velocity of 0.4 m/s was found at a normal walking speed. At that velocity this harvesters design has an active input time of only 0.1 s. This would result in an average

electrical power output 0.84 W per step at a normal walking speed of 1 step per second.

Finally, the efficiency of the system can now be calculated. If the Potential energy equation shown in equation 4-6 is used with the data shown in Table 4-3, then this shows there is 29.4 J of energy potential available from the wearer each step.

$$P_{in} = mgr \tag{4-6}$$

Where, m is the mass of the wearer, g is the earth gravity constant, and r is the radius from the gearbox's input axle centre line and the input bar's tip.

Assuming the wearer is walking at a normal rate of 1 step per foot per second, if the wearer was wearing one harvester, then this person could produce 29.4 W. Taking this wearable energy harvesters active power generation of 8.4 W found in equation 4-5 and the maximum potential power found using equation 4-6, this design of harvester suggests it is has an efficiency of 28.6%

4.5 Fabrication of Initial Harvester Design

To ensure the harvester could fit around, and strap tight to most footwear, a carbon fibre shoe cup was manufactured shown in Figure 4-5. Carbon fibre was used as it has good structural stiffness and very high durability. Both were needed to withstand the forces of the mechanical components creating moments at all fixing points and to survive the loading on the wearer landing on it as they walk.

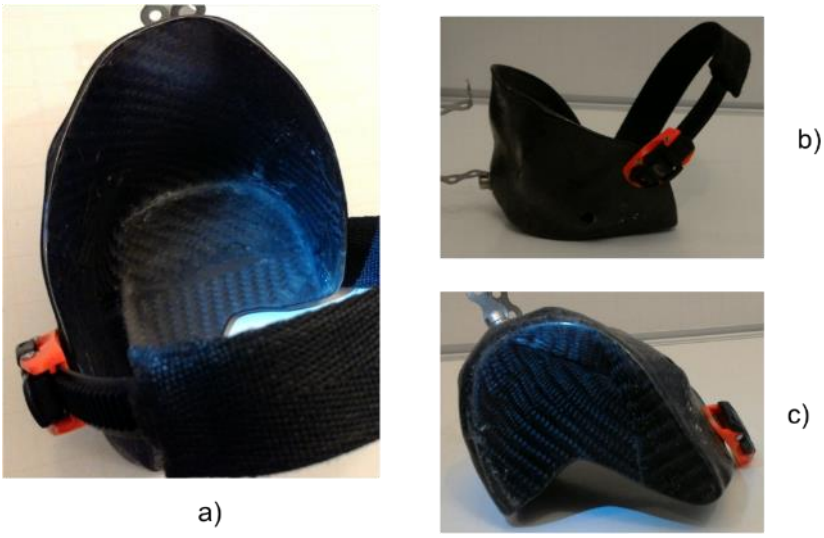

Figure 4-5 Carbon fibre shoe cup for initial design of footfall energy harvester: a) Overview from top showing shoe placement area, b) Side view showing the strapping method, and c) Base of unit showing the conplex carbon fibre weave

The harvester will be sat on the outside of the wearer's shoe, so the covers protecting the mechanical components were also made using carbon fibre, shown in Figure 4-6. Seals were added to reduce the risk of debris or moisture entering the harvester.

Figure 4-6 Carbon fibre covers for initial design of footfall energy harvester: a) Transducer cover amd sealing strip, and b) Showing complex 3D curve of transducer cover.

The chassis of the harvester had to be made to fit to the shoe cup, but also to hold the gearbox input shaft in the correct position. The chassis also needed to withstand rigorous testing resulting in higher fatigue wear than in normal use. To help improve this the return spring was mounted to a replaceable plate instead of directly to the chassis. This will reduce the wear of this connection point. Custom aluminium plates were cut and welded together to create the chassis. By using the design shape shown in Figure

4-7 the structural stiffness of the chassis was improved. This reduced wear of the connection points between chassis and shoe cup, and lessened bending of the harvester. By doing this, more energy would be seen by the transducer, rather than being wasted in distorting and bending the chassis.

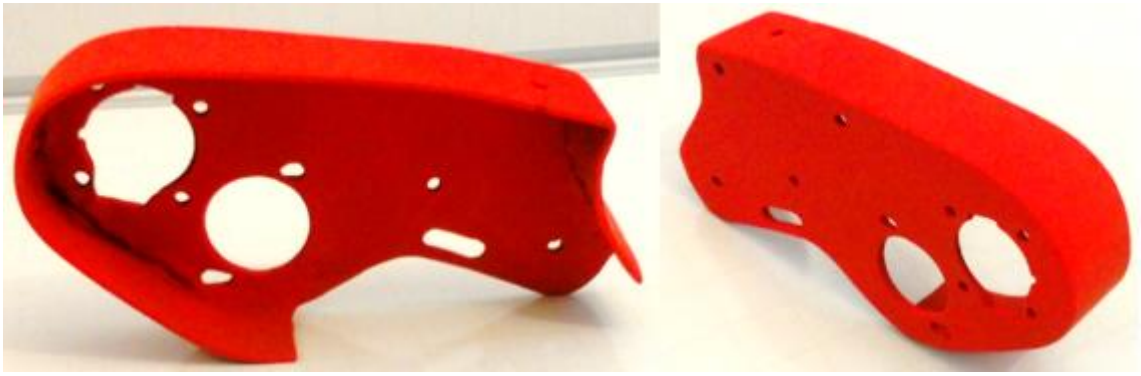

Figure 4-7 Aluminimum chassis for initial design of footfall energy harvester shown from front and back views

The gearbox used was from *Gimson Robotics Ltd.* This gearbox was used because of its high torque strength and a close gear ratio option was available. The motor supplied with the gearbox was not optimal for footfall energy harvesting due to its weight and rotor mass. Having a high rotor mass gives a high motor inertia meaning more energy is needed to start the motor spinning.

This is bad for two reasons;

1. The larger the motor's inertia, the slower the motor accelerates, resulting in lower voltage levels and less electrical energy generated.

2. With slow acceleration of the transducer components, the resulting dynamic torque difference between inputs bar and transducer increases. This torque figure will ultimately lead to the failure of the gearbox and/or the transducer.

A more ideal motor was selected and a custom motor to gearbox motor plate was designed and fabricated. The DC motor used in this harvester's design as the transducer is made by *Portescap*. With an efficiency of 88%,

low stall torque of 48 mNm, and low rotor inertia figures of 4.2, this motor met the design requirements well. It also had the benefit of being lightweight, weighing only 53 g compared to 250 g of the original motor supplied on the gearbox.

Figure 4-8 shows the final footfall energy harvester for the initial harvester design. It is pictured with a UK size 10 shoe, with the input bar protruding below the sole of the shoe.

Figure 4-8 Initial design of footfall energy harvester connected to a males uk size 10 walking boot

A PTFE impact wheel was installed on the tip of the input bar to reduce snagging and wearing of the bar or floor walked on. A double USB socket is located on the top of the chassis for charging or connection to portable devices. To be able to output via a USB port, a voltage regulator circuit needed to be used. This needed to be installed in between the output from the transducer and the input of the USB port. A small, lightweight, and simple regulating circuit that would temporarily store the sharp spikes in electric energy generated from the transducer and produce a regulated 5V output was used. The circuit was purchased online and was from a push-bike phone charging system. It was chosen for its size and weight. The efficiency of the unit is unknown and will drop power the output from the harvester, but will provide the interface needed between transducer and USB output in order to

charge modern portable equipment. The circuit is shown installed in the harvester in Figure 4-9.

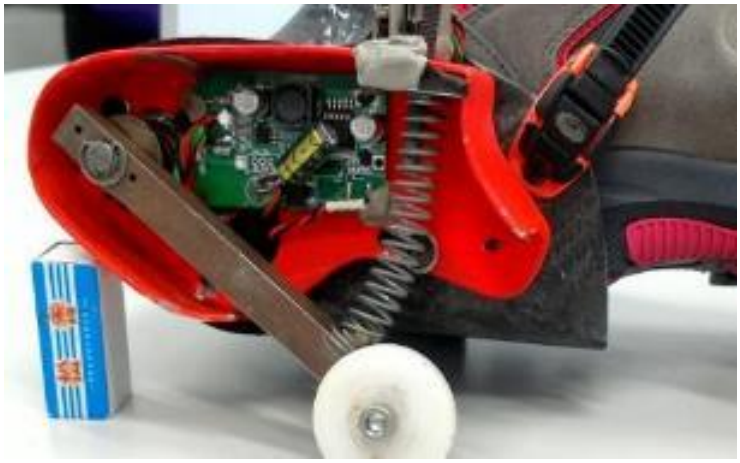

Figure 4-9 Rectifying and regulating circuit installed within the initial design of footfall energy harvester

The final component to specify was the return spring also seen in Figure 4-9. The main purpose of this spring is to ensure the input bar returns to its start position, protruding below the wearer's shoe each time the wearer lifts their foot off the ground, but it can also be used as a harvesting point. As this is used to drive the gearbox and transducer, a heavier spring rate would be better as it would produce a larger energy input during the return phase. The upper limit of the spring force would be down to two factors.

1. The minimum weight of the wearer over the compression ratio of the spring. If the wearer could not compress the spring then no energy would be generated at any point of the gait cycle.
2. The impact to the wearer will increase directly with the increase of the spring rate. From simple preliminary tests, increasing the spring rate had a larger effect on user impact than it had on benefits in electrical energy generation.

4.6 Experimental Set Up

A foot moving towards the floor, landing, and lifting off again, was the objective of the tests. To reconstruct the movement of a foot as if it was being used under differing gait cycles and conditions. The gait cycles and the defining phases were clarified in Chapter 3. As there is no one set walking technique, the test parameters such as; walking styles, speeds, and terrains would need to be able to change. These variables are shown in Table 4-4.

Table 4-4 Three main parameters for testing

Parameter	Range	What it represents
Foot Velocity	0.1 – 0.4 m/s	Different people move their feet at different speeds, meaning different speeds must be tested.
Step Frequency	0.5 – 4 Hz	Strolling, walking, jogging, and running all have different step frequencies, requiring different frequencies to be tested.
Input Displacement	10 – 40 mm	Poor fitting and soft ground will also affect the performance of the harvester by changing the input displacement, this will also need to be varied.

4.6.1 Test Procedures

An *Instron E10,000* tensile testing machine was used to replicate the different motions required for each test. The on-board software called *Wave-Matrix* was used to create different waves of different velocities, frequencies and displacements for the machine to move the harvester to. Each test ran for 50 steps or cycles. The test length changed depending on step frequencies. If the frequency was at 2 Hz, then the test ran for 25 s, but when the frequency was 0.5 Hz, the test ran for 100 s. The tests were set by quantity of step rather than time, in order to compare average step energy generated per step.

In Figure 4-10, photos can be seen showing the equipment used and the harvester installed in the Instron machine. Here the harvester is held in the top clamp and a ground plate is installed in the bottom grips. When the test begins the upper grip holding the harvester is moved towards the floor plate according to the wave-matrix set up. When the input bar contacts the floor plate it is forced upwards and the harvester starts generating energy.

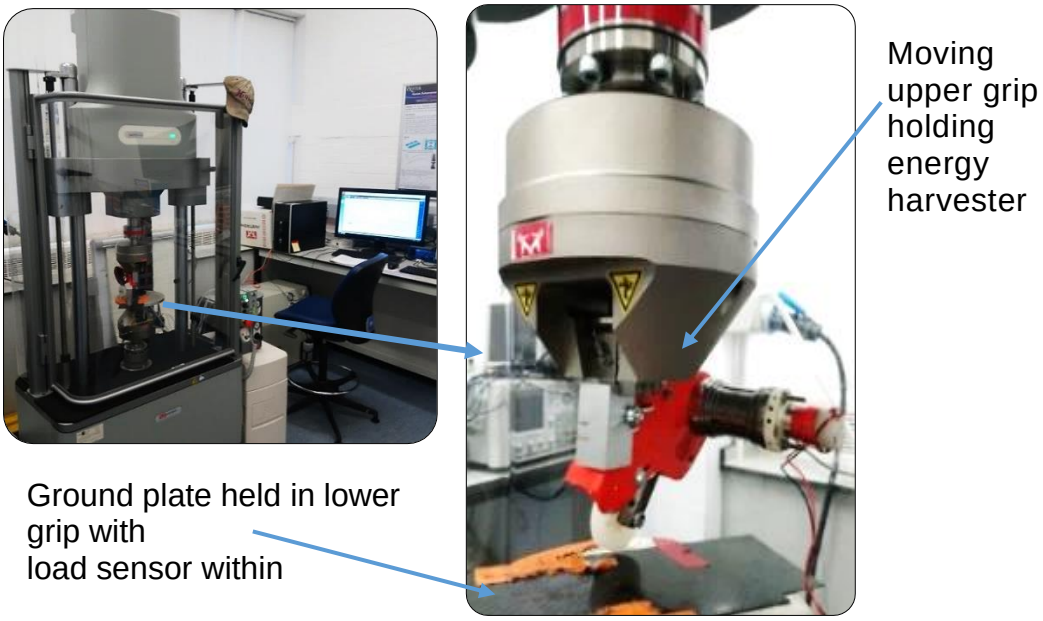

Figure 4-10 Instron machine set up, harvester being held in a moving upper grip and ground plate held in the fixed lower grips with load sensor installed

The terminals from the transducer (motor) were fed out the back of the machine to ensure they didn't influence the harvester or the tests.

The variables shown in Table 4-4 were tested over different electrical loads and the voltage and electric energy generated were recorded.

After hours of testing with a number of component failures along the way, a final set of reliable results were obtained. Each time a component failed, all tests were performed again from the start. This was done to ensure consistency throughout all tests. The results were analysed and the harvester produced different voltage levels under different conditions, (load, frequency etc.) which in turn affected the electrical energy generated in the transducer.

To confirm the harvester true real world potential, tests were perform on a treadmill at the 3 main gait speeds, aiming for 3 different frequency inputs into the harvester when being worn by a human.

a) b)

Figure 4-11 Treadmill tests: a) Heel strike harvester just before landing, b) flat foot harvester just after landing.

Figure 4-11 shows the harvester being tested on the treadmill. Here the harvester is connected to the same resistive load system and data logging program used throughout all the tests.

Endurance testing is perform by walking at a normal speed of 5.4 km/h and 2 steps per second (one step per foot) for a period of one hour. This confirms the harvester has been designed correctly for sustained use.

4.7 Experimental Results from Instron Testing

The first array of results have been grouped into 3 different sets which will be explained individually and then concluded. This results section will then finish showing real world test results, maximum output capabilities from extreme landing condition tests and results from wearing the harvester for longer periods of time.

The theory shows higher efficiency of energy transfer from mechanical to electrical energy will occur the closer the load resistor is to the internal resistance of the motor. But if the connected resistive load on the motor is increased too far, then the motor will be restricted and never have chance to get to higher speeds. Speed and voltage are directly linked, lower speed equals lower voltage. This means there will be a trade-off between maximum energy transfer efficiency and maximum power generated from the harvester. The results from testing the initial design on the Instron machine produced outputs from the harvester that were the same very time. This confirms the test set up was consistent and the harvester transfer the energy the same each test. When data was found to be different an investigation into the harvester confirmed breaking or broken components. Once the harvester was repaired and returned into its intended original state the harvester would once again produce very consistent results. Changes in output results would only be seen from changes from input or changes in the harvester. In this section the results from changing all the different input found from humans walking will be shown and the changes in outputs from the harvester under different input conditions will be displayed. In the following section the results from wearing the harvester will be explained and the variations recorded from the human factors will be shown.

4.7.1 **Results from a Normal Walking Test**

With the Instron machine set to a normal walking pattern at 1 Hz, 40 mm displacement, and an input velocity of 0.4 m/s, the harvester was connected to a 10 Ω resistive load and produced the following results in a 50-step test.

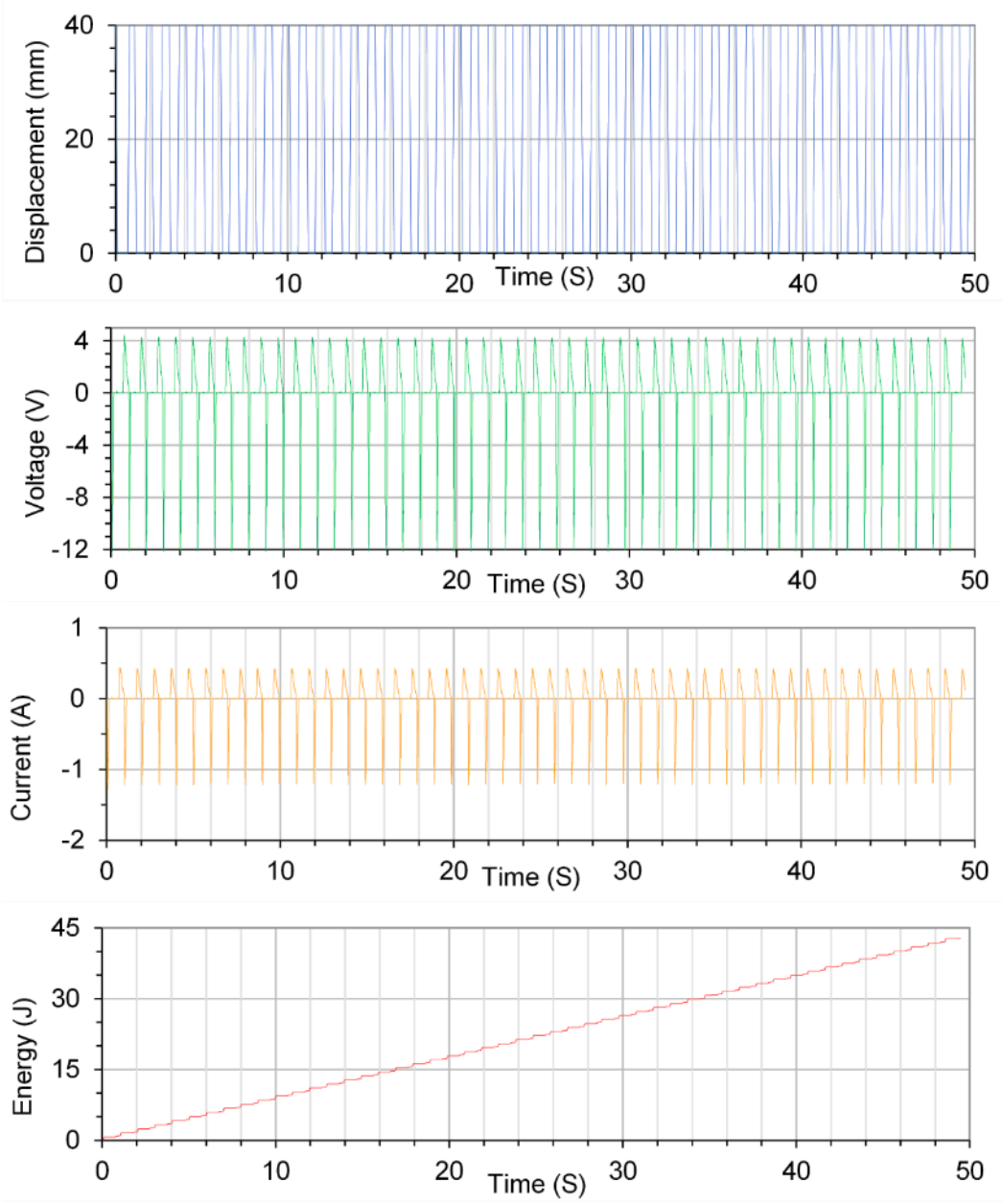

Figure 4-12 Normal walking test results from input condition of 1 Hz, 40 mm displacement and 400 mm/s vertical velocity

It can be seen in Figure 4-12 that under normal input connections the harvester produced over 12 V peak and a total 43 J of electrical energy in 50 s, equalling an average power of 0.86 W.

4.7.2 **The Effects from Varying Input Displacement**

The harvester was installed into the Instron machine and a series of tests were performed where the displacement and load resistors were changed to investigate the effects of changing the input bar displacement. Changes to the input displacement could occur if the wearer was walking on soft ground or had poor fitting of the harvester. The aim of these tests was to see how the load on the harvester affected energy extraction from different displacements.

The graph in Figure 4-13, shows the results from the first set of experiments where the input displacement and load resistor were changed. The input velocity and frequency were set at 400 mm/s and 1 Hz respectively for the whole of this set of tests.

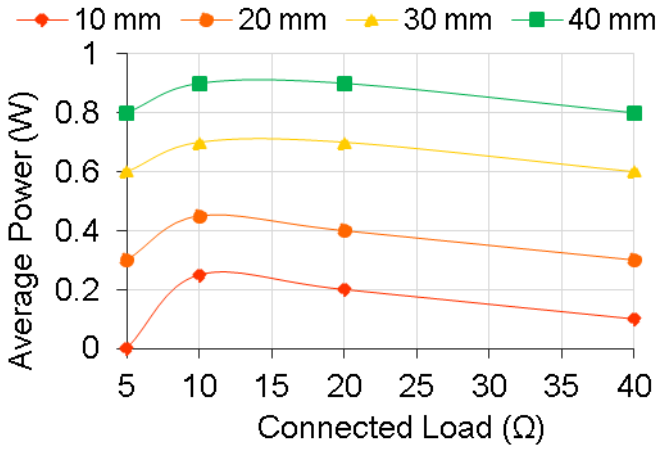

Figure 4-13 Average power generated across different connected resistive loads from different input displacements

The displacement/load graph in Figure 4-13, shows that with increased displacement, average power increased. All of the displacement tests show a decreasing electric energy generation, the further the load resistor value was from the optimum value. This is seen by the drop off in average power seen here after 10 Ω.

With the displacement being low, the maximum angular rotation of the transducer is reduced, resulting in less of an input of rotational kinetic energy

and in turn less electric energy being generated. When the resistive load of 5 Ω was connected, and the input displacement was at the lowest test setting of 10 mm, 0 W of power were generated. The reason for this is down to the losses and free play in the design. The 5 Ω load resistor will create the largest mechanical resistance on the harvester. With the harvester system designed to flex with loading and not break, and the up ratio gearbox having a 2 degree backlash free play, the transducer wasn't able to spin at a high enough velocity to generate any recordable power. With a displacement of 10 mm the inputted angle change was under 6 degrees. Along with the 400 mm/s input velocity, the time in which the 10mm displacement occurred is shorter time than the 40mm displacement tests. This gives the transducer less time to start rotating. This is called spooling up.

From this set of tests, the maximum power seen was 0.86 W. This occurred when the displacement was 40 mm and the harvester was connected to a 10 Ω resistive load. These results clearly show that by having a larger input displacement, the higher the average power the harvester generates. They also confirm that if the connected load is high and the input displacement is low, say due to soft ground or poor fitting of the harvester, the harvester will not generate any useable power. This confirms that fitting is an important factor of this wearable energy harvester design.

The harvester will be set to 40 mm displacement for optimum condition testing later, as this is the best result from the displacement tests.

4.7.3 The Effects from Varying Input Velocity

The graph in Figure 4-14, shows the results from the set of experiments where the input velocity and load resistor were changed. The input displacement and frequency were set at 40 mm and 1 Hz respectively for the whole of this set of experiments.

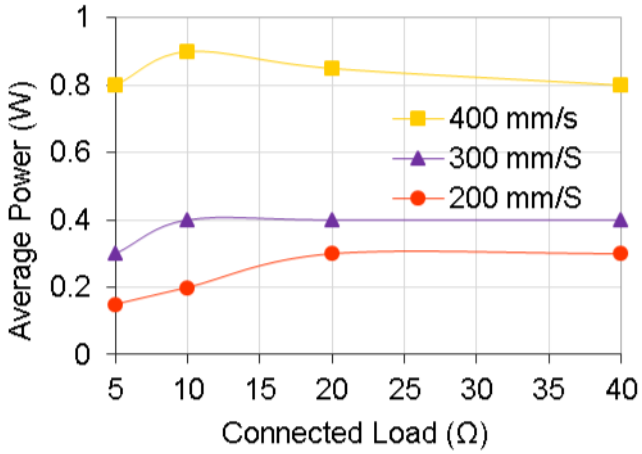

Figure 4-14 Average power generated across different connected resistive loads from different input velocities

It can be seen that the higher the input velocity, the higher the average power generated by the harvester. This confirms that the walking style of the wearer affects the power generated. If the wearer is walking slowly in a relaxed manner, resulting in their foot moving at a reduced rate towards the floor (200 mm/s), then the maximum angular velocity of the transducer is also reduced. As the transducer's velocity is directly linked to output voltage of the harvester, if the input velocity reduces, so does the output voltage, and in turn the average power. The maximum average power generated by the harvester in this set of experiments was seen to be 0.9 W over a 10 Ω resistive load and the voltage generated was 9 V. The voltage increased as the load resistance increased, but the power did not due to the increasing resistive load valve

Maximum average power occurred at 400 mm/s input velocity and this will be used as the input velocity of the optimum condition testing.

4.7.4 **The Effects from Varying Input Frequency**

When the wearer of the harvester walks or runs in different ways the input frequency seen by the harvester will change. In this set of tests, the effects of this change are investigated. Frequency was changed from 0.5 Hz input, seen from someone walking slowly in no rush, up to 4 Hz input. The 4 Hz input is meant to represent someone walking at a fast pace, or even jogging, but wearing a harvester on each foot. Tests were also performed at 1 and 2 Hz which are seen to be the most common walking step rates. The input velocity was set to 400 mm/s with a displacement of 40 mm.

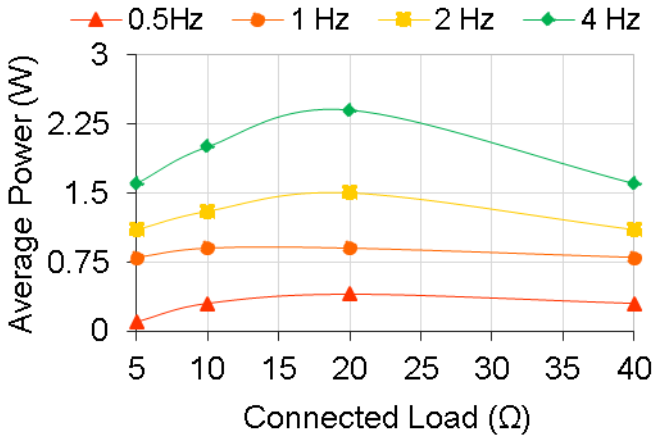

Figure 4-15 Average power generated across different connected resistive loads from different input frequencies

Figure 4-15, shows the results from the frequency tests. Here, it can be seen that under these input conditions the maximum average power was over 2.4 W. This is confirmed to be accurate because at 2 Hz input (half the input), but with the same load resistive load connected, the harvester generated half the amount of electrical energy, (+/-0.2 W). The harvester was designed to operate best at standard walking condition in which the harvester would see an energy input once a second (1 Hz). This is proven from the small changes in average power output at this frequency and these conditions. The further the input conditions move away from the designed conditions of 1 Hz, the less efficient the harvester is.

This is shown from plotting the average power output, over increasing frequencies. This is shown in the offset graph in Figure 4-16.

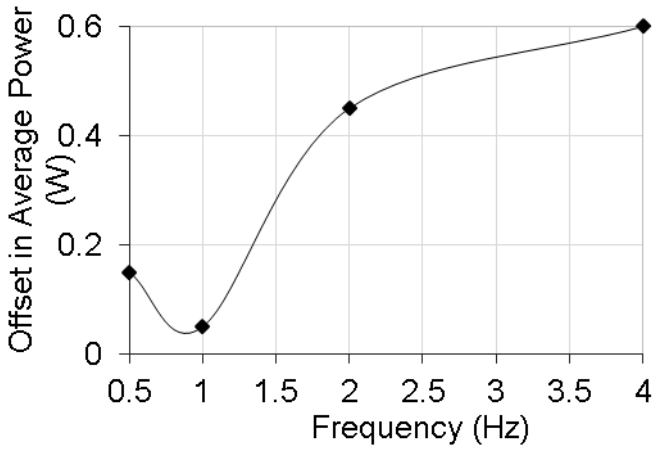

Figure 4-16 Offset in average power generated from changes in input frequency increase from the standard input condision of 1 Hz (data points have been averaged from multiple tests)

It can be seen that as the frequency increases the electrical energy generation does not increase directly. This is due to the losses in the system increasing directly with the frequency increases. This means there is a loss of 0.6 W on average from using the harvester at 4 Hz rather than the designed 1 Hz. This was calculated from knowing the power generated at 1 Hz being 0.9 W. At 2 Hz the theatrical power should have been 1.8 W, but was found to be 1.3 W. giving the power offset of 0.5 W. The same was repeated for 0.5 Hz and 4 Hz frequency inputs and an offset of 0.15 and 0.6 W respectively. This shows the harvester is designed correctly for standard conditions as it has the smallest offset in power across the resistive loads and as the input frequency moves further away from the 1 Hz the lager the offset seen.

4.7.5 **Results from Ground Reaction Forces**

The final pieces of data to analyse from the laboratory tests are the loading or forces recorded from the Instron machine during testing. All data was recorded from the Instron machine. The load data was recorded for two reasons. One, to ensure that the input force was not higher than the 300 N set in Chapter 3, and two, to make sure loading from the harvester would not influence the wearer in such a way it would impact on the walking style.

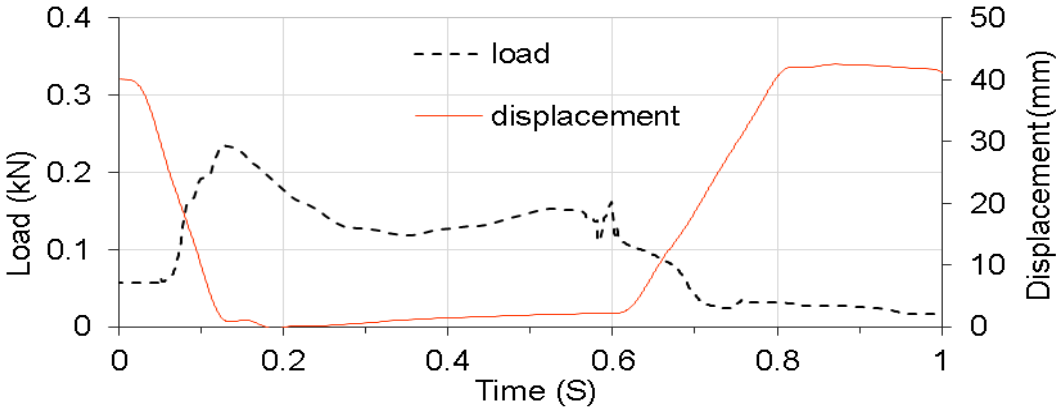

Figure 4-17 Force measured by the load sensor in the ground plate and displacement measured to confirm harvester movements recorded by Instrons machine

The graph in Figure 4-17 shows the displacement and resulting load from the harvester over a single input or step. This is a one second snapshot from a test where the harvester was under heavy load (10 Ω), fast input velocity (400 mm/s) and maximum displacement (40 mm). It can be seen that the maximum load recorded occurs when the harvester is forced down against the ground plate and is seen to be 0.25 kN. This is far below the theoretical maximum load of the wearer's foot on the ground and confirms the harvester's useability by the lightest of wearers.

This is important to ensure the design does not impact the wearer and does not need more force than the wearer can provide. Because the design is "one size fits all", the maximum loading had to be kept low. To ensure lighter weight wearers would be able to use the harvester without finding it awkward or causing them discomfort.

4.7.6 Normal Walking Input Conditions & Optimal Harvester Configuration

From the previous sets of experiments and the average input conditions found from research, a final set of tests were performed under laboratory conditions to confirm the optimal load resistor for normal walking condition with the harvester now configured for maximum energy extraction. A hypothesis can be made at this point;

From the results seen so far, the optimal load resistor will be 10-20 Ω. This is away from the theoretical optimal load for optimum energy extraction from the transducer, which would match the resistance of the transducer (4 Ω). This is because the transducer needs to be able to spool up. The transducer will struggle to build momentum if the energy extraction is too close to the maximum/optimum. This then results in too high a back-torque generation from the EMF's of the electro-magnetic transducer and thus, restricting the transducer acceleration, resulting in less electrical power being generated over a single input period.

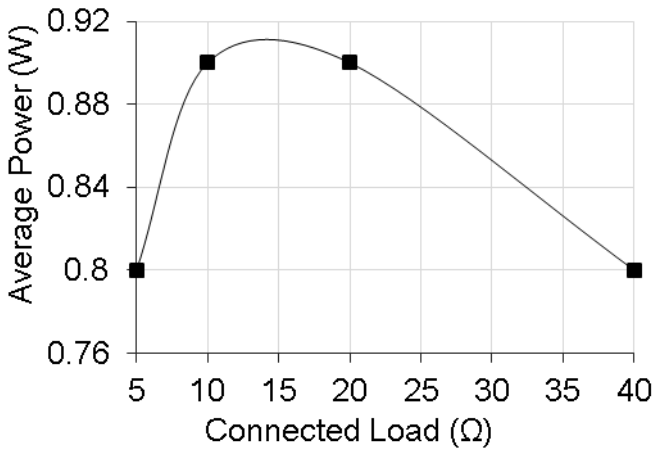

Figure 4-18 Results for finding maximum power extraction from different resistive loads under standard input conditions

It can be seen in Figure 4-18 that this initial design for a wearable energy harvester under normally walking conditions produces its maximum

power of 0.91 W when connected to a 10 Ω load resistor. At 20 Ω the harvester produced 0.89 W.

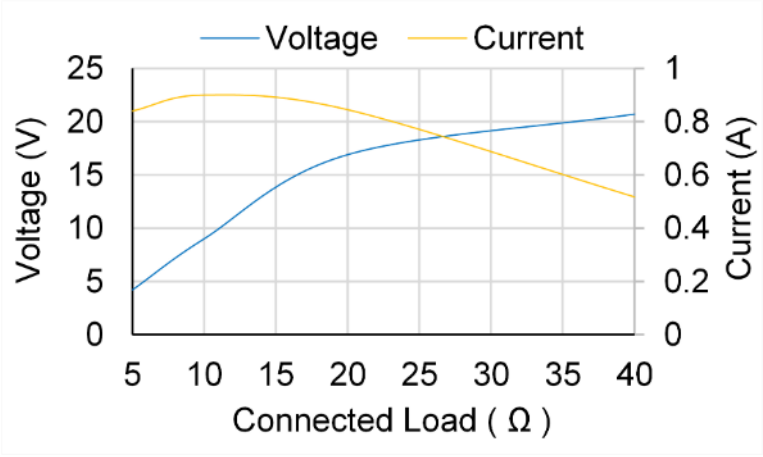

Figure 4-19 Voltage and current generated across different connected resistive loads

From the voltage & current graph shown in Figure 4-19, it can be seen that as the connected resistive load increases, the voltage increases, but the current has a peak and after this starts to decrease with the increasing resistive load.

The voltage increasing is a direct response from the transducer rotating at a higher velocity from having less damping caused by the resistive load. It is important to point out that the DC motor being used as the transducer has a design input voltage of 12 V. When the harvester is producing more than 12 V, the DC motor will be over its designed voltage threshold. This would result in excessive wear on the motor reducing its life expectancy and eventually failure.

The current produced from the harvester is an important graph to study as this denotes an optimum load resistor and can be seen to be 10 Ω. When either a lower or higher resistive load was connected to the harvester, the current being produced is reduced. This results in a lower average power output and reduces the harvester's efficiency.

4.8 Experimental Results from Treadmill Testing

To confirm the real-world capabilities of this wearable energy harvester, tests were performed wearing the wearable energy harvester. Wires from the harvester's transducer were connected to the same setup used in the lab tests as well as the same LabVIEW program. Data was then recorded from the three primary types of gait cycle: Strolling, Walking, Jogging. Each test was performed 3 times and the averages were taken as final results.

The first set of tests were executed as if the wearer was going for a relaxed stroll. As found in research, this is around 3.6km/h (1m/s) where the step frequency was on average 0.5Hz. These tests were designed to see how much power the harvester could generate, if the wearer was not in any rush and inputting at a low rate. One set of results are shown in Figure 4-20.

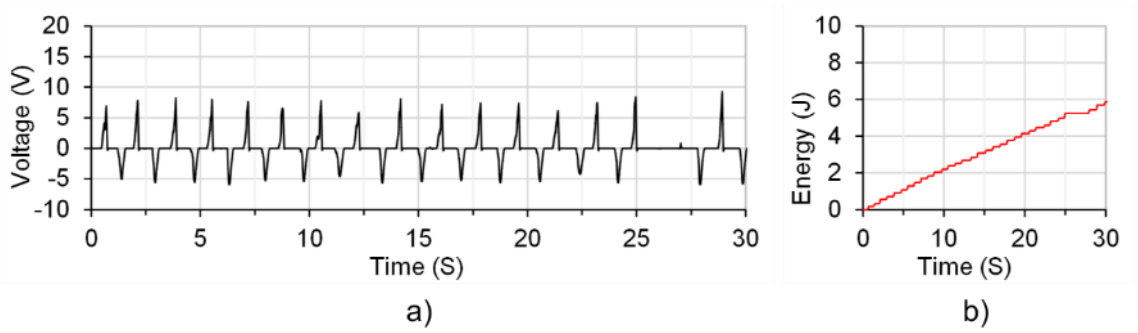

Figure 4-20 Strolling results: a) Voltage generated, and b) Energy generated

These results show that at low speeds and frequency inputs the harvester produced 0.2 W of power on average. In Figure 4-20 b), there is a clear step where no energy was generated. This was found to be because the spring did not return the input bar from the previous step, resulting in no energy inputted, confirming the true real-world nature of these tests.

The second set of results are from the normal walking test. Here, the tests were performed at 5.4 km/s, with an average input frequency of 1 Hz. This would be as if the wearer was walking to work or for a bus. This showed

the average power to be 0.7 W. This was 0.2 W less than the 0.9 W seen in the Instron machine and is down to poor device fitting, and humans being humans, (meaning not very step we take is exactly the same) When the harvester was tested in the Instron machine, every single voltage output was the same, confirming the machine's calibrations and accuracy. But when the harvester is worn by a human, the inputs seen by the harvester change depending on wearer's walking concentration and environment conditions. This can be seen from the voltage spikes in Figure 4-16 a),

The third set of results are from fast walking or jogging tests. From research it was found that an average fast walk or jogging speed of 7.9 km/h is deemed typical for most. When the harvester was tested at this speed, and had target input frequency of 2 Hz, the harvester produced 1.6 W on average. Figure 4-21, shows the average power generated by the harvester under the 3 main gait styles.

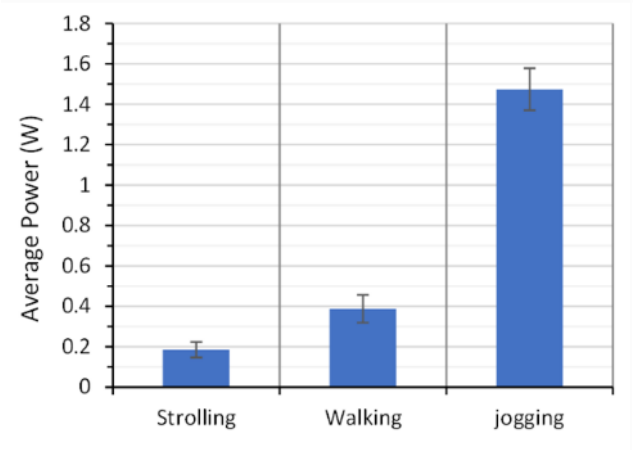

Figure 4-21 Average power generated from the three main gait styles generated on a treadmill shown with standard deviation

The real-world tests show that this wearable energy harvester's design has the potential to produce 0.2 to 1.5 W depending on input style and frequency. The maximum deviation occurred over the jogging speed and was calculated to be 0.1. The results of the standard deviation calculations show the consistency of the tests and the reliability of the harvester.

4.8.1 **Results from Maximum Loading Testing**

The final test performed was a jump landing test. This was done to confirm the harvester's ability to withstand the worst-case scenario of the wearer jumping downstairs or off a wall. Here the harvester was worn, and the wearer jumped as high as they could and landed with a bang. This test was performed a number of times to confirm the results were correct and the harvester would withstand this type of shock loading. The harvester survived and produced some impressive outputs. The maximum voltage seen from the wearable harvester was 28.5 V and produced an instantaneous power level of 40 W. This power level might seem incredible but, is only available during the final part of a jump and this time frame is very small (0.06742 s). If the wearer was to jump once a second, an average power level over a second can be calculated.

This results in an average power level of 1.12 W from a single input.

In Figure 4-22 the results of a jump landing test are shown.

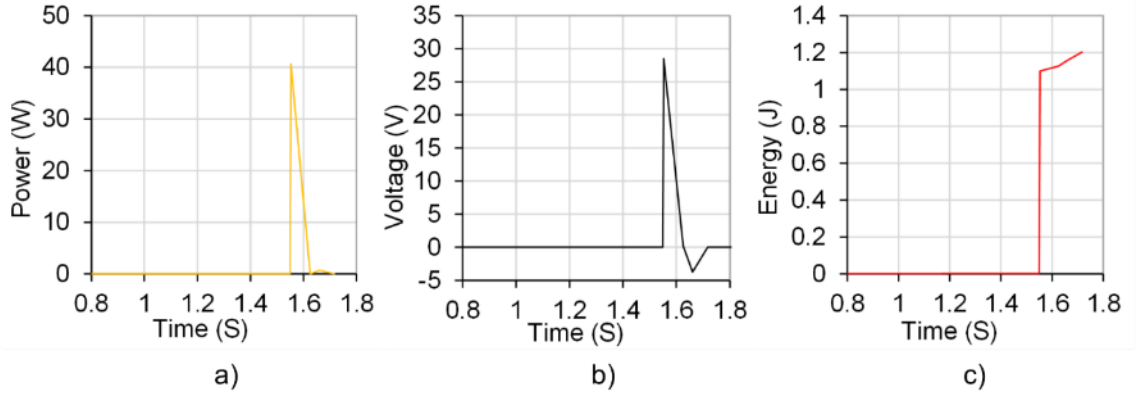

Figure 4-22 Extreme loading test results from a jump landing: a) Instantaneous power, b) Voltage generated, and c) Total energy generated

Figure 4-22 a), shows the power generated. It has a very steep increase as the wearer lands, but also a very quick decay, this results in only a small amount of energy being generated confirmed by the graph shown in Figure 4-22c.

4.8.2 **Results from Endurance Testing**

Here the results from testing the initial design for hour-long tests are shown and discussed. The harvester performed well and was still working efficiently at the end of the tests. This confirms the reliability and durability of the design.

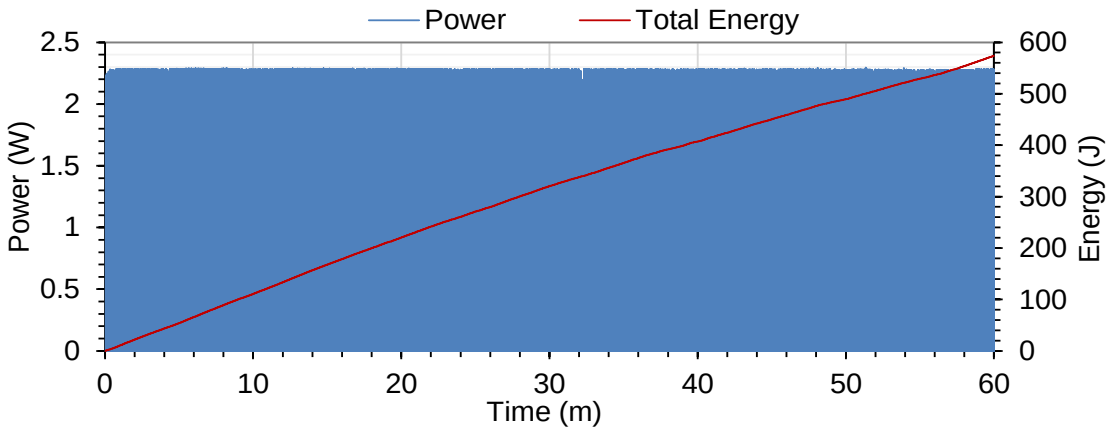

Figure 4-23 Instantaneous power and the total energy generated from the USB port from testing the initial design for an hour of normal walking on the treadmill

Shown in Figure 4-23 are the results from testing the harvester over the whole hour test. It shows the harvester produced 573 J of electrical energy in an hour. The power appears to be a block rather than lines, but as there are over 3600 steps shown here, and it is not surprising the spikes are not visible.

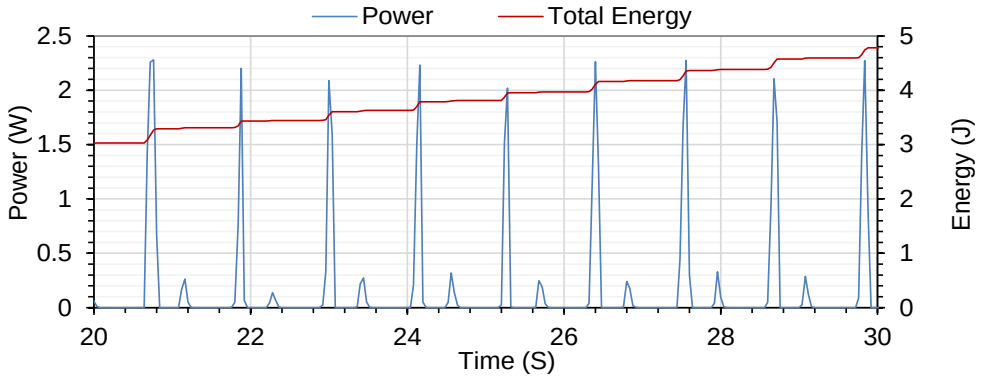

Figure 4-24 10 Second snap shot of the Instantaneous power and the total energy from the USB port from testing the initial design for an hour of normal walking on the treadmill

Shown in Figure 4-24 is a 10 second snapshot, showing the power spikes and the energy increasing and this shows each step taken on the treadmill directly relating to the electrical energy generated by the harvester.

If the total energy generated is divided by the total time in seconds then the average power can be calculated. This results in an average power of 0.16 W. Even though the instantaneous power is over 2 W, the average is a lot lower. It is clear that even though the design produces watt-level of electrical power, it would take a very long time to charge your portable device due to the losses and inefficiencies of the cheap power management used.

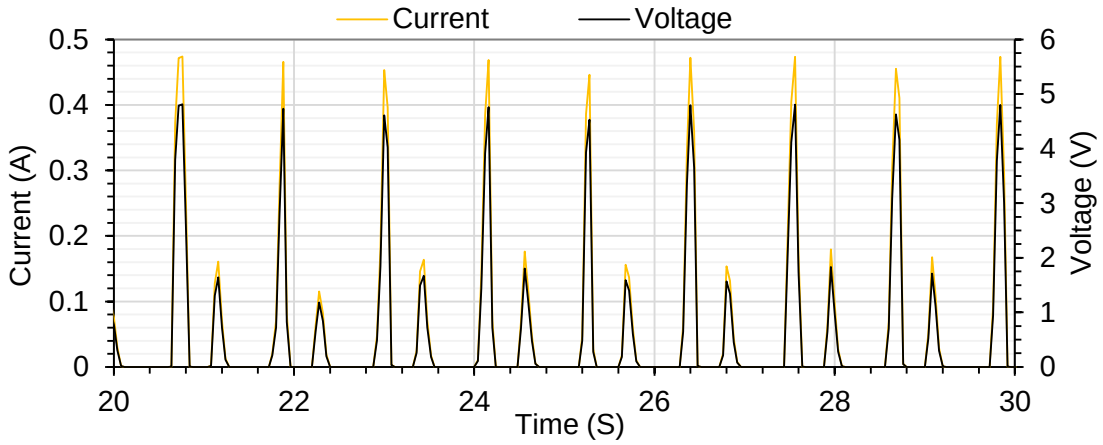

Figure 4-25 10 Second snap shot of the voltage and current generation from the USB port from testing the initial design for an hour of normal walking on the treadmill

Figure 4-25 shows the voltage and the electrical current generated by the harvester in the same 10 second snap shot as shown before. It can be seen here that with the basic power management circuit installed for outputting via a USB port, the voltage is limited to a maximum of 5 V to protect any device connected to the USB port. It also shows the shape spikes from the inputs from footfall.

Due to the on/off nature of the electrical power generation from this design, it was not able to change a portable device. Each time a device was connected, the device kept trying to charge but then refusing to due to the extreme surges of power. In Figure 4-26 are the results from testing the harvester for another hour, but measuring directly from the transducer.

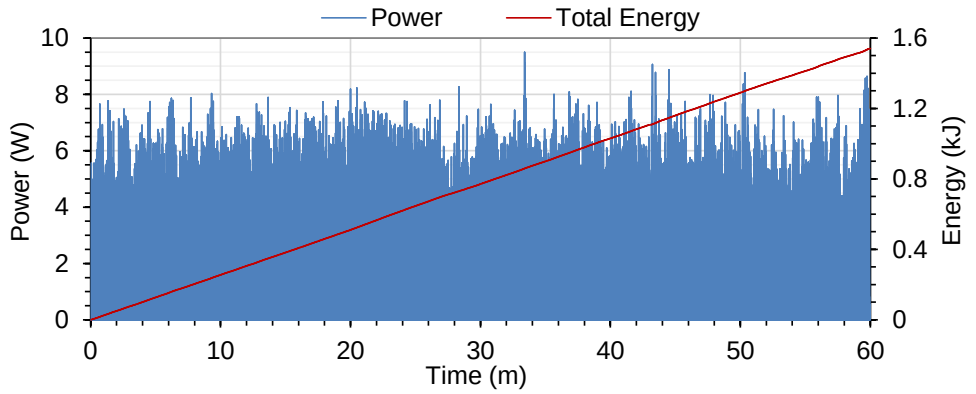

Figure 4-26 Instantaneous power and the total energy generated directly from the transducer of the initial design from testing the initial design for an hour of normal walking on the treadmill

It can be seen in Figure 4-26 that the harvester actually produces 1.54 kJ. This is lot higher than the regulated output from the USB, due to the higher voltage spikes seen. Figure 4-27 shows that the maximum voltage is higher than what will useable for 5 V USB charging, hence the need for the regulating circuit.

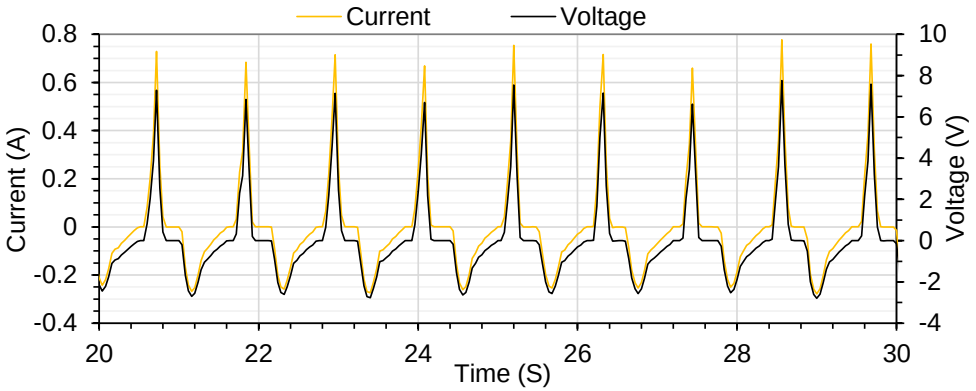

Figure 4-27 10 Second snap shot of the voltage and current generation directly from the transducer of the initial design from testing the initial design for an hour of normal walking on the treadmill

For this harvester design to charge a portable device a bespoke power management circuit would be needed and that is not the focus of this research project. After wearing and using this harvester design for an hour, the shoe cup and strap both started to become uncomfortable. If this harvester prototype design was going to be used in a commercial application such as ankle weights, then the ergonomics of the design would need to be improved, but again that is not the focus of this study.

4.9 Conclusions and Discussion on Test Results

The wearable energy harvester that has been created, tested and analysed here shows the potential of the design and energy extraction method. From all the tests performed in laboratory conditions it can be said that this design of wearable energy harvester produced a maximum average power of 2.4 W over a 10 Ω resistive load.

Under normal walking conditions with only one harvester being tested, the average power from the one harvester was 0.9 W. The tests also confirmed the design produces an average of 0.7 W when the harvester is worn in real world testing, and can withstand extreme conditions, such as a jump landing.

This would suggest that if a harvester was worn on both feet, then the total average power output would be 1.4 W under normal walking conditions and would not load the wearer in an over dramatic way.

The only error in the experiments was the small reduction in energy generated when wearing the harvester compared to the Instron machine. This can be put down to the fitting strap and the flexible nature of shoes that the harvester is trying to securely fix to. If the harvester was fixed in a more rigid way, the energy generated would match the Instron test results better. This would however lead to the wearer feeling more and more discomfort from wearing the harvester.

The valuable points from this design are; the use of an input bar that protrudes below the shoe line, and the use of a large ratio planetary gearbox to increase the small angle change of the input bar into multiple revolutions of the transducer. These points will be used to evolve a wearable energy harvester design seen in the next chapter.

The bad points or feedback from others is the weight on the foot. Even though the harvester only weighs 1.2 Kg, the people that wore the harvester said it was too heavy. This could be reduced if more expensive materials and components were used, but from feedback the weigh on your foot feels “too much”. So, maybe moving the mass away from the foot might be explored.

From the tested performed here a large variation on power generation was seen from the different walking patterns resulting in lower power from slow footfall speeds and displacements, but good power output levels for fast walking and larger displacements with very low deviation in each set of tests. To improve this a harvester will need to be designed so that it generates a more average power output no matter what the walking style. The next design will not investigate the different power generation from different walking styles as it will be designed to overcome this change seen from this design.

Overall, this design performed well but also showed the way to an improved design. 0.9 W of electrical power were seen from one-foot harvesting under normal walking conditions. The harvester also withstood heavy shock loads and different input style, but this came at the cost of increased weight of the whole harvester’s design.

Chapter 5 Improved Design, combining Backpack and Foot Units

This chapter will explain the steps taken to evolve a footfall energy harvester with the aim to improve the energy extraction, increase the average power outputted, and decrease the impact to the wearer. The design principles and the mechanics behind the harvester are explained, leading on to the tests that were performed on the harvester and finishing with the results being analysed.

5.1 Understanding the New Parameters for the Improved Design

In the previous chapter exploring the initial design, the results showed the potential of the harvester's basic design principles. However the experimental tests and results also showed areas where the design could be improved. The key improvement needed was to reduce the mass the wearer would have on their foot. The forces seen in footfall limit the material selection for key components to materials which have high strength and durability. These materials normally come with a high density meaning the mass of the component is also high. This left two options;

1. Reduce component weight, but also reduce maximum power output due to risk of component fails.
2. Move the heavy mechanical components away from the foot.

Option two was investigated by a design of harvester that has the main mechanical harvester component in a back pack worn by the wearer. Two foot units were design and strapped to the wearer's shoes. The footfall forces can then be transferred up to the back pack.

The first stage of the design process was to create a simple table listing the good points of the initial footfall harvester design that will be carried through to this design and the key points that need to be improved. Table 5-1, shows the key points that were considered.

Table 5-1 Parameter analysis of initial wearable enrgy harvester design

Initial design parameters	Good	Bad	Solutions
Input bar protruding below the shoe line	This proved to work and converted the footfall force into torque well	The bar was of fixed length and was not adjustable for different wearers	Add adjuster to end of bar. Wearers can change input displacement to suit them
High up ratio planetary gearbox	Transformed a small angle change into multiple rotations, but saw a high fatigue rate occurring during testing	Limited gear ratios. Too high a ratio results in large torque figures at start up, too low and the angular velocity seen by the transducer is small and results in low power	Reduce the sudden input velocity of when the foot is placed on the floor via the addition of a spring. This will result in the ability to have a larger gear ratio.
Whole harvester mounted on outside of shoe.	Direct transfer of foot forces into harvester	High cost of harvesting due to wearer having to lift the weight of the harvester each step they take	Move harvester into backpack worn by wearer and transfer the force up to the main components

The heavy components in the initial design were the up ratio gearbox, and the chassis. The gearbox was heavy due to needing to withstand sudden torque increase each time the input bar was forced upwards. The chassis was as light as it could be being made from aluminium, but it still needed to be made from 3.5 mm thick plate to enable it to withstand fatigue from repeated shock loading at connection points. The following design has been developed to move these components up off of the foot and as close to the wearer's centre of gravity. This will also reduce the cost of harvesting as the harvester's mass is now closer to the wearer's centre of gravity reducing the amount of energy consumption of the wearer carrying and using the harvester.

5.2 Improved Harvester Design

The final design for the improved footfall energy harvester became very complex in order to improve multiple bad points found with the initial design. The harvester has been nicknamed SS12. The number is relative to the development stages taken to get to this final design shown.

5.2.1 Overview of improved design

The basic energy extraction method is similar to the initial design, but this is where the similarities end.

Figure 5-1 Photographs of finished prototype for the improved design

Error! Reference source not found. shows the finished prototype of the improved design. It can be seen with foot units strapped to the shoes and the backpack being worn.

Footfall forces are extracted via the foot units and the energy is transferred via high tension cables up to the main unit in the backpack. In the backpack there is a mechanical assembly that converts the shape spikes from footfall

into a smooth rotational movement which is transferred into the electro-magnetic transducer.

The foot unit that straps to the wearer's shoe ensures an input bar protrudes below the shoes outsole and is forced upwards when the wearer places their foot onto the ground. In this design the input bar rotates around a pivot on the foot units and the opposite end of the input bar pulls on a lightweight high tension cable. This cable transfers the input displacement of the input bar up into the main unit that is held within a backpack. The end of the cable in the main unit connects to an input arm. When the cable is pulled, the input arm rotates. Fixed into the input arm is a Sprag clutch that is engaged when the cable is pull and free wheels when the input arm in pulled back via a return spring. The return spring pulls the input arm, cable, and input bar on the foot unit back to their starting positions ready for the next input. When the input arm is pulled by the cable the clutch forces an input shaft to rotate. This shaft can only rotate in one direction due to another Sprag clutch being used as a holding clutch fixed into the casing of the main unit. This shaft is connected to the inner end of a reel spring. Each time there is an input on the input arm the spring is winding up, and adding to tension held within the spring the reel spring cannot unwind via the input shaft due to the holding clutch. The opposite end of the reel spring (the outer end) is connected to a large cup in which the entire reel spring sits within.

Once the reel spring holds enough tension the outer cup starts to rotate. The cups rotation is now unwinding the reel spring. The spring can be "winding up and unwinding at the same time in the same direction. This is a very unique feature of this design. The cup is connected to a high ratio and high

torque multi stage planetary gearbox. Connected to the back of the gearbox is a small, light-weight electric motor. As the spring cup starts to rotate the gearbox input shaft, the motor starts to rotate at a lot high velocity and starts to produce an electric output. On the back of the motor is a flywheel. This flywheel aids in increase the maximum tension held within the reel spring before the motor starts to rotate and also helps regulate the motor speed which improves in the electric energy production.

For a clear understanding of the harvesting procedure, the device has been divided into 3 different areas and these areas are as follows:

The foot units

The Kinetic energy rectification

Angular velocity increaser, transducer and Inertia controller

5.2.2 **Foot Units**

This resembles the initial harvester design in only two ways. One, being that the unit is strapped to the wearer's shoe via a quick release SIDI buckle and a flexible strap making it a retrofit wearable energy harvester. The strap includes a piece of elastic sewn in to improve fitting and strap tension. The second is the energy input method. This is done by an input bar that protrudes below the shoe line. Figure 5-2 shows a detailed design render of the evolved foot unit.

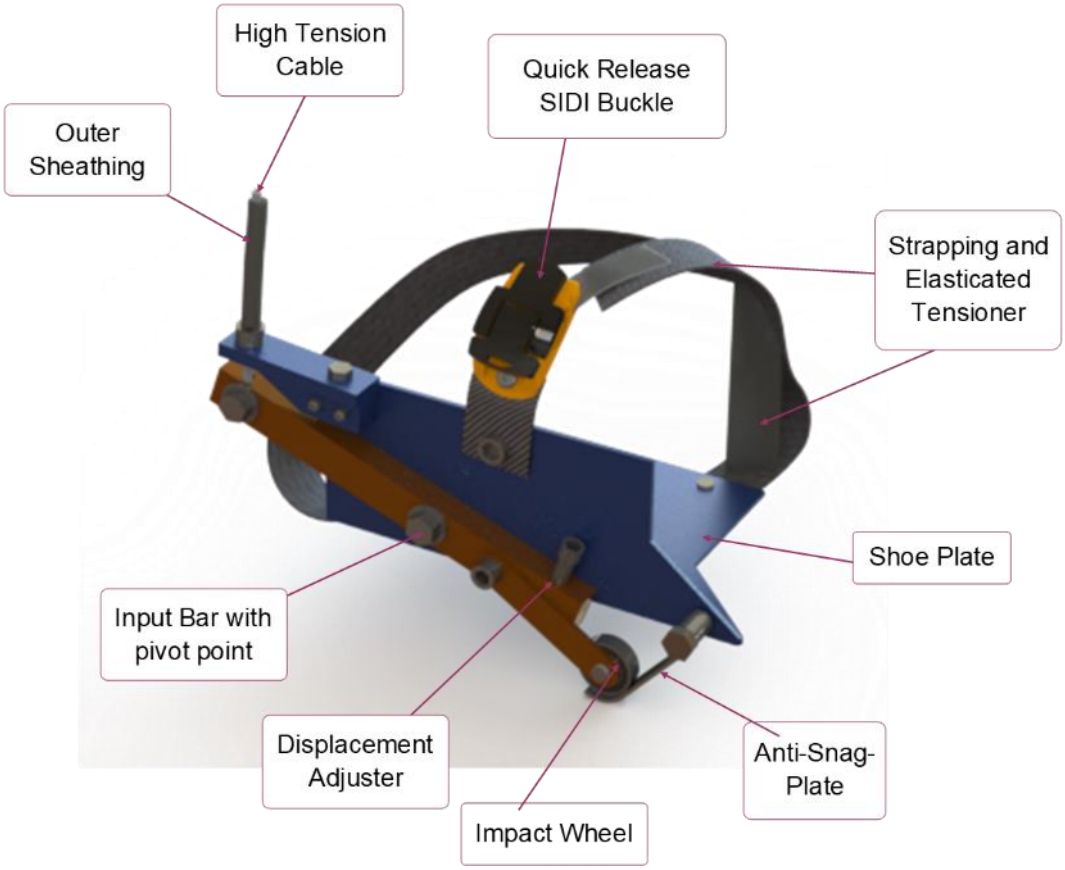

Figure 5-2 Foot unit of the improved wearable energy harvester design (right foot unit shown)

This proved to be a productive way of inputting the footfall energy into the harvester via the initial design. This design however does not have the input bar connected to the gearbox input shaft, it instead rotates round a pivot point and acts as a lever. The input bar includes an anti-snagging-plate similar to the first design to ensure safety of the wearer and reduce the risk of the input bar becoming a trip hazard. One end of the lever sees the input force from the foot moving towards the ground and the opposite side of the lever (input bar) pulls a high-tension cable. This cable runs up behind the wearer's legs to the main harvester. In this design the main part of the harvester has been moved to a backpack, it results in lightweight foot units making it easier to wear a foot unit on both feet.

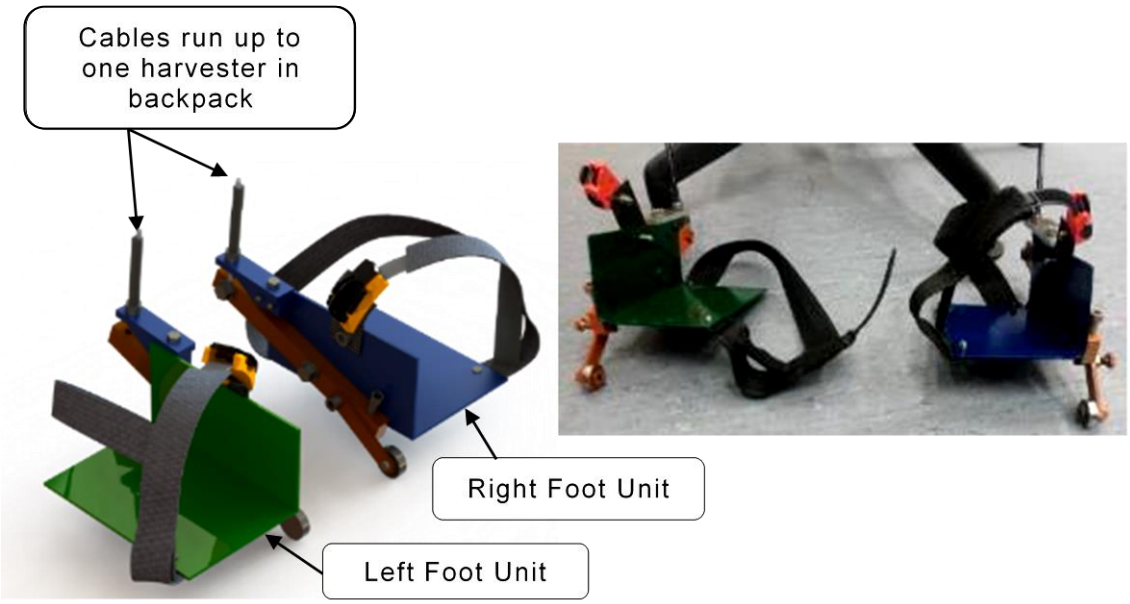

Figure 5-3 Design of the foot units for the improved harvester design

Each foot input will go into the same harvester. The mass of the foot unit in the initial design was the whole mass of the prototype harvester, weighing 1.2 kg per unit. This design means that the footfall force from both feet can be harvested without doubling the weight of the harvester. This will reduce the weight carried on each foot, which will improve cost of harvesting compared to the initial design. The design renders and the final prototyped foot units are shown in Figure 5-3.

5.2.3 **Kinetic Energy Rectification and Mechanical Energy Storage**

Here the sharp sudden spikes of force seen in footfall harvesting are captured, sorted and outputted in a controlled smooth continuous pattern. This will reduce the problems of electrical storage and rectifying, which has been proven to be costly in terms of energy use generated by the harvester. Figure 5-4, shows a labelled render of this section of the harvester.

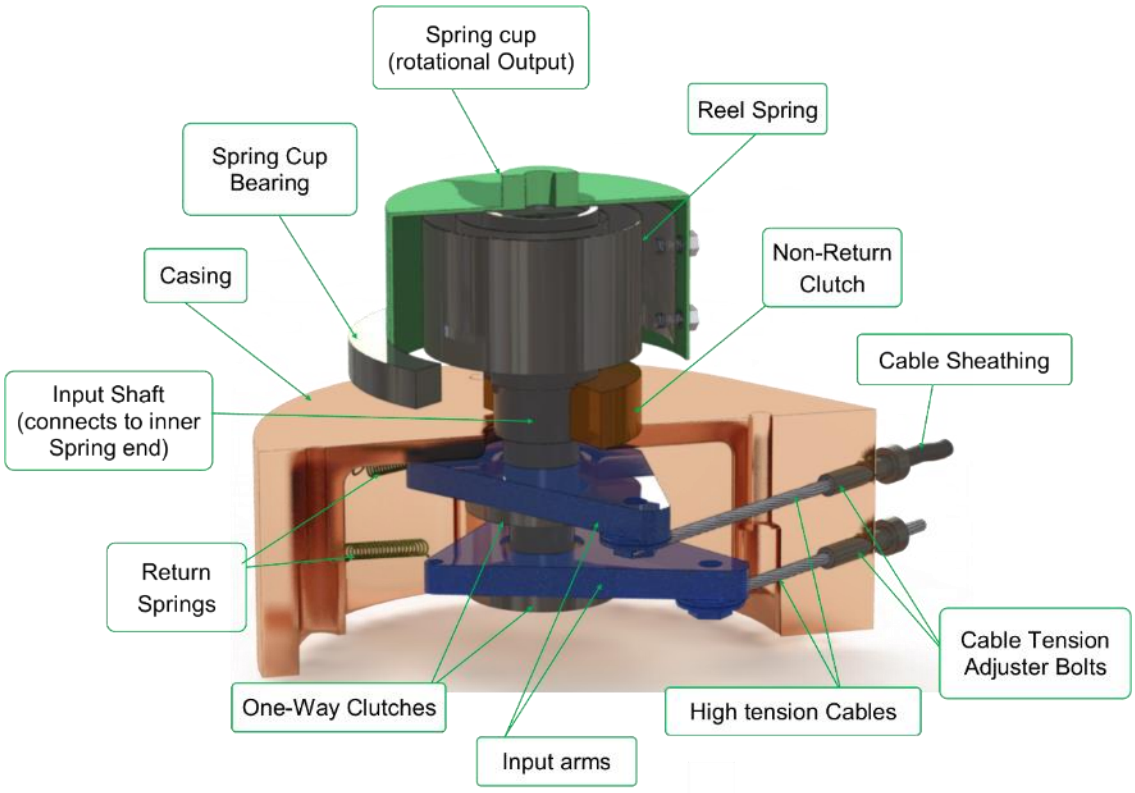

Figure 5-4 Footfall rectifier system and mechanical storage section view

The cable being pulled by the foot unit is connected to an input arm. The input arm incorporates a Sprag clutch and a return spring. The clutch connects the input arm to the input shaft. This means when the cable is pulled the input arm rotates and in turn, rotates the input shaft. When the foot is lifted and the tension on the cable is reduced, the return spring rotates the input arm back to its starting position.

This at the same time pulls the cable back, and re-protrudes the input bar on the foot unit. When the return spring is rotating the input arm backwards, the Sprag clutch is disengaged and the input shaft is not rotated.

The input shaft transfers the motion of the input arm through into a spring area. The shaft runs through another Sprag clutch (non-return clutch). This clutch is connected to the input shaft and the casing of the harvester. This clutch only lets the input shaft move in one direction. The end of input shaft in the spring area is connected to a torsional spring or reel spring. When the input arm is rotating due to the footfall force on the cable, the input shaft is also rotating and this is adding tension to the spring. The spring cannot unwind by rotating the input shaft backwards due to the second Sprag clutch. The spring spirals round the input shaft and the opposite end is connected to a spring cup. Each footstep adds more and more tension to the spring until the spring holds enough tension to overcome the inertia of the rest of the harvester. While this stage is in operation, the spring can be being wound-up and unwound at the same time.

This is the first time a spring has been used this way, making this design very unique.

There are three stages to the spring operation

1. First stage, wind up.

   Only the input shaft is rotating in pulses from footfall and is winding up the spring adding tension to the spring system.

2. Second stage, active harvesting.

   Here both input shaft and spring cup are rotating. This is again broken down into two sections,

   1: Acceleration of spring cup,

   2: The frequency of winding and unwinding depending on input frequency and load out loading or damping.

3. Third stage, unwind

   This is when the wearer has stopped walking and the input shaft into the spring is no longer rotating from any inputs. The spring still has enough tension to maintain the rotation of the spring cup and keep outputting energy. This will slowly decay and its rate will be dependent on the loading or damping of the harvester.

Once the energy has entered the spring, the only way it can come out is via the next stage of the harvester. In this stage, the energy can be stored in the form of potential energy held within the spring and output after the input energy has stopped.

To aid in explaining what is happening to the spring illustrations were created and are shown in Figure 5-5.

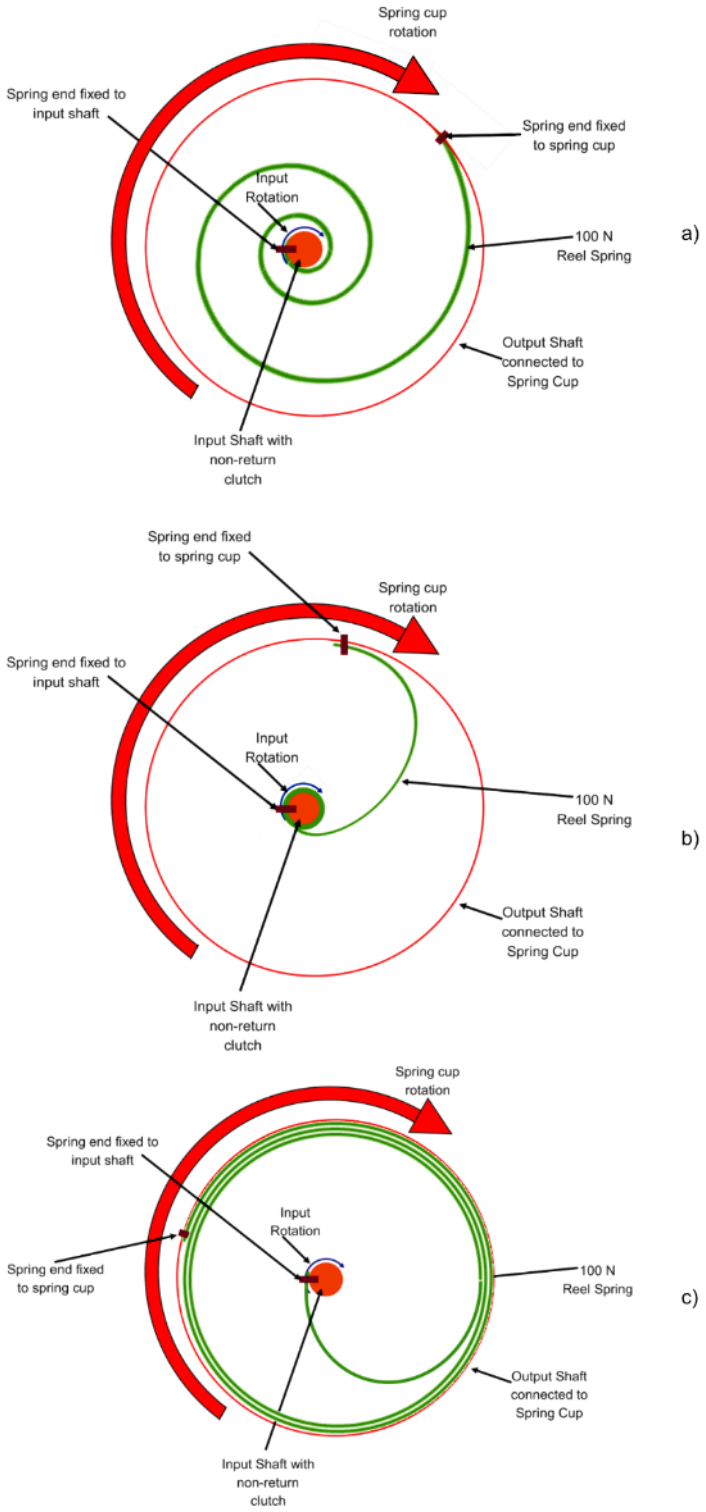

Figure 5-5 States of the mechanical energy storage system via the installed reel spring: a) Natural spring state, b) Full tension state from fully winding up, and c) Fully relaxed state unwound spring providing easy start up for next use

Figure 5-5 a) shows how the reel spring sits after installation into the harvester. The internal end is fixed to the input shaft and the outer end is fixed to the spring cup (output shaft). The input shaft can only rotate clockwise due to the non-return clutch. The input shaft is rotated each time the input arm receives an input from footfall.

Before the gearbox, transducer and flywheel start spinning, the reel spring winding itself up until it holds enough tension to overcome the systems static inertia. Figure 5-5 b) shows what the reel spring would look like it the spring cup was never allowed to rotate.

Once the spring has stored enough energy to break the static inertia, the spring cup will start to rotate. Once the system is up to speed and inputs stop, the system keeps spinning and unwinds the spring. Figure 5-5 c) shows what the spring would look like after completely unwinding.

5.2.4 Angular Velocity Increaser, Transducer and Inertia Controller

In this stage the low angular velocity of the spring cup rotating from the spring tension is transferred through an up-ratio gearbox and into the transducer.

Figure 5-6 Harvester's up ratio gearbox, transducer and interchangeable flywheel

Figure 5-6 shows the final render of this section where the gearbox input shaft connects to the spring cup. The gearbox is a 416:1 planetary gearbox by Portescap. This ratio was chosen as it will output into the transducer at a rate which will be very close to the transducer's optimum RPM for maximum efficiency of the transducer. This gearbox is very small and light, but has a maximum torque transfer capability of 22Nm. This torque figure means the gearbox will not fail from sudden shocks, increased loading and lots of testing.

The transducer is another DC motor. This is a brushed DC motor by Maxon. This motor was chosen as it had an output shaft on each end.

There were not many motors available with shafts on each end which resulted in this one being the best option for the harvester. The motor needed to have shafts at each end so one end can have the pinon for the gearbox and then the other can have flywheels added and removed for testing.

The harvester will have a flywheel connected directly to the transducer. This is done for two reasons;

- To add static inertia to the system to increase the spring tension before the transducer starts spooling up.
- To increase the time of the energy recovery stage.

The flywheel on the transducer end of the system will act as a damper to the pulsing incoming wave of spring energy and also as an extra energy storage system. Here the energy will be in the form of kinetic energy.

5.3 Improved Design Theoretical Analysis

In this section an analysis of the improved design will be explained with the aim to justify how the spring and flywheel were chosen and work together to increase the average power generation from this design of harvester.

First, the initial conditions will be set in order to perform the theoretical analysis. The environment conditions will be the same as used in the initial harvester design, but the harvester design parameters have changed.

Table 5-2 Input Conditions and Improved Harvester Design Parameters

Symbol	Environment Condition	Unit	Value
m	Wearer Mass	kg	75
Freq	Step Frequency per foot	Hz	1
v	Footfall Velocity	m/s	0.4
g	Gravity	g	9.81
	Harvester Conditions		
r	Input Bar Length	m	0.1
y	Input Displacement	m	0.04
Lev rat	Lever ratio	1:	0.75
r_a	Input Arm length	m	0.05
k	Spring constant Force	Nm	100
S_{od}	Spring outer diameter	m	0.038
Gb rat	Gearbox Ratio	1:	416
Gb eff	Gearbox Efficiency	%	40
Ke	Motor Speed Constant	V/RPM	1.1
Km	Torque Constant	mNm/A	15.7
R_m	Motor Terminal Resistance	Ω	4
R_l	Connected Resistive Load	Ω	10 - 40

5.3.1 **Selecting the Spring**

A constant force reel spring was chosen for the mechanical storage system of this improved design to provide the same resistance to the wear each step and also provide a smooth constant acceleration force to the transducer. Having a spring with too high a force would result in the wearer feeling the resistance to winding up the spring and causing them to either change walking style or feel discomfort. Having a spring with too little force would result in the spring not providing the transducer with a smooth acceleration. A soft spring would wind up to maximum tension then directly transfer the force from the input to the output, making the spring redundant. A reel spring was also chosen due to its size and mass, both being low. The reel spring chosen for the improved design has a constant force of 100 N. This would provide none if very low resistance to the wear and provide the transducer with a smooth acceleration. Each time the wearer walks the footfall force inputs energy into the spring.

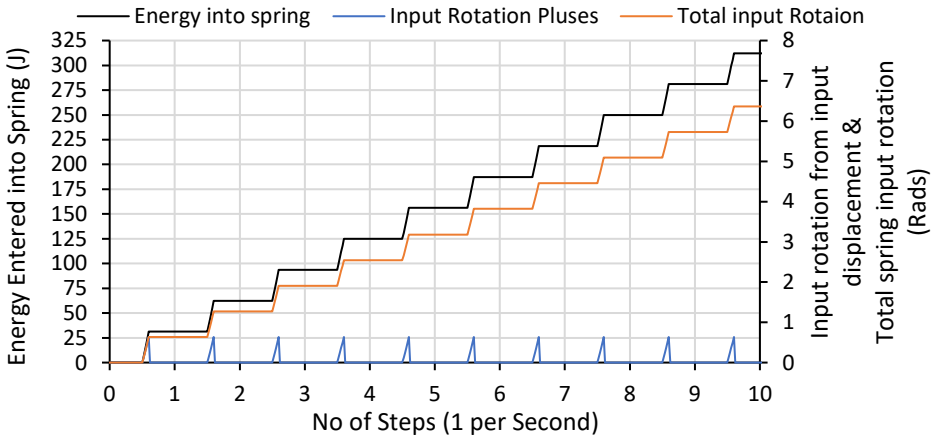

Figure 5-7 Input displacement spikes from footfall, Total input rotation of spring and Accumulated energy entered into the mechanical energy storage system

It can be seen in Figure 5-7 that each time the wear places their foot on the ground a spike of input rotation (blue line) is seen entering the spring. This rotation is increasing each step the wear takes (orange line). Using the data

shown in Table 5-2, and calculating this input rotation value along with the torque applied to the inner end of the spring, the energy entering the spring can be calculated. It has been calculated that 31.4 J will be entered into the spring each step. This energy is stored in the spring and can only be released through the transducer. As the spring chosen is a constant force spring the output force will be constant into the transducer, but the rate will be determined by the inertia of the transducer and the flywheel installed.

5.3.2 **Selecting and Sizing the Flywheel**

By adding a flywheel to the transducer two effects will result. One being the smoothing of the input energy coming from the stored energy in the spring and the footfall input pluses, and the second is to increase inertia of the transducer improving the average rotational speed of the transducer. The second factor will also aid in unwinding the spring once input into the spring have stop resulting in the transducer producing electrical energy after energy input from footfall has stop. The constant force spring will output a constant force once starting to move the transducer and flywheel. Knowing the spring force of 100 N and the spring cups diameter 0.038 m, the spring will output 3.8 Nm of torque into the gearbox. The gearbox has a up ratio of 1:416, this will result in a torque output from the gearbox and input into the transducer of 0.0091 Nm (9.13 Nmm).

By knowing the torque input into the transducer and flywheel, the angular acceleration can be calculated using Newtons second law rearranged and using the inertia of the flywheel and transducer. This is shown in Equation *(**5**-**1***.

$$\alpha = \frac{\tau_{in}}{I} \qquad (5\text{-}1)$$

Where α is the angular acceleration, τ_{in} is the constant torque input from the spring and I is the inertia of the transducer and flywheel system. I will change depending on the flywheel used and will affect how quickly the transducer will accelerates. If the flywheel is too heavy, then the transducer will take a longer time to reach is target operating speed which will reduce the harvester average power output.

The target rotation speed is calculated from the motor data sheet. The motor is a Maxon A-Max 32. This motor runs at 4590 RPM when supplied by 12 V. The target voltage is 5 V for charging portable electronic devices and from the motors data sheet, with no load connected to the motor, the motor would produce 5 V at 1912.5 RPM. By knowing the target RPM and calculating the angular acceleration of the transducer with different flywheels, Equation*(5-2)*can be used to calculate the time taken for the harvester to reach 5 V.

$$T = \frac{\alpha}{\omega_t - \omega_1} \qquad (5\text{-}2)$$

Where T is the time taken to reach target RPM, α is the angular acceleration, and ω_t and ω_1 are the target RPM and the starting RPM respectively.

$$I = m \times k \times r^2 \qquad (5\text{-}3)$$

I is calculated by the moment of inertia equation shown in Equation***(5-3)***, where is the m is the mass of the flywheel, k is the moment of inertia shape factor set to 0.606 for a flat solid disc and r is the radius of the flywheel set to 0.04 m.

By using these equations the time for the transducer to accelerate to its optimum RPM to produce its selected voltage can be calculated and is shown in Figure 5-8.

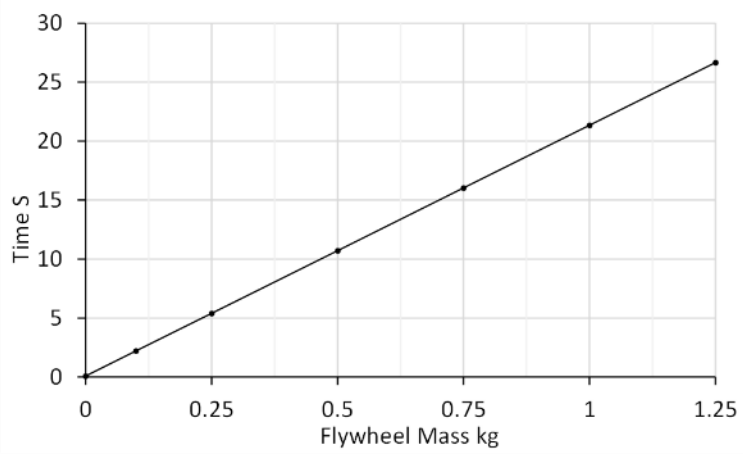

Figure 5-8 Time taken for transducer to reach target RPM to produce 5 V with different flywheel masses installed

As the transducer accelerates towards its target RPM the voltage will increase to achieve its target voltage at its target RPM. With an increasing voltage the current draw across an external resistive load will also increase. With an increasing current draw will come an increasing back EMF or back torque. To calculate the back-torque generation from the transducer, Equation*(5-4*)can be used.

$$T_{gen} = \frac{V}{R_m + R_l} \,.\, Km \qquad (5\text{-}4)$$

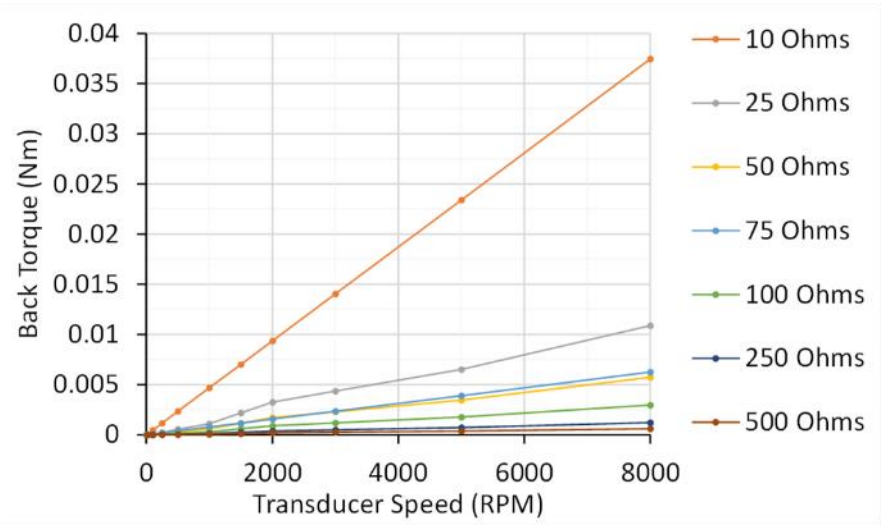

Figure 5-9 Back torque generation by the transducer from increasing rotational velocity when connected to different external loads

The results shown in Figure 5-9 confirm that as the connected resistive loads is increased the back torque also increases. There is a large increase of back torque when connected to the 10 Ohms load and increasing the connected load any further would result in damage to the energy harvester mechanical components. Figure 5-9 also shows that as the connected resistive load decrease the back-torque generation decreases at a progressive rate.

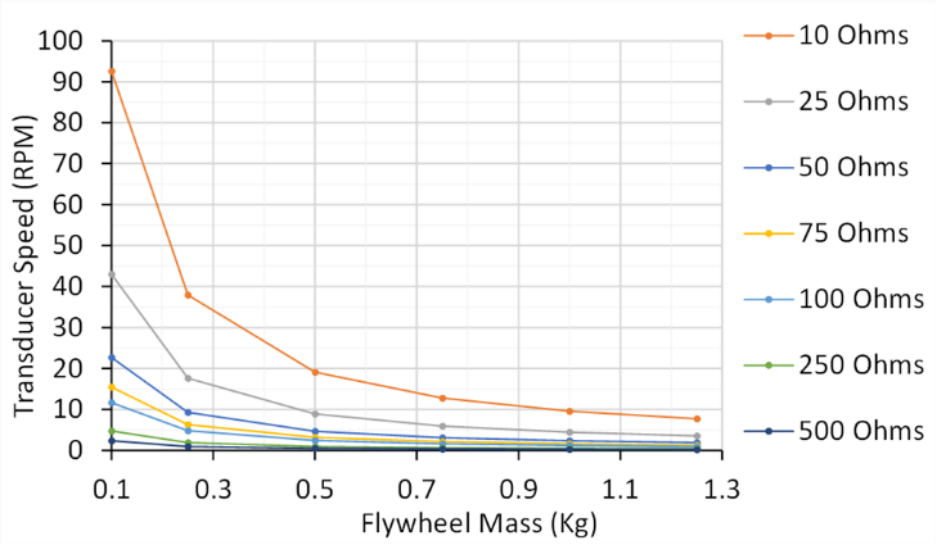

Figure 5-10 Transducer speed reduction per second when using different mass flywheels and connected to different external resistive loads with no input

In Figure 5-10 it can be seen that with a heavier flywheel mass the rotational velocity reduction that will occur in between the incoming input pluses from

footfall and spring during normal operation is dramatically decreased. This shows the importance of the flywheel. If a flywheel is used the rotational velocity reduction of the transducer caused by the back-torque coming from the EMF generation can be reduced. By reducing the speed drop a higher average voltage can be maintained. Figure 5-10 also shows the larger the resistive load the larger the transducers velocity reduction will become. 10 Ohms shows the highest velocity drop with only a lightweight flywheel installed. The difference between a lightweight flywheel and a heavy flywheel when connected to 10 Ohms is 85 RPM. When the 500 Ohms load is connected the difference is on 2.1 RPM from using a light or a heavy flywheel.

From this it would suggest that using a heavy flywheel is better for the energy harvesters design but looking back at Figure 5-8 it is clear that a heavier flywheel increases start time dramatically. It is also clear the connected resistive load has the largest effect on back-torque generation and the transducer velocity fluctuation resulting in less average voltage. This means if a too large resistive load is using the benefits of getting a larger current draw might be not worth the side effects of reduced average transducer velocity resulting in higher transducer velocity drops per second and increased the back-torque which would lead to over stressing the light-weight mechanical components.

From the equation used and the graphs displayed the following power results can be predicted from the Improved design and are shown in Table 5-3.

Table 5-3 Improved harvester design electrical power outputs when connected to different resistive loads

Transducer Speed and output		Connected Load						
		10 Ohms	15 Ohms	20 Ohms	25 Ohms	50 Ohms	75 Ohms	100 Ohms
RPM	Voltage	Watts	Watts	Watts	Watts	Watts	Watts	Watts
1000	2.525	0.638	0.425	0.319	0.255	0.128	0.085	0.064
1500	3.788	1.435	0.957	0.717	0.574	0.287	0.191	0.143
1750	4.419	1.953	1.302	0.976	0.781	0.391	0.260	0.195
2000	5.051	2.551	1.701	1.275	1.020	0.510	0.340	0.255
2250	5.682	3.228	2.152	1.614	1.291	0.646	0.430	0.323
2500	6.313	3.986	2.657	1.993	1.594	0.797	0.531	0.399
2750	6.944	4.823	3.215	2.411	1.929	0.965	0.643	0.482
3000	7.576	5.739	3.826	2.870	2.296	1.148	0.765	0.574

From Table 5-3 it can be seen that there is only a small ranger in which the harvester will produce the correct voltage and enough power to charge a portable electronic device. The area highlighted in light orange shows the maximum range the harvester would be able to charge a portable electronic device but would not be healthy for the device's battery life due to the unstable charging conditions. Outside of this (no highlights) and the voltage and or power would not be correct, and the device would not charge at all. The area highlighted in orange show the area in which the harvester will be producing enough power at the correct voltages to charge a portable device at a suitable rate. The 10 ohms load column shows the highest power output, but the 10 ohms load effected the harvester heavily. 50 Ohms and above the harvester will not produce enough power to charge a portable electronic device.

From the analysis performed surrounding the selection of a suitable spring, a 100 Nm spring will be chosen for the improved harvesters design. This will output enough torque to constantly rotate the transducer at the target speed when connected to a resistive load that will produce enough power for charging a real-world device. The flywheel is used as a transducer velocity fluctuation stabilizer and from these calculations a flywheel with an inertia of between 0.25 g/m2 to 0.49 g/m2 would be of optimum size. Knowing the size and weight constraints of the improved wearable energy harvesters design the flywheels mass will between 0.2 and 0.5 kg depending on it shape. Tests will be performed on flywheels between 0 and 0.85 kg to confirm the optimum flywheel mass and inertia. This can then be used to produce a final flywheel design which can be less mass but of the same inertia for optimum results.

5.4 Experimental Conditions and Procedures

Here how, why, and what was tested will be explained. The tests will use the normal walking test procedure from the initial design. This is done for consistency and ease of comparison. The normal walking conditions are shown in Table 5-4.

Table 5-4 Input conditions used to test the improved harvester design

Factor	Value
Displacement	40mm
Velocity	0.4m/s
Frequency	1 Hz *

* 1 step per second per foot. (1Hz & 2Hz will be tested for 1 & 2 foot inputs)

5.4.1 Test Procedures

The Instron tensile testing machine was used again, along with the same wave matrix programming. The ground plate is the same as design one to ensure the same ground reaction is seen. The aim of the tests will not only be to find the optimum resistive load for maximum energy extraction, but also to find the relationship between flywheel mass and optimum load and how each part effects energy extraction, leading on to confirm the electrical energy generation capability.

The tests started with no flywheel and the load resistance decreased from 100 Ω down to 10 Ω. When preliminary tests were performed on this harvester design, it was seen that when the load resistance was below 10 Ω the back torque generated became so high that the input system failed and needed rebuilding multiple times. From the results from the initial design, decreasing the load resistor past 10 Ω confirmed there were no increases in power output, so will not be investigated any further here.

From the tests and results seen in the previous chapter, the walking input pattern will be set to a normal average input for the Instron tests and then changed on the treadmill tests to confirm the design now delivers a average power output no matter what the walking style. This is shown in section 5.6 - Results from Treadmill Testing.

In total 42 different test set ups were performed made up from 7 different resistive loads and 6 different flywheel inertias. Each flywheel mass was tested on each resistive load valve in order to confirm the optimum resistive load for given flywheel mass.

Figure 5-11 shows the harvester installed into the Instron testing machine. Here the foot unit was held in the top grips and moved toward a ground plate held in the lower grips.

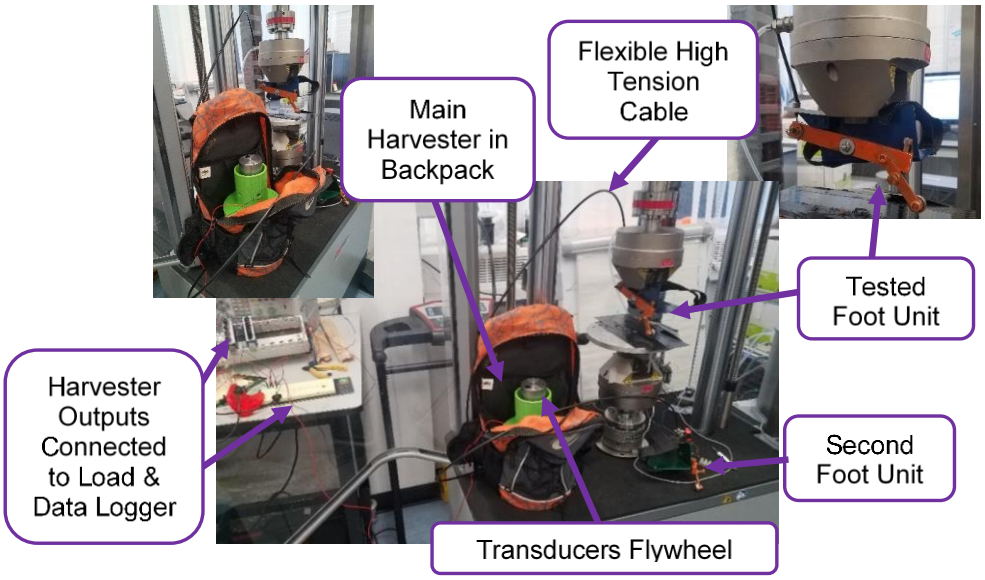

Figure 5-11 Harvester being testing in the Instron testing machine

Increasing the flywheel mass attached to the transducer is also tested. Each time an increased flywheel mass is added, a new set of tests were performed where the load resistor is increased as before.

The aim of these tests is to confirm the optimum flywheel mass or inertia of the high velocity components (transducer). Five flywheel masses were tested, and the results analysed.

From these results, an optimum flywheel mass and resistive load were known for normal walking. These harvester conditions were then tested on a treadmill at the three typical gait speeds of 3.6, 5.4, and 7.9 km/h. This was done to confirm the results from the Instron machine under normal walking conditions and to see how the harvester would perform being worn and used by a human would react under different walking patterns.

Figure 5-12 Improved design of wearable energy harvester shown being tested on the treadmill

The treadmill tests were performed multiple times and averages were taken. Figure 5-12 shows the energy harvester being worn and tested on the treadmill.

Endurance testing is perform by walking at a normal speed of 5.4 km/h and 2 steps per second (one step per foot) for a period of one hour. This confirms the harvester has been designed correctly for sustained use. The

results from the endurance testing aim to show the harvesters ability to change a portable electronic device available on today domestic market.

5.5 Experimental Results from using the Instron Machine

This section contains the organized results from the testing of the evolved energy harvester design. The results from the experiments have been analysed and their findings reported throughout this section. A maximum load resistor value was set at 10 Ω. This was done for two reasons;

- The data from testing the previous harvester design showed a sharp drop off in power below 10 Ω.
- When preliminary tests were performed on this harvester design, loads below 10 Ω resulted in extreme fatigue to components.

The results have been organized into four areas.

- Optimum load resistor for harvester with no flywheel
- 3 stages of harvesting relative to the reel spring stages
- Optimum load resistor for harvester with different flywheels
- 2 foot harvesting, the optimum conditions and maximum power extraction

The results section contains a section on the how the flywheel and resistive load relate to each other and what the optimum flywheel mass and load would be of maximum energy extraction for this design verified by the real-world testing on a treadmill. The improved harvester design will be shown to charge a modern portable electronic device with no on-board electronics, power management or electrical store vessels such as capacitors or batteries. Unlike the initial design the outputs from the improved harvester changed very small amounts during the Instron testing. The tests were consistent, and the harvester was not breaking. The changes occurred due to the previous test set up and end state of the spring. If a low resistance load was connected, then the spring would be completely unwound before the next

test started. Whereas if a large resistive load was connected then the spring would stop in a semi-wound state until this load was removed. The results shown in this section display average results from multiple tests. Standard deviation is used to confirm the changes in outputs are very small.

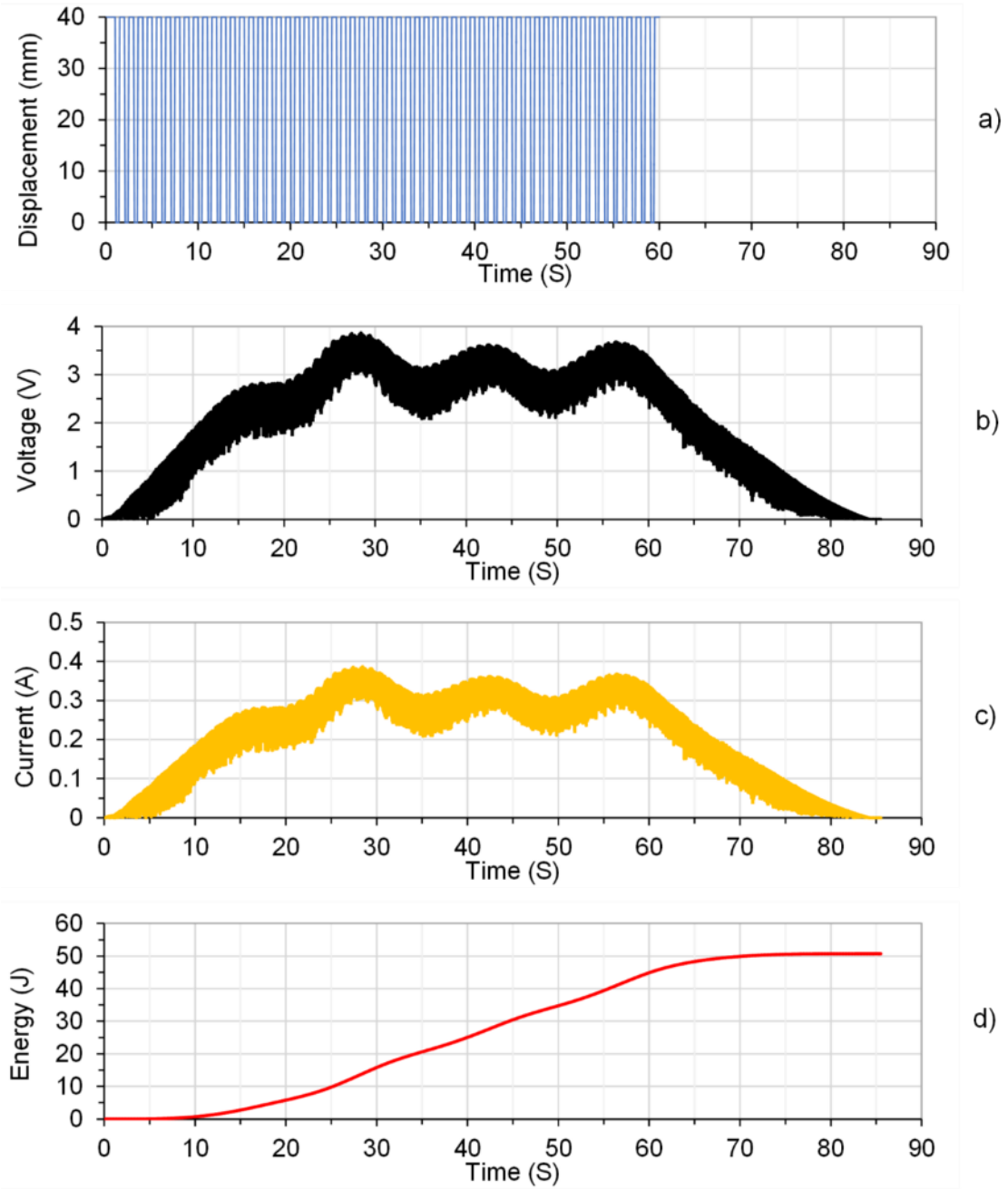

Figure 5-13 Improved harvester design results when connected to a 10 Ω resistive load: a) Input displacement, b) Voltage generated, c) Current generated, and d) Total Energy generated

Shown in Figure 5-13 is a complete test result from one of the many tests performed on the Instron machine. It can be seen that the input displacement is the same as used with the previous harvester, yet the outputs

are completely different. It also shows how the harvester continued to generate electrical energy after the inputs had stopped. It also shows how noisy the voltage signal is from the harvester transducer. This is down to the DC motor being used in this design. The motor was selected for its output voltage and motor constant value, but more importantly as the motor shaft extended out the back of the motor. Only a few motors have this feature making it suitable for installing different flywheels to the system with the need to dismantle. The drawback being the quality of the motor as a whole is not as good as the motor used in the first design.

5.5.1 Locating the Optimum Load Resistor with No Flywheel

The first set of tests performed were to find an optimum load resistor for the basic harvester set-up. This was performed to find the maximum power from the harvester without any flywheel connected and this provided a datum for the flywheel tests to compare to. The tests were performed at an input frequency of 1 Hz, normal walking frequencies for one foot harvesting. The load resistor was changed from 250 Ω down to 10 Ω and the input conditions from the Instron machine were the same as those used in the first design testing chapter.

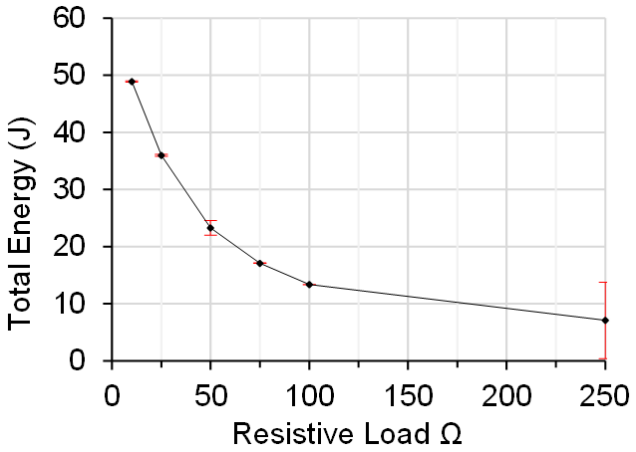

Figure 5-14 Total energy generated by the improved harvester design in 60 s when connected to different resistive loads including standard deviation error bars

The graph in Figure 5-14 shows that as the load resistor was increased, the total energy generated also decreased. The best result was over the 10 Ω resistor where the total power seen was 48.9 J. When this harvester was connected to the 250 Ω resistive load, this design only produced 7.1 J.

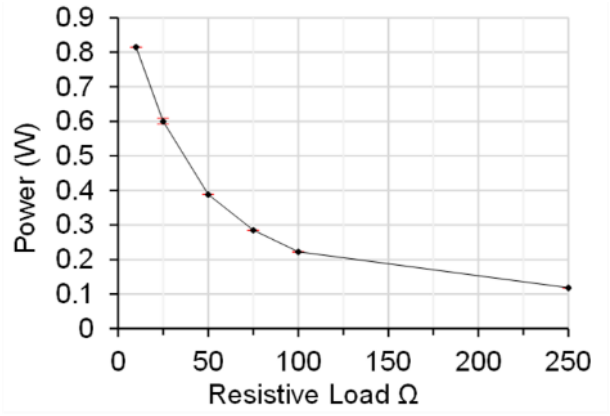

Figure 5-15 Average power generated by the improved harvester design in 60 s when connected to different resistive loads including standard deviation error bars

Figure 5-15 shows that the lower the resistive load, the higher the average power output will be. Below 10 Ω the harvester failed, and as a result, produced no power. The maximum average power seen from testing the harvester under these conditions was 0.55 W. This average power was calculated by taking the total energy generated and dividing it by the total time the harvester ran for in each test. The time each test ran for changed depending on the resistive load connected, even though the input wave time

was the same, 60 steps in 60 seconds. An explanation for this is the integration of the reel spring.

The graph in Figure 5-16 shows the total harvester run time of each test over different resistive loads. In this context ‘run-time’ is define as the total time the harvester was working for. This is from the first input into the harvester, to when the harvester final stopped generating electrical energy. This is important as this harvester continues to output electrical energy after the inputs have stopped.

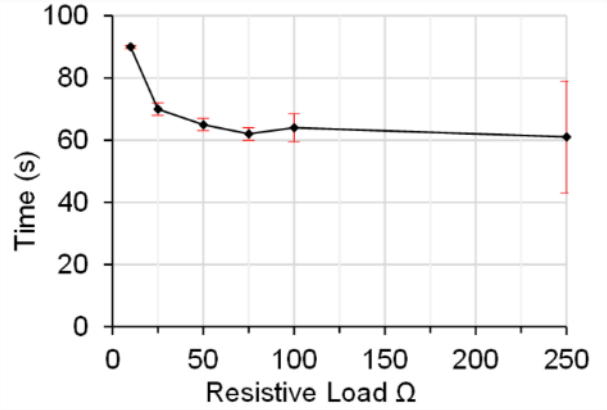

Figure 5-16 Total run time of each test of the improved harvester design when connected to different resistive loads including standard deviation error bars

It can be seen here, that as the resistive load increases, the run time of each test decreases. When the harvester was connected to the 10 Ω resistive load the test time increased from the 60 s of input to 90 s. This resulted in a drop in average power due to the total energy generated being over a longer time frame. When the average power is calculated, the longer the harvester extended its run time by, the lower the average power became. A better representation of the harvester’s average power is power per step and this is shown in Figure 5-17.

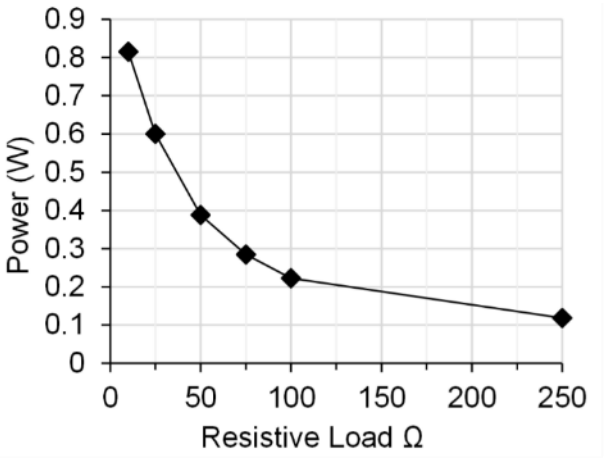

Figure 5-17 Average power generated per step

This shows how much power the harvester generated during an active input period. This shows that a wearer wearing only one foot unit and walking in a normal manner would produce an average power output of 0.82 W. This can be seen as 0.82 W per step.

Figure 5-18 shows the energy generated from the harvester over one whole test when connected to a 10 Ω resistive load. The input wave was as seen in Figure 5-13 and ended at 60 s, but this harvester's design continued to generate energy for a further 30 s.

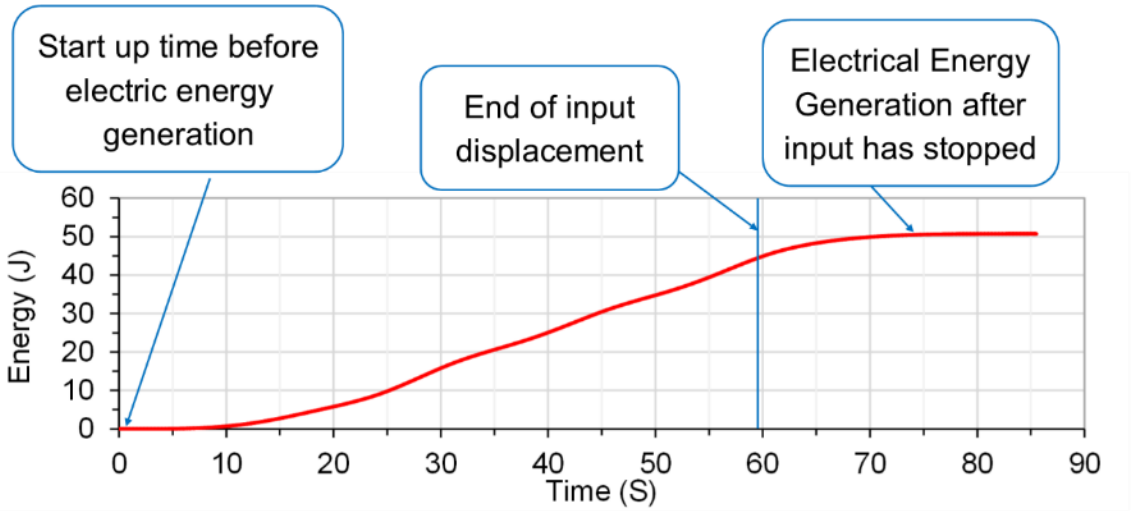

Figure 5-18 Energy generated with no flywheel installed when connected to a 10 Ω resistive load

Figure 5-18 verifies there is no direct connection between the energy inputted and the energy outputted from the harvester.

Figure 5-19 shows the first 6 seconds of a test in more detail. During this time 6 input displacements have been entered into the harvester, yet the total electrical energy generated is increasing at a steady independent rate.

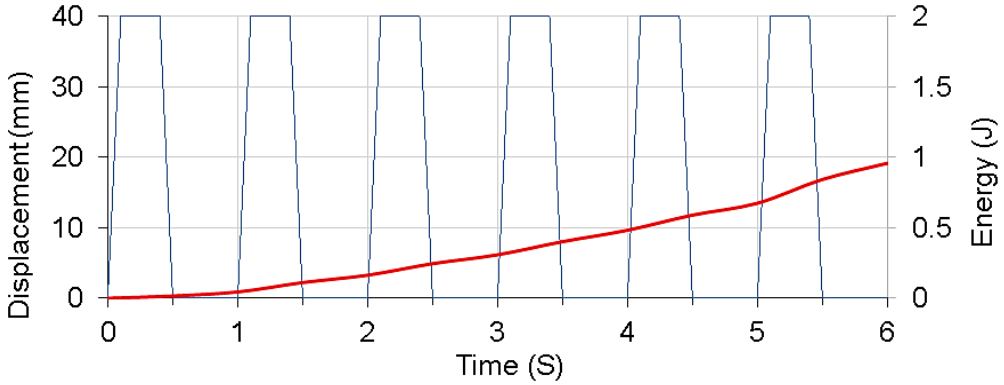

Figure 5-19 Detailed view of the first 6 seconds of test results showing displacement and total energy generated

From the first step of energy in, there is no energy coming out. This is due to the reel spring starting to wind up. This confirms the 3 stages of the reel spring and these stages can now be described differently in a more accurate way.

5.5.2 3 Stages of Harvesting Relative to the Reel Spring Stages

In this section the reel spring stages will be explained in terms of harvesting and outputs seen from the harvester. The three stages explained earlier in this chapter were called:

- Stage 1: Wind up
- Stage 2: Active harvesting
- Stage 3: Unwind to stop

These stages can now be described in more suitable terms after analysing the results of the first set of tests and are now described as follows:

- Stage 1: Acceleration Period
- Stage 2: Active Harvesting
- Stage 3: Energy Recovery

These stages will now be examined to understand the effects the connected resistive load has on the harvester in terms of energy outputted, time of stages and voltage levels seen. This section an explanation of the spring states. Only one set of results are used for the explanation, so no error bars are displayed.

Stage 1: Acceleration period

This is from the first input into the harvester up until the harvester transducer first outputs above its average voltage. In this stage the spring is starting to wind up from the input pulses from the wearer and the torque being applied to the transducer is slowly increasing. Once the transducer is spinning at a speed higher than the average speed of the input pulses, the transducer's velocity starts to reduce. It is at this point that the end of stage 1 can be seen, and the transducer has stopped accelerating.

The length of time was found to change depending on the load resistor connected to the harvester. Figure 5-20 shows the time the harvester spent in stage 1 over different resistive loads.

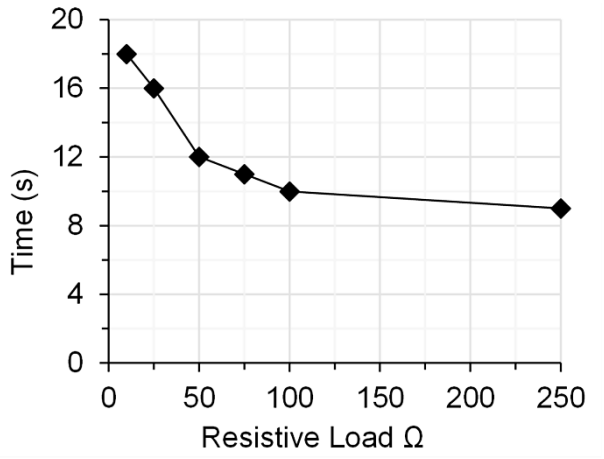

Figure 5-20 Time spent in stage 1 when connected to different resistive loads

When connecting a lower resistive load, the time it took the harvester to reach its average voltage increased. It took 18 s for the harvester to produce 5.3 V when connected to a 10 Ω load, but only 9 s for the harvester to produce 7.8 V when connected to a 250 Ω load. This shows how changing the electrical resistive load can affect the time of stage 1, but as mentioned there is also a change in voltage seen at the end of this stage.

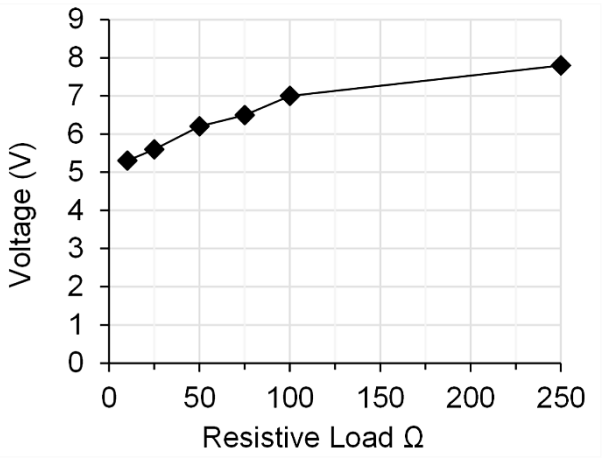

Figure 5-21 Voltage generation in stage 1 over different resistive loads

Figure 5-21 shows the voltage seen at the end of stage 1. A trade-off between start up time and voltage output can now been seen. If a lower resistive load is connected, more tension can be added to the spring before

the end of stage 1 is reached. This results in higher stored energy levels in the spring. At the same time a lower resistive load means lower voltage due to the damping effect the load has on the harvester's acceleration. The optimum situation for stage 1 would be, a low start up time, but a high voltage level. The optimum resistive load for stage 1 for this situation would be 250 Ω. From the 250 Ω tests the harvester had a stage 1 time of only 9 s and the highest Voltage level of 7.8 V. The draw back to this is a low energy generated in this stage over this load.

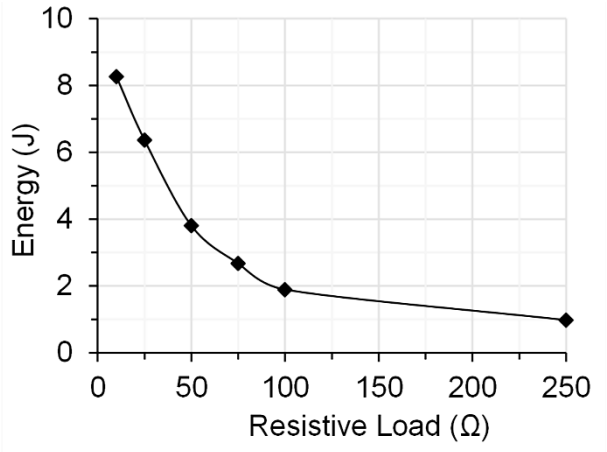

Figure 5-22 Electrical energy generated in stage 1 over different resistive loads

The graph in Figure 5-22 shows that over the 250 Ω resistive load the harvester would only generate 1 J of electrical energy in this stage, whereas over the 10 Ω resistive load, the tests showed an electrical energy generation level of over 8 J. As the aim of this wearable energy harvesting research is to produce as much electrical power as possible, the 10 Ω resistor would be deemed better as it produces a higher electrical energy level.

Stage 2: Active Harvesting

Here inputs and outputs are both happening at once, yet are not related to each other. The length of this stage is dependent on the length of time the inputs continue occurring for. The longer the wearer walks, the longer the active harvesting time. In this stage the spring will be applying torque to the transducer and receiving torque from the input shaft. This means the spring is winding up and unwinding at the same time.

Figure 5-23 shows the voltage out from the harvester when connected to a 10 Ω resistive load during stage 2.

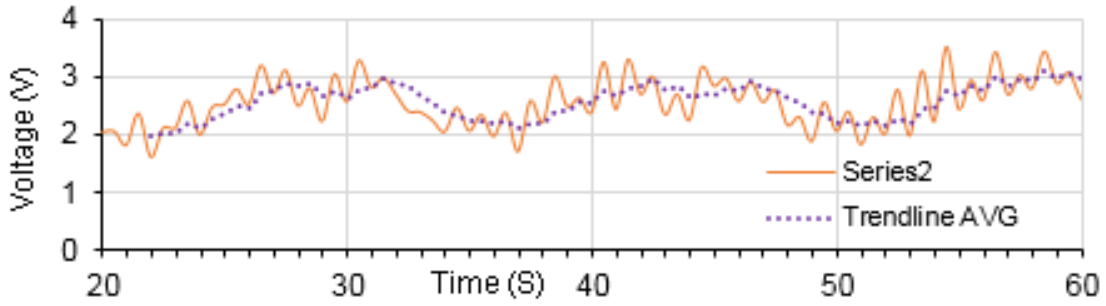

Figure 5-23 Voltage output from harvester over a 10 Ω load during stage 2

As the transducers output voltage is directly related to the output speed of the spring, as the springs output speed changes, so does the voltage. The trend line shown in Figure 5-23 shows a harmonic wave that can be related to the spring tension. The spring has absorbed the sharp spikes of energy from the input wave displacement and transferred them into a smooth output into the transducer.

If the energy generated in stages 1 and 3 is subtracted from the total energy generated, then the result is total energy generated during stage 2. Total energy generated in stage 2 is shown in Figure 5-24a.

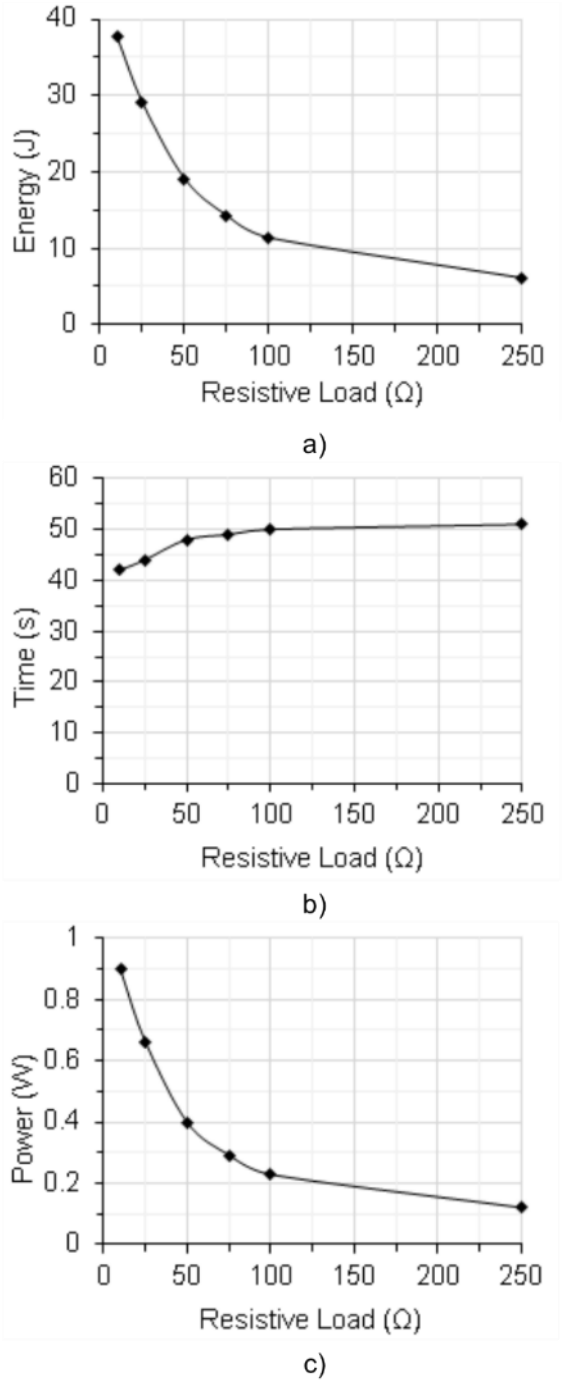

Figure 5-24 Stage 2 active harvesting results: a) Total energy generated in stage 2, b) Length of time for stage 2, c) Average power generated during stage 2

It can be seen that as the resistive load increases, the total energy and the average power generated decreases. The increase in time of stage 2

shown in Figure 5-24b, only changes by 9 s and this increase occurs due to the increase in time of stage 1, reducing the length of stage 2.

When the harvester was tested connected to the 10 Ω resistive load, the harvester produced 38 J of energy in 42 s. This results in an average power of 0.9 Watts in this stage. When the harvester is in active harvesting (stage 2), it is clear that the optimum resistive load for this stage is 10 Ω. Lower than this and the harvester broke.

Stage 3: Energy Recovery

This is when the inputs into the harvesters have stopped, yet the harvester has stored energy that the transducer can now use to increase the electric energy generated. This is done by the spring tension. When the harvester first started up, tension was added to the spring before the transducer started outputting energy. This happens as the tension in the spring is building up and at the start there is not enough tension in the spring to break the static inertia of the system. However, once the stage 1 and 2 have occurred, there is enough tension in the spring to keep the transducer generating for some time after the inputs into the spring have stopped.

Figure 5-25 shows electrical energy produced in stage 3 when the harvester was connected to a 10 Ω resistive load. It shows that after inputs have stopped this design of harvester produced 2.92 J of electrical energy.

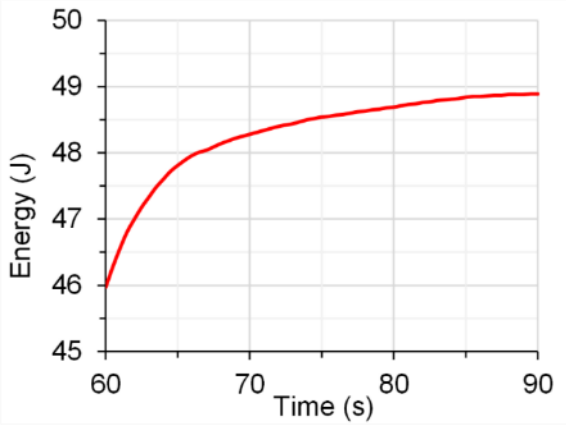

Figure 5-25 Electrical energy output from harvester over a 10 Ω load during stage 3

This confirms that the reel spring is acting as a temporary energy storage device and that energy entered into the spring, must exit via the transducer. Figure 5-26 shows that as time passes the spring tension reduces and the electrical energy generated slows down.

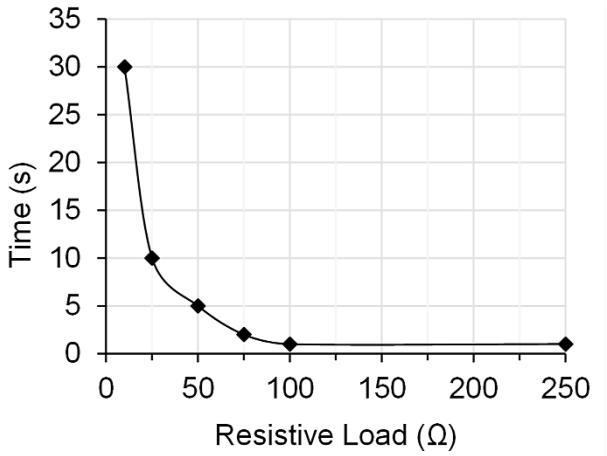

Figure 5-26 Time spent in stage 3 when connected to different resistive loads

The Graph in Figure 5-26 shows the length of time stage 3 ran for before the harvester stopped outputting energy. It can be seen that the higher the resistive load connected to the harvester, the shorter stage 3 becomes. This is the same as stage 1. This means by having a lower resistive load connected, the harvester takes longer to start up, but also longer to slow down, confirming the energy into the spring can only exit via the transducer, just not necessarily at the same time as it was entered into the spring.

From studying the 3 stages and the effects the resistive load had on them, it can be confirmed that the resistive load affects the following aspects of the stages.

- The total energy generated in the test
- The length of the whole test
- The length of stage 1
- The maximum Voltage seen
- The length of stage 3.

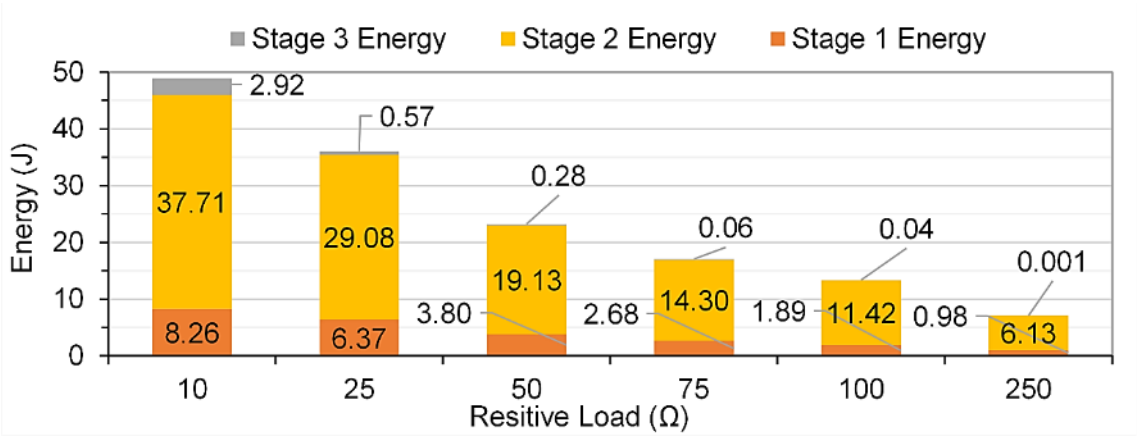

Figure 5-27 Energy generation in each stage over different resistive loads

The graph shown in Figure 5-27 shows the energy generated in the 3 stages when connected to different resistive loads. It shows that as the connected load increases, the energy generated decreases. Maximum electrical energy generation occurs when the harvester is connected to the 10 Ω resistive load.

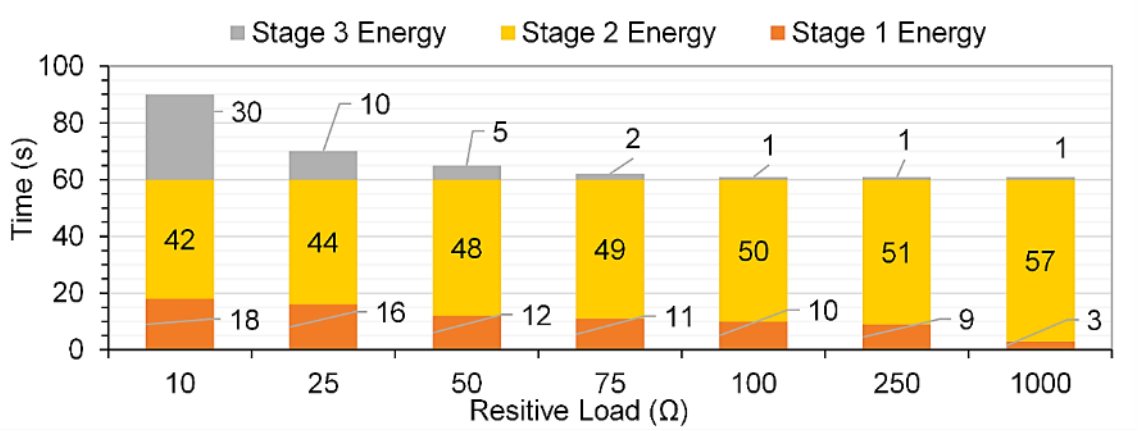

Figure 5-28 Time of each stage over different resistive loads

The second effect the resistive load has is to change the length of the stages. The graph shown in Figure 5-28 shows the times for each of the stages. If stage 1 increases in time, then so does stage 3. By increasing the time of stage 1 the tension in the spring is increased. This is confirmed by the 10 Ω load tests, where it has the longest stage 1 time of 18 s, and then the longest stage 3 time of 30 s.

5.5.3 Optimum Load Resistor for Different Flywheels

In this section a set of results will show how the optimum load and flywheel were found. The mass and shape of each flywheel give a different inertia to the harvester. The aim of using a flywheel is to decrease the amplitude to the harmonic wave seen Figure 5-23 in and optimize energy extraction in stage 3. Changing the flywheel mass will also change the length of stage 1 and thus increase energy in stage 3. Table 5-5 shows the data of the flywheels used in this set of experiments.

Table 5-5 Flywheels used for testing the improved design of wearable energy harvester

Fly No.	Radius	Thickness	Mass	Volume	Moment of Inertia	
	mm	mm	g	mm³	g·mm²	kg·m²
0	0	0	0	0	0	0
1	30	20	96	56,549	43,200	0.00004
2	30	6	220	16,965	99,000	0.00010
3	30	18	450	50,894	202,500	0.00020
4	30	12	633	33,929	284,850	0.00028
5	30	20	849	56,549	382,050	0.00038

The data shown in Table 5-5 Flywheels used for testing the improved design of wearable energy harvester reveals a steady increase of inertia that can be added to the harvester and this can be seen in the graph shown in Figure 5-29.

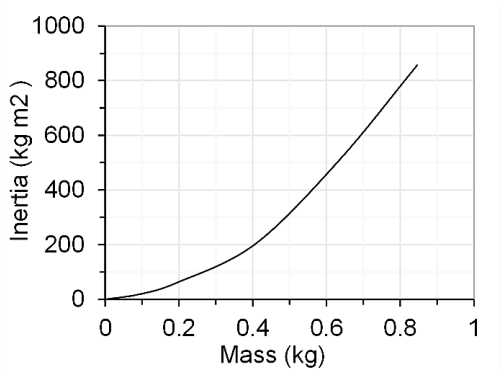

Figure 5-29 Flywheel inertia increasing with mass

Figure 5-29 shows that the flywheels were sized to increase the inertia steadily even though the steps between the masses are different.

Tests were performed in flywheel groups. Each flywheel was connected and tested over a decreasing resistive load, then swapped for the next flywheel and the each load was tested again. In Figure 5-30 a graph is presented showing the total energy generated from those tested.

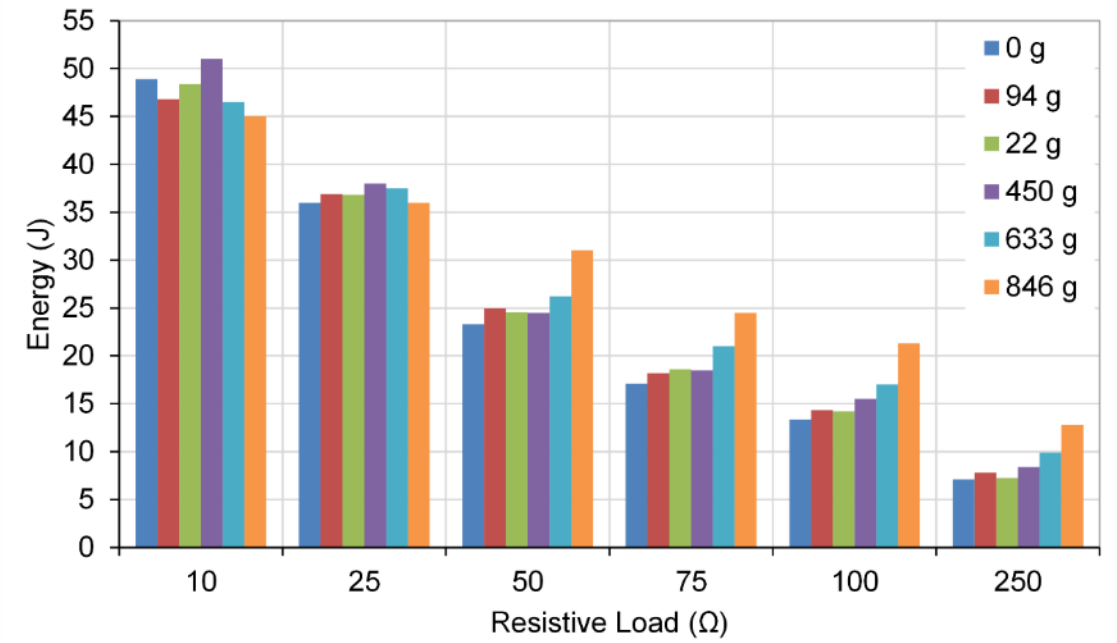

Figure 5-30 Total energy generated over different resistive loads with different flywheels installed from 0 g to 846 g

The maximum energy extraction occurred over the 10 Ω with all flywheel masses. As the connected load decreased, so did the total energy output. However, as the resistive load decreases the benefits of having a heavier flywheel increased. The graph shows that as the connected load increases a heavier flywheel mass performs better compared to other masses connected to the same load. The 849 g flywheel produced the lowest energy over the 10 ohms load tests, but the highest energy over the 250 Ω load tests. These results only show that the larger the load, the higher the energy extraction. They do not really explain the effects the flywheels have on the stages. To gain better understanding of the benefits of a flywheel on this harvester's design, the effects of harmonic dampening on the voltage outputs will be explained.

Figure 5-31 shows the effect the increasing flywheel mass had on the harvester's output voltage when connected to a 50 Ω load resistor.

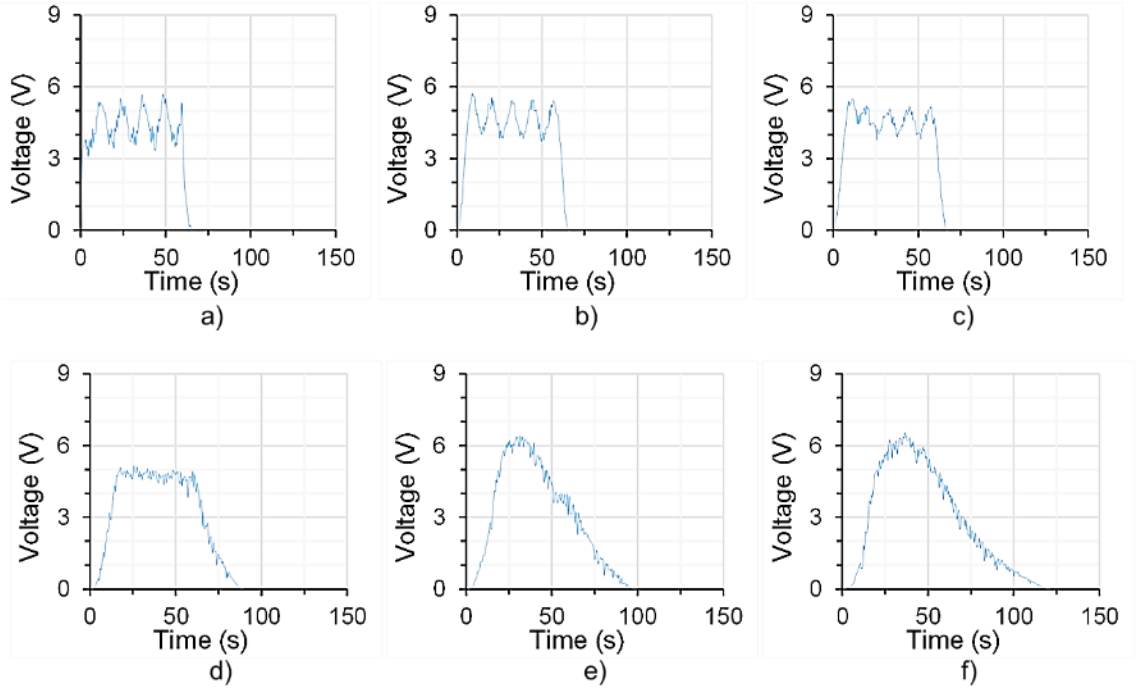

Figure 5-31 Voltage output from improved harvester when connected to a 50 Ω resistive load and different flywheels: a) 0 g, b) 96 g, c) 220 g, d) 450 g, e) 633 g, f) 849 g

In Figure 5-31 it can be seen that as the flywheel mass increases, the voltage ripple is reduced. When no flywheel was installed, the voltage ripple was 2.25 V. This results in a lower average voltage. Whereas the voltage ripple when the 450 g flywheel was installed was only 0.6 V and had an average voltage during active harvesting of 4.7 V. This is a clear improvement on the average voltage during active harvesting with no flywheel installed which was seen to be 4. V. This is an increase of 0.4 V on average simply by connecting the flywheel.

These results also show that by having a flywheel installed that is too heavy, the harvester took far too long to accelerate and consequently active harvesting was barely achieved. The peak voltage is higher on the largest flywheel test (849 g flywheel), but the average voltage is much lower at 2.8 V over the whole test.

This set of results shows that a flywheel will reduce the voltage ripple, which in turn improves the average voltage and that having too heavy a flywheel the harvester doesn't reach its optimum run speed in active harvesting.

These effects are confirmed and seen over all the flywheel tests. As the load increased on the harvester, the effects the flywheel had also increased. Shown in Figure 5-32 are the voltage outputs from the harvester when connected to a 25 Ω resistive load and with different flywheels installed.

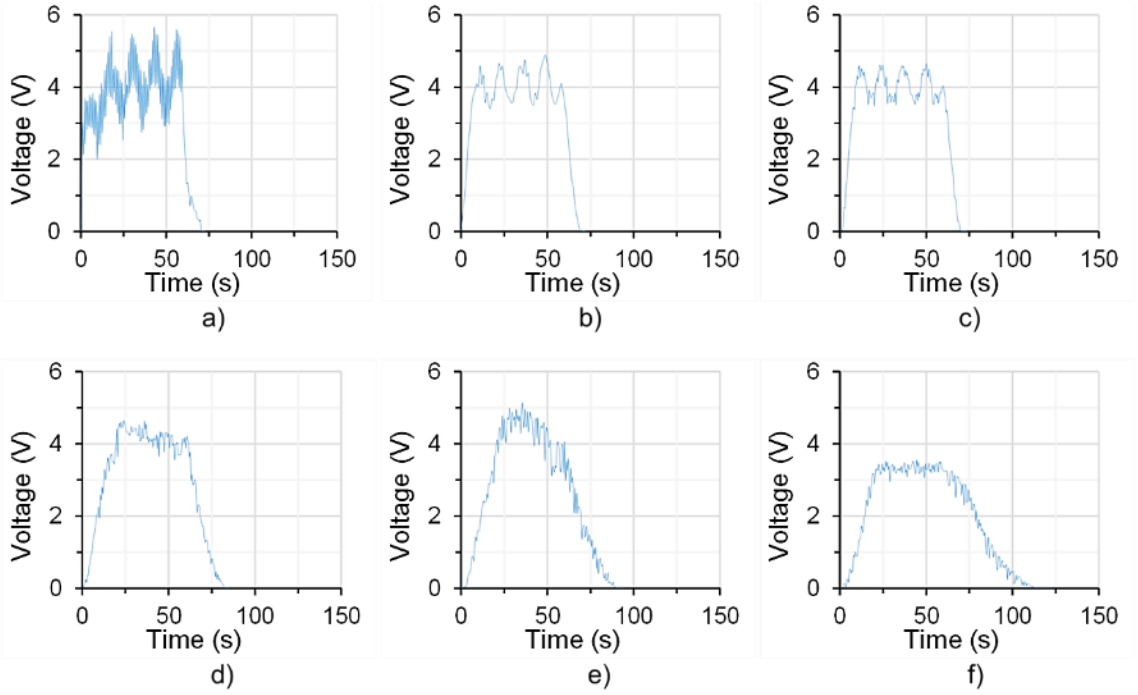

Figure 5-32 Voltage output from improved harvester when connected to a 25 Ω resistive load and different flywheels: a) 0 g, b) 96 g, c) 220 g, d) 450 g, e) 633 g, f) 849 g

When comparing the graphs in Figure 5-32 it is clear to see that having a flywheel is better than no flywheel, comparing graph A, to graph F, but it can also be seen that the maximum voltage seen is also reduced.

To conclude on the flywheel section, it can be seen that as the flywheel mass increases three things occur.

1. The voltage ripple is reduced
2. The length of stages 1 and 3 are extended
3. The peak and average voltages are increased

The optimum flywheel mass for this harvester was found to be 450 g. This gave the best advantages, with the least disadvantages. When a heavier flywheel was connected no more power was generated, yet the wearer would have to carry the extra mass, making it redundant. The best result seen was when the harvester was connected to the 10 Ω resistive load (Figure 5-14), but the average voltage level was low at 3 V (Figure 5-13b). This would mean the harvester would need to include a voltage step-up converter in order for the harvester to charge portable electronic devices. This would lead to increased energy losses, and less available power. It was also found that when the harvester was connected to the 10 Ω resistive load, the fatigue level was high and would result in a short life expectancy. Increasing the resistive load value will increase the voltage level and improve the life of the mechanical components. The improvements to the life of the components is from the reduction of back torque generated by the transducer. The less load connected to the transducer, the less back torque it generates. With a lower torque value to overcome all bearings, axles, cables, and springs will be subject to lower stresses and increase their life expectancy.

5.5.4 The Optimum Resistance for Two Foot Harvesting and Maximum Power Extraction

Now that different flywheels and resistive loads have been investigated, the final stage is to confirm the optimum conditions for the harvester when receiving inputs from both feet. This is a key part of this wearable energy harvester's design; the harvester can harvest from two inputs without increasing the weight of the main body of the harvester, and only the addition of the foot unit.

From the previous sets of tests, the optimum flywheel design will now be used. This flywheel should increase the spring tension in stage 1 and thus increase the peak voltage seen and improve the average voltage, but without excessively extending the time frames of stage 1 and 3 and thus reducing the average power output. The best flywheel from the previous test was flywheel 3. This had a mass of 450 g and had an inertia figure of 202,500 g/mm².

The final flywheel design has a reduced mass of 264 g, but has the same inertia as flywheel no. 3. This was achieved by changing the shape of the flywheel, and the final flywheel design can be seen compared to flywheel no. 3 in Figure 5-33.

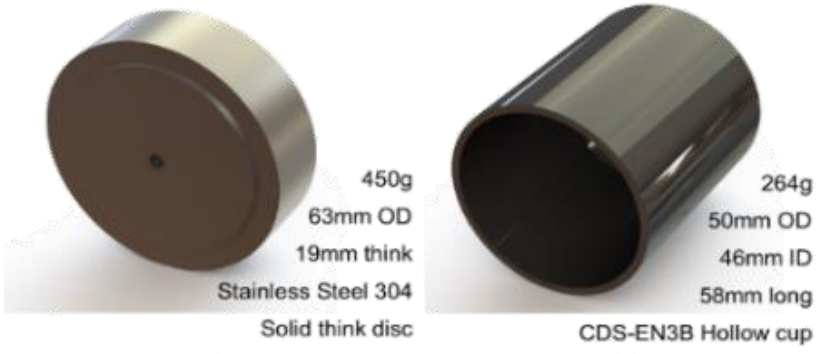

Figure 5-33 Flywheels for improved energy harvester design: a) Best flywheel from tests results, and b) Optimum design for final flywheel ensuring same itertia as 'a)'

This was done to help reduce the mass of the harvester, but provide the transducer with the extra inertia for best energy extraction.

With the final flywheel installed in the harvester, tests were performed with the input into the harvester set at a frequency of 2 Hz. This was as if the harvester was harvesting from both feet when walking at a normal rate. Tests were performed in order to find the optimum resistive load for the final flywheel and the increase frequency. Tests were performed with a resistive load of between 100 Ω down to 10 Ω. The graphs in Figure 5-34 shows the total energy and voltage generated from the harvester from this set of tests.

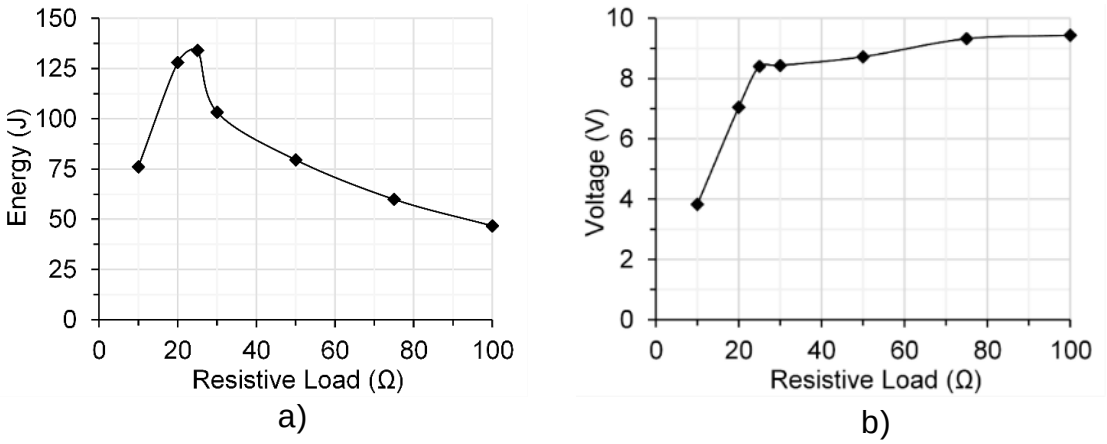

Figure 5-34 Results from a 2 Hz input wave over different resistive loads: a) Total electrical energy generated, and b) Voltage generated from the harvester

It can be seen that the optimum load resistor in this set of tests was 25 Ω. When connected to the 10 Ω resistor it was found that the voltage dropped off sharply and resulted in lower electrical energy generation shown in Figure 5-34 a. This is in agreement with the last set of results that showed a large voltage drop when connected to a 10 Ω load and is shown in Figure 5-34 b). The graph shown in Figure 5-34 b), shows the average voltage output over the different resistive loads. This shows the voltage over the 10 Ω resistor was 3.8 V and also shows that the voltage increase after 25 Ω

resistant's becomes far less significant. With the optimum flywheel installed and a 25 Ω resistive load connected, the voltage ripple was reduced to 0.65 V fluctuation peak to peak and this was seen as very good in comparison to the other flywheels and connected loads.

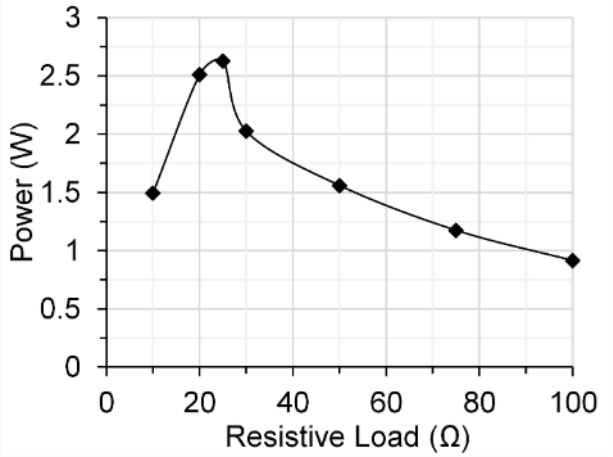

Figure 5-35 Average power generated by the improved harvester design over different resistive loads from a 2 Hz input wave

The graph shown in Figure 5-35 shows the average power available from the harvester. It shows that when connected to the 25 Ω resistive load the harvester produced 2.6 W. This confirms the optimum load resistor to be 25 Ω when inputting at 2 Hz. Because of this, the 25 Ω resistor will be used for the real world testing on the treadmill.

5.6 Results from Treadmill Testing

Here the results from wearing the harvester and walking on a treadmill at the 3 main gait speeds will be examined. These tests were performed to confirm the harvester's true wearable potential and confirm the power outputs from a human inputting the energy into the harvester. The input displacement is now set to 40 mm displacement and the input foot velocity will be allowed to be natural. The tests were performed 3 times for a length of 1 minute. Averages were taken and are shown throughout this section and the standard deviation is shown. The optimum load resistor found from the previous

Instron tests was connected (25 Ω) along with the optimum flywheel installed. The same LabVIEW data logging program was also used.

Unlike the initial design, this harvester should not be affected by changes in frequency and should produce the same average power per step once the wearer has been walking for a few steps and the harvester goes into the active harvesting stage.

5.6.1 **Results from Strolling on the Treadmill**

Here the input frequency was targeted at 0.5 Hz to represent someone walking slowly, in no rush at 3.6 km/h. The graphs shown in Figure 5-36 shows the output voltage and the total energy generated by the harvester during this test.

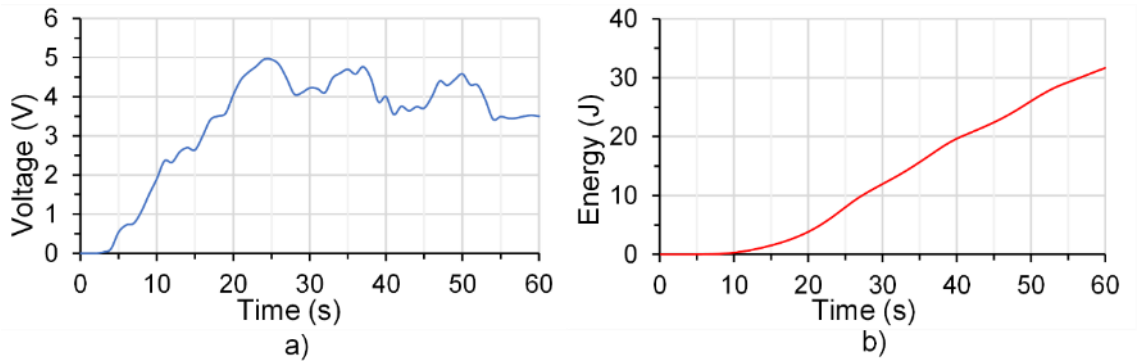

Figure 5-36 Treadmill test results from slow walking at 0.5 Hz: a) Voltage output, and b) Total energy generated

The total energy generated in this test was 31 J in the 60 s test time. This results in an average power output of a little over 0.5 W. This is lower than expected and is down to the voltage being low and having a long start up time in stage 1. The average voltage of this test was found to be 3.4 V.

It can be seen in Figure 5-36 a), that the harvester took 24 s before reaching it maximum voltage. This is also shown prominently in the first 10 seconds on the total energy generated graph shown in Figure 5-36 b). After 8 s the

harvester had only generated 0.09 J. After this point the harvester started to build momentum and began to generate higher electrical outputs.

5.6.2 **Results from Normal Walking on the Treadmill**

The same test was performed as in the previous section, but now the input frequency will be targeted at 1 Hz, and a normal walking speed of 5.4 km/h will be set. Figure 5-37 shows the results from the normal walking tests performed on the treadmill.

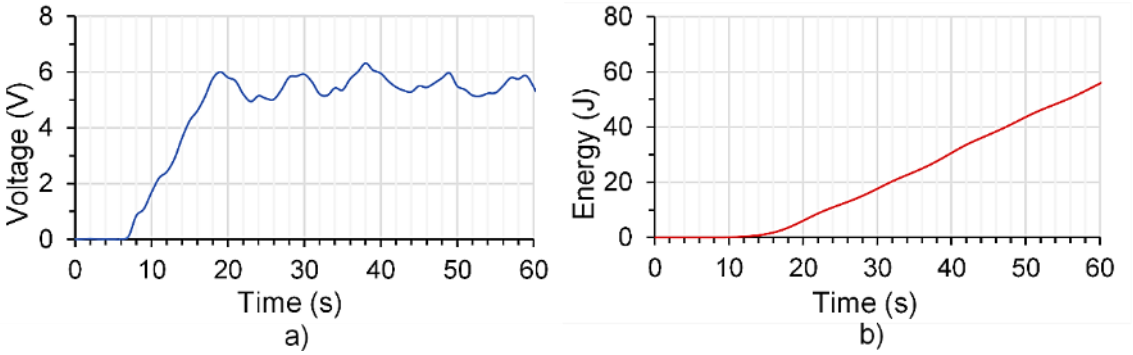

Figure 5-37 Treadmill test results from normal walking 1 Hz: a) Voltage output, and b) Total energy generated

It can be in seen in Figure 5-37 b) that the total energy generated was 58 J and that by 10 s the harvester had outputted 0.1 J. Figure 5-37 a) shows a smoother voltage ripple compared to the slow walking tests and this results in a higher average voltage of 4.4 V. This means the average power from this test was just under 1 W.

This is correct as with double the input frequency compared to slow walking, there is double the input energy and in turn from this design, double the average power under normal walking conditions.

5.6.3 **Results from Jogging on the Treadmill**

The last tests performed on the treadmill were at a high walking speed or jogging for some. The speed on the treadmill was set 7.9km/h and the input frequency was targeted at 2 Hz. The results from this test can be seen in Figure 5-38.

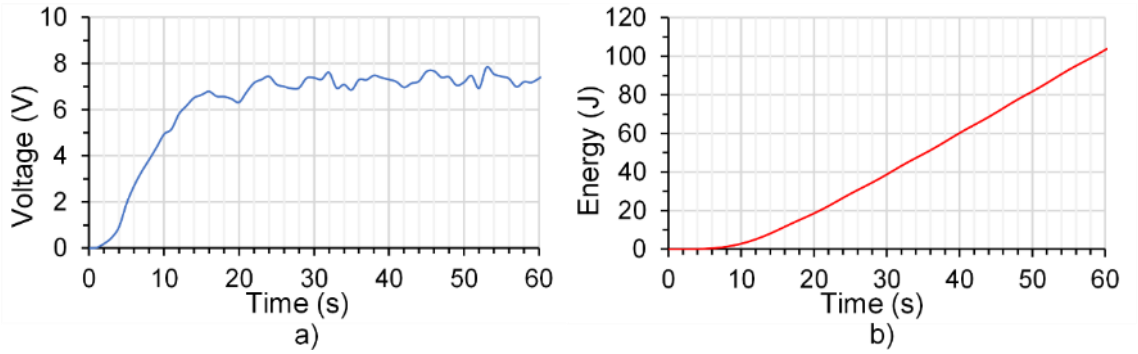

Figure 5-38 Treadmill test results from fast walking 2 Hz: a) Voltage output, and b) Total energy generated

Here the total energy generated was found to be 103 J in 1 m of walking at this speed. This results in an average power output of 1.7 W. The voltage ripple is now almost smoothed out and has the ideal voltage level with an average of 6.5 V.

It can be seen from the treadmill results that the harvester produces different average power levels depending on the input frequency seen by the harvester. This suggests the harvester is now producing the same power per step and if the step rate changes, then so does the average power.

The graph shown in Figure 5-39 Compares the electrical energy generated by the harvester and shows the increase clearly depending on input frequency.

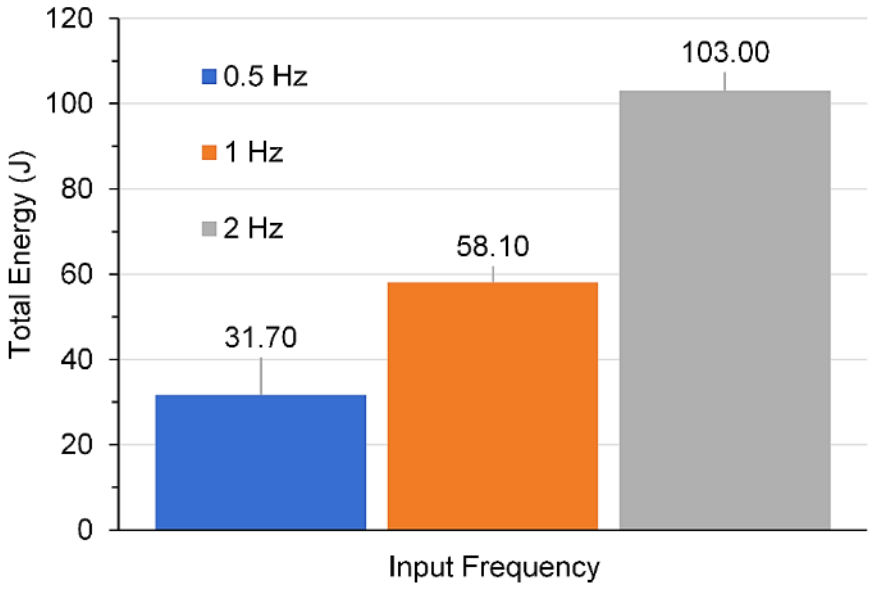

Figure 5-39 Total energy generated from the improved harvester design tested on the treadmill at the three typical giat speeds of 3.6, 5.4 and 7.9 km/h

If this total energy is then used to calculate the average power over the treadmill test time then you get the results shown in Figure 5-40.

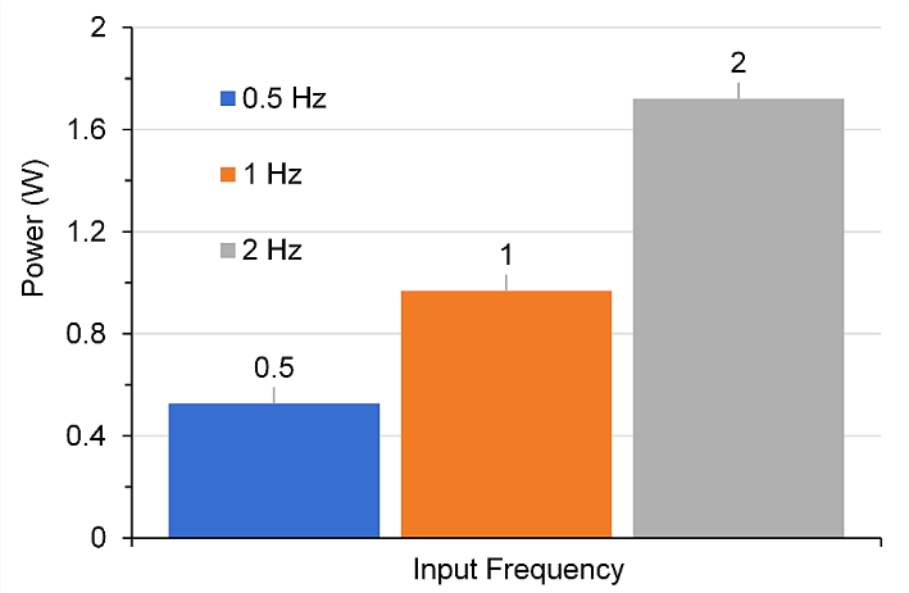

Figure 5-40 Average power generated from the improved harvester design tested on the treadmill at the three typical giat speeds of 3.6, 5.4 and 7.9 km/h

Lastly, the average power can then used to calcute the power per step. This is done by knowing the step frequency and the length of the test, thus total step per test. This results in the graph shown in Figure 5-41.

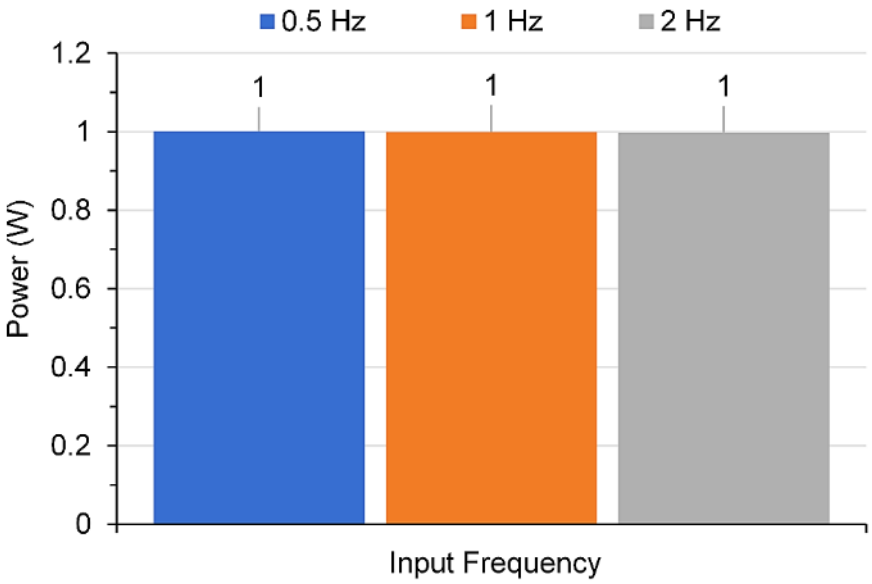

Figure 5-41 Power per step generated from the improved harvester design tested on the treadmill at the three typical giat speeds of 3.6, 5.4 and 7.9 km/h

This confirms that the harvester on average produces 1 W per step in real world testing.

5.6.4 **Results from Endurance Testing**

Here the results from testing the improved design for an hour are shown and discussed. The harvester was connected to a Samsung Galaxy S7. The battery in the phone was drained down until the phone displayed 0% battery and turned itself off. The outputs of the harvester were connected to the inputs of the phone and the voltage and current was recorded. The harvester performed well, but it was seen that one of the tension cables had become very worn by the end of the test. This confirms the reliability and

durability of systems design, but also confirms the need for the future design to remove the tension cables.

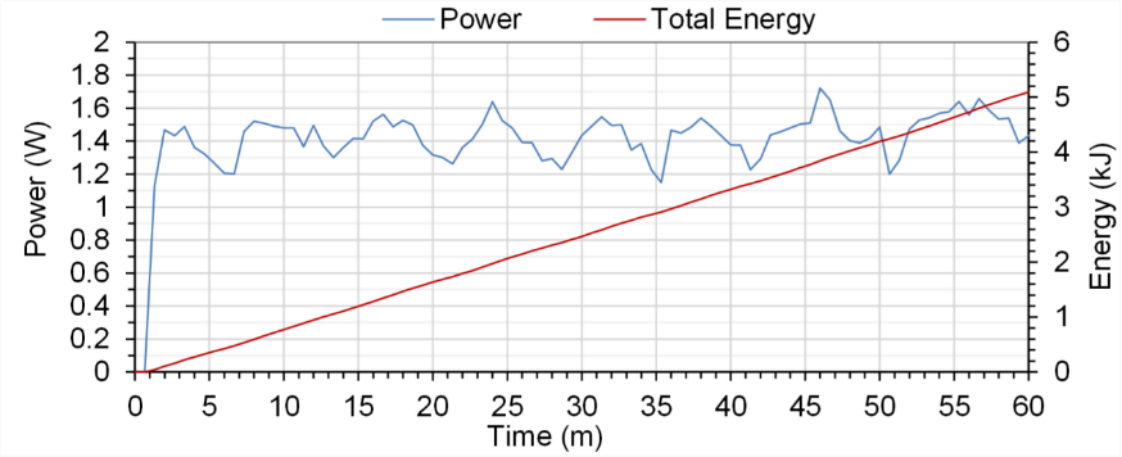

Figure 5-42 Instantaneous power and the total energy generated from the improved design from an hour of normal walking on the treadmill

The graph shown in Figure 5-42 shows that the improved design produced 5 kJ of energy in the one hour test; the power fluctuations are from the noisy Maxon motor output and the lack of power management. When the harvester produced a voltage higher than 7 V, the phone stopped charging and the current dropped to zero.

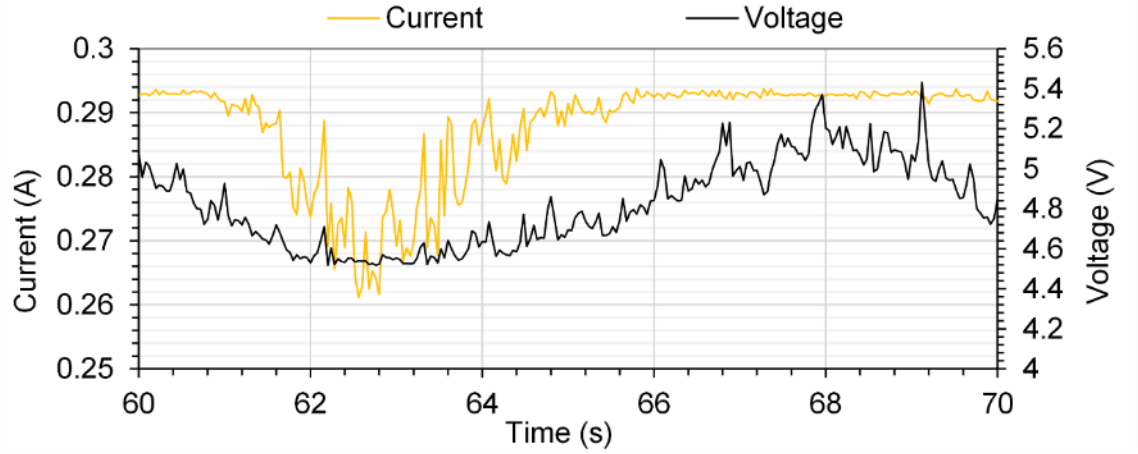

Figure 5-43 10 Second snap shot of the voltage and current generation from the improved design from an hour of normal walking on the treadmill

In Figure 5-43 the noise from the harvester can be seen. This shows the shape spikes of voltage which in turn affects the current.

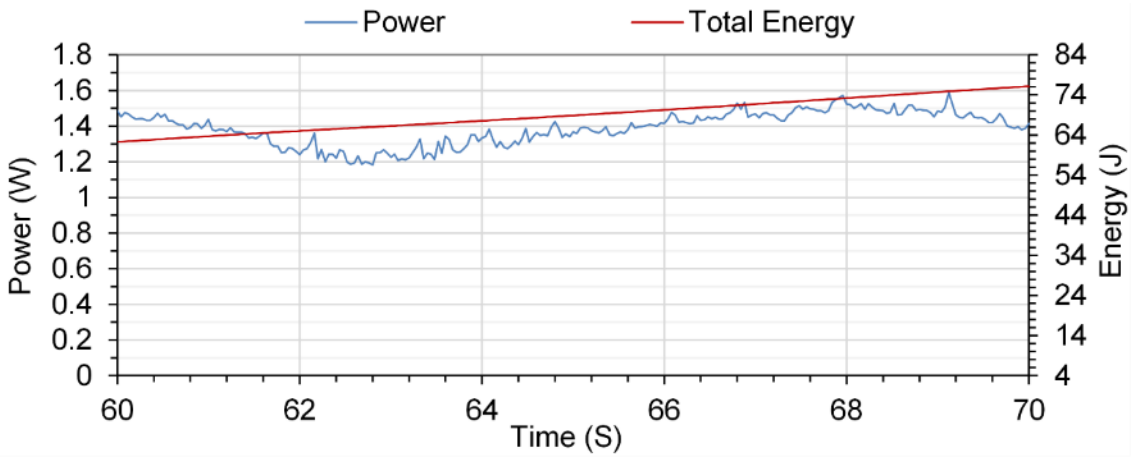

Figure 5-44 10 Second snap shot of the instantaneous power and total energy generated from the improved design from an hour of normal walking on the treadmill

In Figure 5-44 the Instantaneous power can also be seen not be a smooth output due to the noisy voltage output, but the total energy continues to raise at a steady rate.

When the Samsung Galaxy was turned back on after the test, the harvester had managed to charge the device by 12% according to the device's battery display. Knowing the total energy generation was 5325 J and the size of the battery in the device to be 3600 mAh or 47952 J, then we know that a little over 11% of the battery's capacity was generated by the harvester, which confirms the device's battery display to be correct.

The treadmill recorded the Calories burnt during the session and displayed a total of 319 C. This equals a metabolic rate 371 W. By using the equation to calculate the metabolic rate shown in equation 6-1, entering my personal data instead of average data, this calculated the metabolic rate to be 368 W. This confirms the accuracy of the equation and that walking speed has a very large effect on the metabolic consumption rate. Overall the improved design performed very well during the endurance testing.

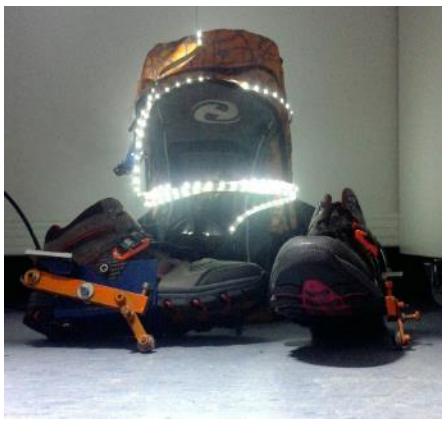

Figure 5-45 Photograph of improved harvester design powering 4 Meters of flexible LED lighting

In Figure 5-45 a photo of the harvester powering 4 meters of LED lights can be seen. This shows the available power from the harvester is more than capable of powering lighting for safety system for night workers. This would be far safer than just relying on reflective strips on clothing for safety purposes.

5.7 Conclusions and Discussion on Test Results

From the tests performed it was found that this design of this wearable energy harvester produced an average power output of 2.6 W when connected to a 25 Ω resistive load under normal walking conditions. This was the best power output generated by the harvester with the optimum flywheel installed and receiving an input of 2 Hz (1 steps per foot, per second)

The results from testing the improved harvester design without any flywheel installed showed a reduction in power output and only achieved 0.55 W from receiving a 1 Hz input. When the input frequency was changed there was no large change in power. This shows how the spring is working as an internal energy buffer, extracting the shape spikes of footfall force and converting them into a smooth 1 W power output.

The final weight of the improved harvester prototype was 5 Kg, including bag, both foot units and cables. It can also be seen that the main body of the harvester in the bag is quite large. The size and weight of this wearable energy harvester design can be reduced dramatically, but a harvester design that would withstand hours of tests and be able to change the flywheel with ease, meant that the size and weight were neglected at this stage of the research.

Comparing the improved design to the initial design it was found the improved design produced a better average electrical power output with any need for electrical rectification. The improved design also harvested from both feet rather than just one foot with the initial design. This showed not only an improvement in electrical power generation, but also an improvement in using and wearing the harvester. After the endurance testing was completed, the improved harvester didn’t show any signs of reduction in output and charged a smart phone by 12% in a one hour test. This confirmed the improve designs ability to produce enough electrical power from a wearable energy harvester, harvesting from human footfall.

Chapter 6 Comparing Wearable Energy Harvesters

In this chapter the effects of using wearable energy harvesters will be examined in forms of energy extraction and energy expenditure. This chapter will present a novel way that wearable energy harvesters are compared to one another. First, the designs presented in this thesis will be compared to other researcher's work in simple forms such as, power generated, increased energy consumption of the wearer from using the harvester and the harvester's power to weight ratio. The chapter will continue onto calculating the cost of harvesting and compare this to others designs of wearable energy harvesters. Then the introduction of a new term called "User Impact Factor" will be explained and shown to be a useful way of justifying the design and use of an energy harvester over conventional methods or other harvester designs.

6.1 Existing Comparison Methods

Some wearable energy harvester only increase the wearer's energy consumption due to carrying the harvester. This would be where the harvester works off vibrations from the wearer or a force that does not increase muscles work, such as footfall force.

Footfall harvesters that use footfall forces have the advantage of not using any direct muscle force to input energy into the harvester. These harvesters use the mass of the wearer and the ground reaction to create an energy input into the harvester. This means that extra energy consumption by the wearer can be calculated as if the wearer was simply carrying a mass in the form of energy harvesters.

6.1.1 Max Average Power Generation

By carrying or using a wearable energy harvester, the energy consumption of the wearer must increase. Table 6-1 shows a list of wearable energy harvesters, which harvest energy from humans walking.

Table 6-1 Wearable energy harvesters that harvest from human walking patterns

Design No.	Researcher /Year	Harvester's Mass (kg)	Harvesters Location (Location factor)		Harvested power (W)	Ref
1	Rome, 2005	25	0.1	Back	6	[13]
2	Shepertycky, 2015	3	0.1	Lower Back	3	[12]
3	Xie, 2015	0.35	0.8	Foot	0.5	[32]
4	Li, 2008	2	0.5	Knee	4	[37]
5	Rao, 2013	0.22	0.8	Ankle	0.0003	[109]
6	Zhang, 2015	0.06	0.8	Foot	0.0014	[110]
7	Qian, 2018	0.23	0.8	Foot	0.02	[1]
8	Fan, 2017	0.022	0.8	Foot	0.0002	[86]
9	Pritchard, 2017	1	0.8	Foot	1	--
10	Pritchard, 2018	5	0.1	Lower Back	2.6	--

Table 6-1 shows the mass, location and power generated by key wearable energy harvesters including the two designs developed during this research project.

If just the power output of the harvester is looked at, then one would simple say design 1, is the best as it produces the highest power output. It can also be seen, that design 1 has the largest mass of all the harvesters.

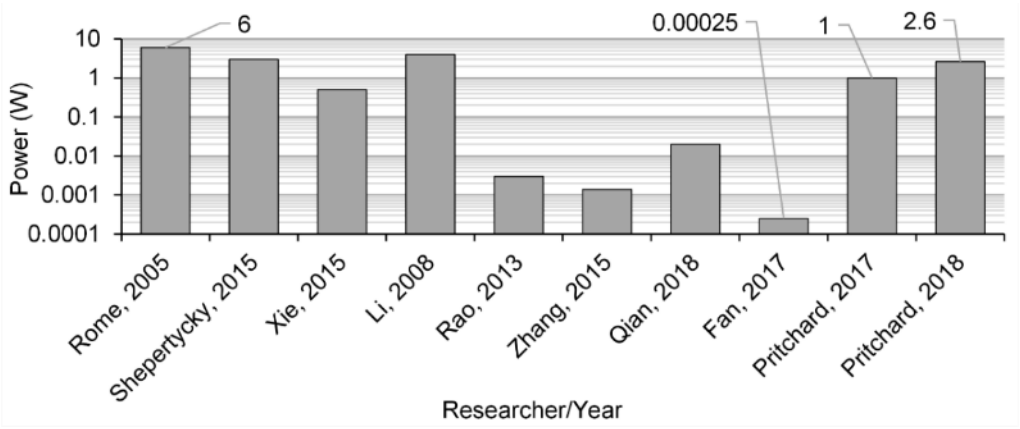

Figure 6-1 Power generated by the key wearable energy harvesters listed in table 6-1

Figure 6-1 shows the harvesters compared by their average power outputs under normal walking conditions. Comparing wearable energy harvesters by power output only does give the researcher a clear impression of the harvester. Wearable energy harvesters researches the need to look at the harvesters in different ways to ensure all factors that affect the user have been considered.

6.1.2 Increased Energy Consumption of the Wearer

The energy consumption of a human walking can be calculated using equations relating to human energy expenditure when walking and carrying different loads in different situations, locations, and speeds.

Equation 6-1 shows how this metabolic energy consumption can be calculated [106].

$$Met = 1.5W + 2(W + m)\left(\frac{m}{W}\right)^2 + \eta(W + m)(1.5V^2 + 0.35VL) \quad (6\text{-}1)$$

Where Met is the metabolic energy consumption in Watts, W is the weight of the wearer, m is the additional mass of the harvester, η is the terrain coefficient, V is the walking velocity and L is the location of the additional mass around the body.

To help understand the location factor, first the centre of a human must be know. Figure 6-2 a), shows Leonardo-da-Vinci's Vitruvian man. This was an early look at the geometry of the human body and the discovery of a university centre of gravity we all have. The image of a human clearly shows the centre of the human body is located at the centre of the circle. This results in all humans centre of gravity being in the lower torso, just behind the belly-button.

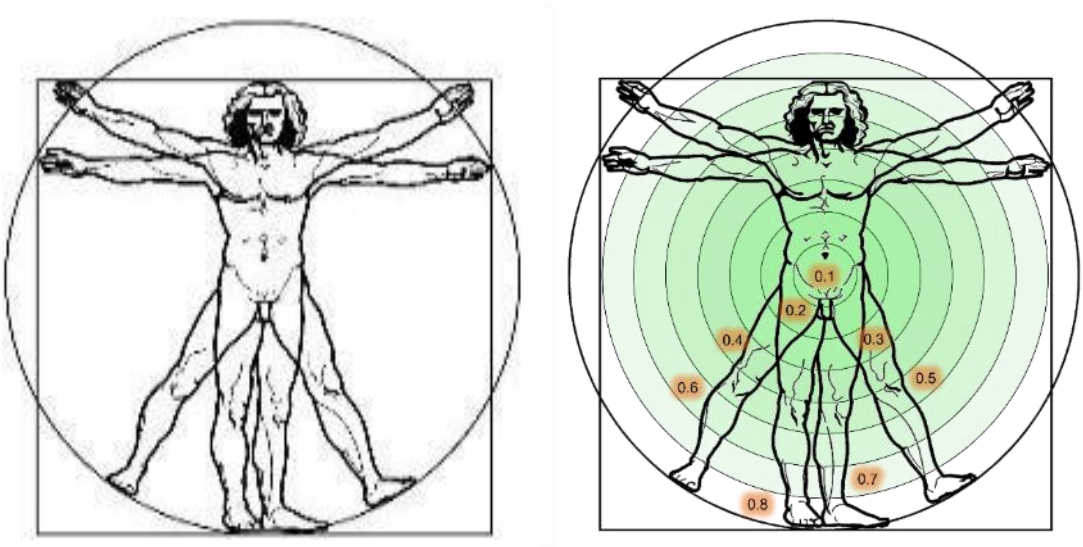

a) b)

Figure 6-2 Leonardo-Da-Vinci-Vitruvian-Man: a) Leonardo-da-Vinci-Vitruvian-man, b) Vitruvian Man with location factor added

Shown in Figure 6-2 b), is the same drawing by da-Vinci, but with location factor rings added. This shows the further away a harvesters mass is from the wearer's centre of gravity, the higher the location factor it is given.

Using this equation 6-1, a wearer not carrying any additional loads or harvesters, weighing in at 80 kg, walking at a normal walking pace of 1 m/s, on perfect terrain, would use an average of 240 W whilst walking. This 240 W consumption figure will be used as a baseline figure for calculating the increased energy consumption of the wearer carrying and using a wearable energy harvester.

Now, using the baseline figure of 240 W, the increased energy consumption from carrying and using the harvester's needs to be calculated and is done using equation 6-2, and having the baseline figure subtracted from the result to leave just the increased energy consumption. Each design of wearable harvester will have different effects on the increase of energy consumption of the wearer due to its mass and location. This is calculated by Equation 6-2 and these results are shown in Figure 6-3.

$$\Delta MET = Eq\ 6-1\ with\ harvester - Baseline \quad (6\text{-}2)$$

Where ΔMET is the increased energy consumption, $Eq\ 6-1\ with\ harvester$ is the total energy consumption of the wearer using the harvester, and $Baseline$ is 240 W calculated earlier.

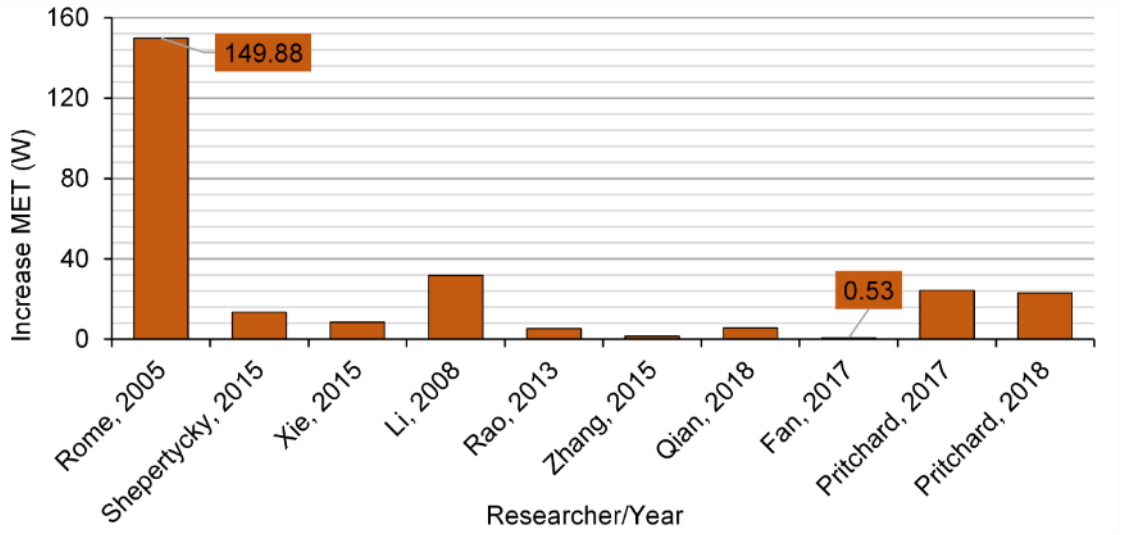

Figure 6-3 Increase energy consumption due to carrying/wearing the key wearable energy harvesters listed in table 6-1

Figure 6-3 shows the increase of energy consumption of the wearer, wearing different designs of wearable energy harvester. It is clear to see that the mass of the harvester has the biggest impact of consumption of the wearer, with the backpack harvester coming in with the highest increase in metabolic energy consumption of 150 W. This is not surprising as the backpack has a load of 25 kg added for it to work effectively. As where the design produced by Fan in 2017, only weighs 22 g. This shows very little increase in energy consumption of the wearer as it is so lightweight.

The two designs investigated here, have an average increase in energy consumption when compared to other harvester designs. The initial design has a higher energy consumption than that of the improved design. This is due to the mass of the harvester in the initial design being location on the wearer's foot. Even though the improved design, weighs almost 5 times that of the initial design, the main part of the harvester in the improved design

is located closer to the wearer's centre of gravity, meaning less energy is used when carrying and using the harvester. If the wearer was to wear and use the wearable energy harvester shown in the initial design (SS3), this would give an increased metabolic energy consumption of just under 25 W. As where using this equation again but with the improved harvester design (SS12), this second design would only have a metabolic energy increase of 22 W or 8%. This confirms the design improvement were very beneficial with regards to energy consumption of the wearer. The improved design reduced the energy consumption when carrying and using this design of wearable energy harvester.

The error in just looking at the increase energy consumption, is the fact it neglects to take into account the power output of the harvester. Design No.7, by Fan in 2017 shows the lowest increase, but also produces the lowest power. This design would be no use if you were aiming to charge or run a portable electronic device as the power output is too low. This means that the power output of the harvester also needs to be considered.

6.1.3 **Power to Weight Ratio**

Another comparator that has been used across multiple industries for decades, is the power to weight ratio. This is a useful way of determining how useful something is compared to its weight. This is important for harvesters that are going to be on the move and not in a fixed location. The power to weight equation is shown in equation 6-3.

$$PTW_{Ratio} = \frac{Harvester's\ Output\ Power}{Harvester's\ Mass} \quad (6\text{-}3)$$

Figure 6-4 shows the results of the simple power to weight equation being applied to the same group of harvester designs. The larger the PTW figure the better the harvesters design is with regards power density.

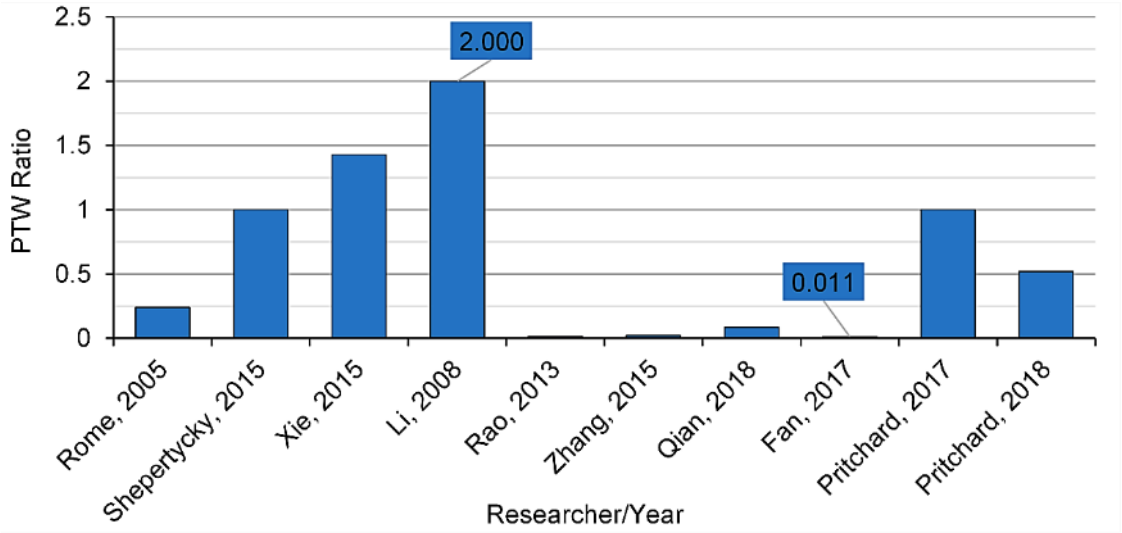

Figure 6-4 Power to weight ratio of the key wearable energy harvesters listed in table 6-1

This shows a different picture compared to looking at the increased energy consumption. Due to the power levels and weight of the harvesters being so far apart from one another, this shows that having a heavier harvester is ok, as long as it produces higher power to match the increased mass.

Here, the best performer regarding energy consumption from earlier, Fan from 2017, is now the worst in terms of power to weight. This is due to the very small amount of power the harvester produces. The best performer with regards to power to weight is the harvester design by Li in 2008.

The power to weight analysis approach shows the potential of the initial design (SS3), as it has the third highest power to weight ratio of the harvesters compared here, equalling almost 1 W of power, from a 1kg harvester. As where the improved design (SS12) is a lot heavier and the power output does not increase directly with the mass of the harvester resulting in a lower power to weight ratio figure.

The limitations of looking at the power to weight ratio, is the fact it doesn't take into account the effects on the wearer. This is why researcher created the term "cost of harvesting".

6.1.4 **Cost of Harvesting**

Cost of harvesting (COH), as found earlier in the research is currently the most common way, wearable energy harvesters are compared to each other. This helps quantify whether a wearable energy harvester is better than conventional methods such as batteries or manual portable power generators. The cost of harvesting equation is shown in Equation 6-4.

$$Cost\ of\ Harvesting\ = \frac{\Delta MET}{Electrical\ Power\ Generated} \qquad (6\text{-}4)$$

By using equation 6-2, and published data on the harvester's power outputs, the cost of harvesting can be calculated and the results are shown in Figure 6-5. The lower the cost of harvesting figure the better the harvester with regards to Cost of Harvesting.

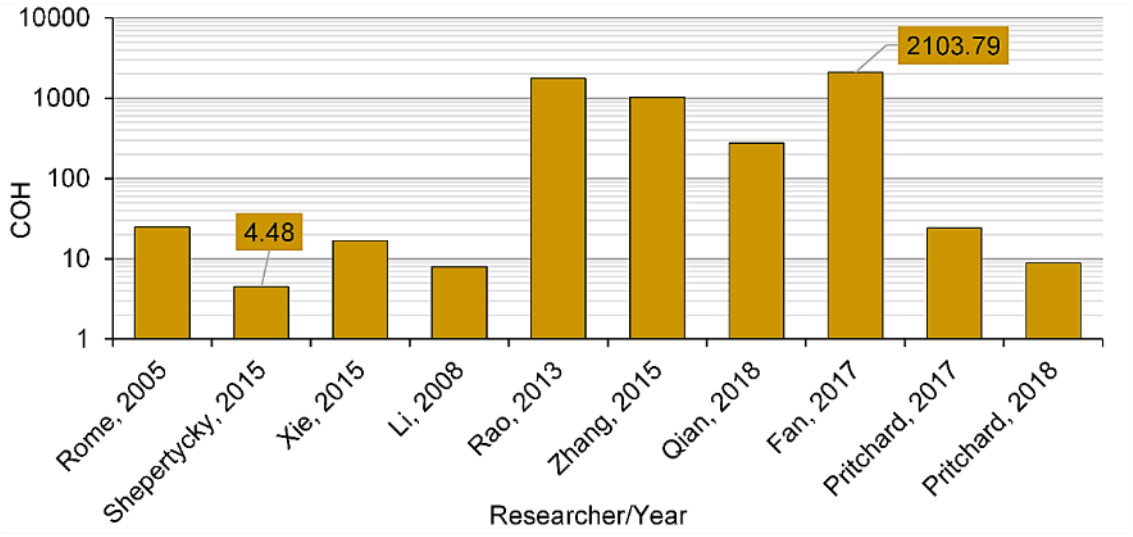

Figure 6-5 Cost of harvesting of the key wearable energy harvesters listed in table 6-1

This shows a different order of results again compared to the previous comparison approaches. This time Shepertycky's design returns the best cost of harvesting figure of 6.06. As where Fan's design, which has previously been at the top of the list, comes out the worst in the cost of harvesting scale. This is due to the power output of the harvester's designs.

Due to Fan's design only producing 0.25 mW, its cost of harvesting is very high. This shows that cost of harvesting does not give a clear indication whether any of these harvesters are more beneficial over conventional systems. As well as not making easy to compare to each other, in terms of usefulness.

Wearable energy harvester's need to ensure there available power output is beneficial over the extra metabolic energy consumption from carrying and using the harvester. If the harvester was to consume too much energy from the wearer, this would be detrimental to the wearer and could cause them to become exhausted. Looking at the two design developed here, the improvement from moving the mass of the harvester away from the foot can be seen. By moving the mass of the improved design to the lower back, it gives the improved design the lowest location factor resulting in a lower

cost of harvesting compared to the initial design. But this approach doesn't take into account the mass the wearer will feel and have to live with when carrying the harvester and this is why a new term called "User Impact Factor" was created.

6.1.5 **Summary**

By comparing wearable energy harvesters in different ways, harvesters can be seen as good or bad depending on the harvesters individual strengths and weaknesses. This means it can be hard to form an opinon on whether a harvesters design is viable for future developments.

Table 6-2 Comparator comparisons

Comparison Method	Advantages	Disadvantages
Max Average Power Generation	Easy to see power levels available	No idea on weight, location, useability
Mass of Harvester	Shows how much the wear is going to need to carry. Useful when planning expeditions where weight is important.	No idea on power output,
Location of Harvester	Important to know if harvesting from one location or needs an input from one particular place	Might limit imagination of integration of new designs if only thinking about location.
Increased MET from Harvester	Very important to ensure harvesters are not detrimental to the wearer.	Hard to know whether this loss is worth it, without looking at power available
Power to Weight Ratio	Incorporates power generated and weight of harvester making it easy to predict future designs	Ignores location of harvester and the effect the harvester has on the wearer.
Cost of Harvesting	Good to know power generated over metabolic energy consumed.	No clue on effects of the size and location of the harvester

After studying comparison methods used in energy harvester and other fields of power generation Table 6-2 with created. It became clear none

of them incorporated all of the important aspects for designing a wearable energy harvester. A comparator that includes; power, mass, and energy consumption using the location factor, would give a richer picture of the harvester's feasibility and future changeability.

6.2 New Comparison Method: User Impact Factor (UIF)

The user impact factor, aims to improve the ability to simply see which deign of wearable energy harvester is most suited to be a wearable energy harvester. The user impact factor takes into account the mass of the harvester, power output from harvester and the increased energy consumption of the wearer. By doing this, it combines all of the previous attempts to quantify a wearable energy harvester's feasibility, useability and performance, into a simpler form, the User-Impact-Factor or *UIF*.

$$UIF = \frac{\Delta MET}{PTW_{Ratio}} \qquad (6\text{-}5)$$

Equation 6-5 shows how the user impact factor is calculated. Where ΔMET is the increased energy consumption of the wearer from using the harvester shown in equation 6-2, and the PTW_{Ratio} is the power to weight ratio of the harvester from equation 6-3. The lower the user impact factor, the better the wearable energy harvester design is at generating power without effecting the wearer. The results of using equation 6-5 are shown in Figure 6-6.

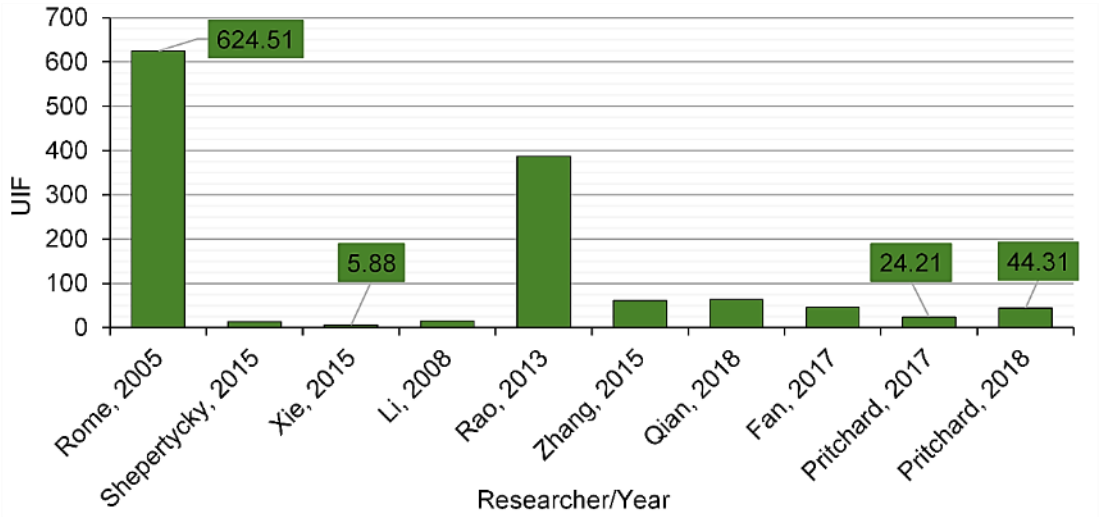

Figure 6-6 User impact factor of the key wearable energy harvesters listed in table 6-1

This shows another different picture of optimal wearable energy harvester design.

By taking into account of the harvester's mass and power output, via the power to weight ratio, and not just the power output like in the cost of harvesting equation, the user impact factor will always indicate whether a harvester is heavy resulting in a higher user impact. Due to the backpack having the heaviest mass, this is by far the worst on this scale and the design by Xie in 2015 is the best.

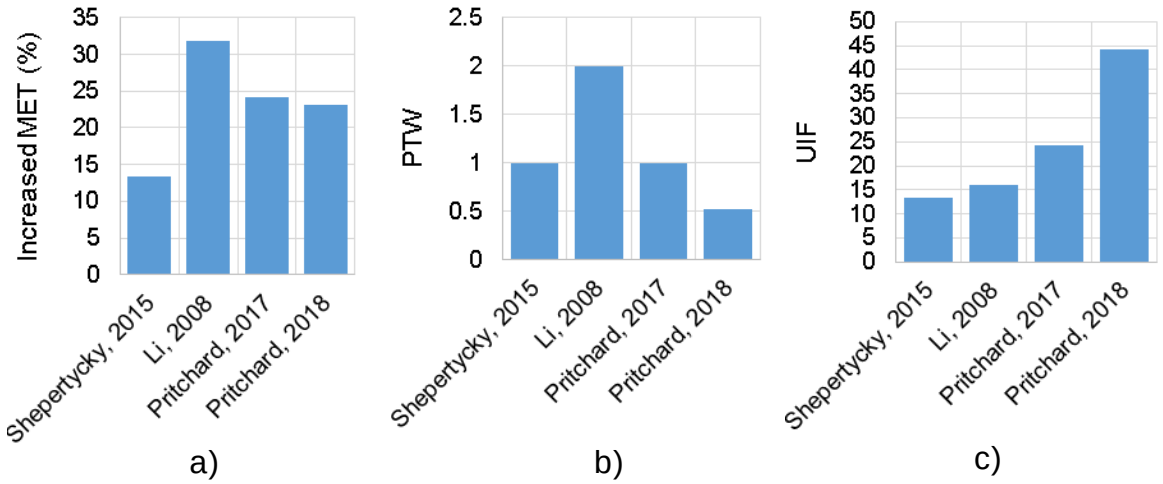

Figure 6-7 Comparison of four selected footfall harvesters: a) Increased energy consumption, b) Harvesters power to weight ratio, and c) the new User-Impact-Factor

The graphs shown in Figure 6-7 shows 4 wearable energy harvesters compared via increased metabolic energy consumption, Power to weight ratio and the new user impact factor.

The user impact factor shows how practical a wearable energy harvesters design is rather than just looking at its energy consumption or power output.

6.3 Conclusion

It has been shown in this chapter that the existing ways of comparison between wearable energy harvesters didn't make it easy to determine which harvester is better, more useable, or has the potential to be developed. By using the user impact factor as a comparison method, it has been possible to compare harvesters of different styles, transducers, locations, and power levels to each other in a way that incorporates more important variables.

Using the User impact factor comparator shows the wearable energy harvester with the best results to be that by Xie, published in 2015 [32]. This has a rating of 5.88 UIF. The weight is low, and has a good power density

with a recorded power output of 0.5 W. This means that this harvester has good potential for development and little impact to the wearer.

The two designs shown throughout this thesis (*inertial design and the improved design*) had an average UIF rating of 24.21, 44.31, respectively. The improved design has a higher UIF compared to the first which was not intended. The second design is very complex and was state of the art when first created. This meant the reduction of mass from the harvester was not a concern, rather concentrating on achieving reliable results was paramount. A lightweight design has been worked thought and has a suggested weight of 1.5 kg. If this mass is used to calculate the user impact factor, then the improved design has a rating of 3.8 UIF. Far below any other wearable harvester to date.

The traditional comparison method such as power-to-weight and cost-of-harvesting only take into two variables for their calculations. PTW uses the power generated by the harvester and the overall weight of the device but does not look at the increased energy consumption or the size of the harvester being used. The COH uses the increased energy consumption of the wearer over the electrical energy generated by the device but does not include the mass, location or size of the harvester being used. By not including key elements of that effect the usefulness or practicality of wearable energy harvesters, it is hard to see whether a wearable harvester design has potential for future development or even commercialization. The new comparator created in this work, The User-Impact-Factor (UIF) will provide better understanding of existing harvesters practicality as being used as a wearable energy harvester. The UIF uses 3 elements for it calculations

instead of two. These are; the increase in metabolic energy consumption of the wear, electrical power generated when using the harvester and the weight of the harvester design generating the power. By including these three key elements the UIF improves the ability to compare wearable energy harvester designs.

In this chapter the explanation of the new term was concentrated on over a detailed analysis of existing harvester designs. Without being able to test all of the wearable harvester designs in one controlled laboratory situation, a theoretically approach had to be created in order to gain all the information about the harvesters to convey the new comparison method. Not measuring the metabolic energy consumption of wearers using the different harvesters meant calculating it by existing prediction on human energy consumption [106]. This worked as an explanation of the new term, but more testing would have resulted in more details. Because of this, the new comparison method would need further validation in order to prove its accuracy, but time and harvesters were unavailable to confirm this. Further research could easily confirm this new comparator in the future.

Further discussions on the applications and improvements of the designs are presented in the following chapter.

Chapter 7 Discussion and Conclusions

In this chapter, a discussion on the applications that both harvester designs could fit into are presented. It continues on to discuss the developments the designs would need to undergo in order to work in the application more effectively. The chapter will conclude with overall conclusions. A review of the research aims and objective will be presented along with the research contributions. The problems found along the way will be examined and how these issues were addressed is explained. A closing statement is presented to bring the thesis to a close.

7.1 Applications and Developments of Both Harvester Designs

Here each design will be looked at in terms of its real world applications. If the designs were changed for applications, what would be changed and how? The obvious development for any wearable energy harvester would be making the devices smaller, lighter and less noticeable by the wearer. This research project was to concentrate on new and novel design approaches for wearable energy harvesting applications. This meant size and weight were not as important as making the novel harvesters designs withstand rigorous testing, and still be able to be demonstrated as a proof of concept in the future. This meant having a large factor of safety margins to ensure the harvesters would last, but this came with the cost of increasing weight and size.

7.1.1 Application for the Initial Design

Research revealed that the fitness community use ankle weights to increase their energy consumption while out jogging. Figure 7-1 shows a pair of ankle weight used by the fitness community. These were found to commonly range from 0.5 kg up to 5 kg per ankle. The initial design weighs 1.2 kg and could act as an ankle weight as well as a wearable energy harvester.

Figure 7-1 JBM adjustable ankle weights from 0.5 kg to 5 kg per ankle

Ankle weights that could charge portable electronic devices seem a strong target market and with the weight on the foot no longer a problem, the initial design could be evolved to fill this gap.

7.1.2 Augmentation of the Initial Design

This design would be ideal for this situation with only the need to improve the shoe cup design to give more comfort to the wearer as the harvester would need to be used while jogging. The hard carbon fibre shoe cup does do the job, but would wear quickly and after some time of wearing the harvester, the wearer would start to feel the impact of continuously landing on the hard carbon fibre. A complex composite that is made from more soft and flexible materials could be used. This would need rigid

structural components imbedded into the material for fixing of the gearbox, transducer and importantly, protective casings.

Additional features could be added to this wearable energy harvester mounted on the foot that would also be of benefit to the fitness community. These could include; a GPS sensor, a step counter, accelerometers and a wireless transmitter. These could be powered directly from the harvester and communicate to the portable device being changed. This data could then be accessed via an app on the device.

7.1.3 **Applications for the Improved Design**

When planning an expedition, an age old problem since the invention of global communication using electronic devices has been powering these devices. Generally expeditions do not have access to a mains power grid so have had to rely on batteries or power generators to recharge or run their electronic needs. This comes with a big drawback. Batteries are heavy and the longer the expedition, the more batteries that will need to be carried. This results in higher energy consumption of anyone involved in moving the batteries. This was shown in section 3.4.2.

The power generators would consume more energy from the user as they are having to convert their metabolic energy into electrical. Any increase in energy expenditure will result in the need to carry and consume larger amounts of food.

If a wearable energy harvester was designed to continuously charge all their portable electronics, then there would be no need to carry extra batteries or waste their own energy manually generating electrical power.

Military personnel known as ground troops currently carry very heavy backpacks with all of their supplies. A large amount of this mass is from carrying a big battery used for communication and location. Backpack harvesters designs researched by many require a mass to move within the backpack to recharge a smaller battery held within the backpack.

The improved design of footfall energy harvester presented here, could also be used to recharge the military personnel's battery and the weight of the prototype shown would still be less than the weight of carrying larger batteries making it a worthwhile investment.

7.1.4 **Augmentation of the Improved Design**

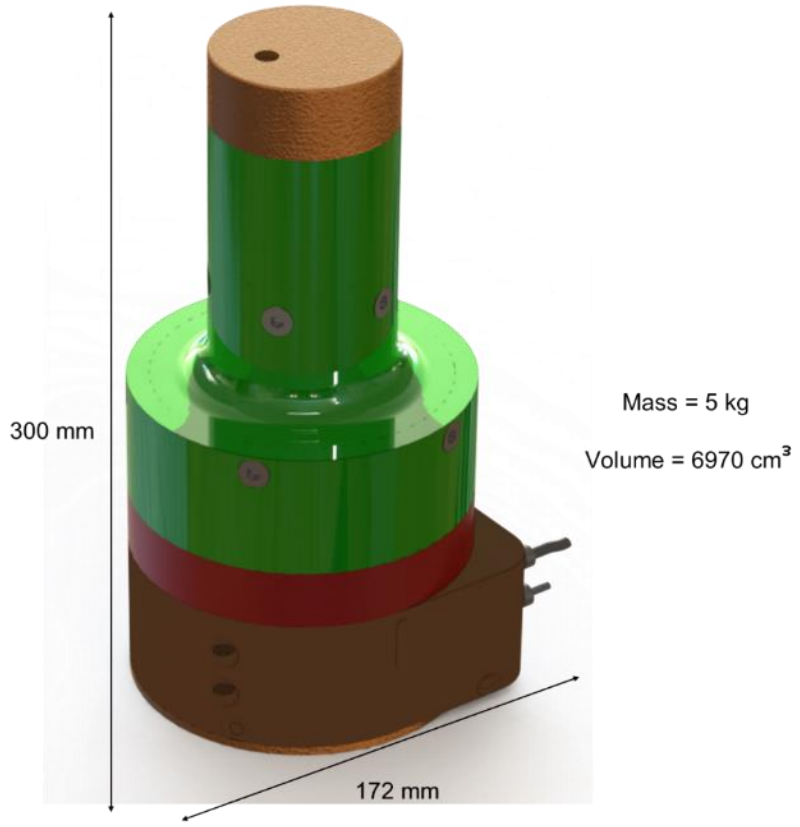

Figure 7-2 Improved harvester prototype design geometry

The improved design seen in Chapter 5 was very complex and having to start somewhere, the weight and size of the device was not optimised in the prototype shown. This is shown in Figure 7-2. This prototype's final

weight was 5 kg which is high for a wearable energy harvester. With vast optimization the future design of a footfall energy harvester would dramatically reduce energy consumption of the wearer and improve the harvester's efficiency. Therefore the size and the weight have both been reduced and the geometry is shown in Figure 7-3.

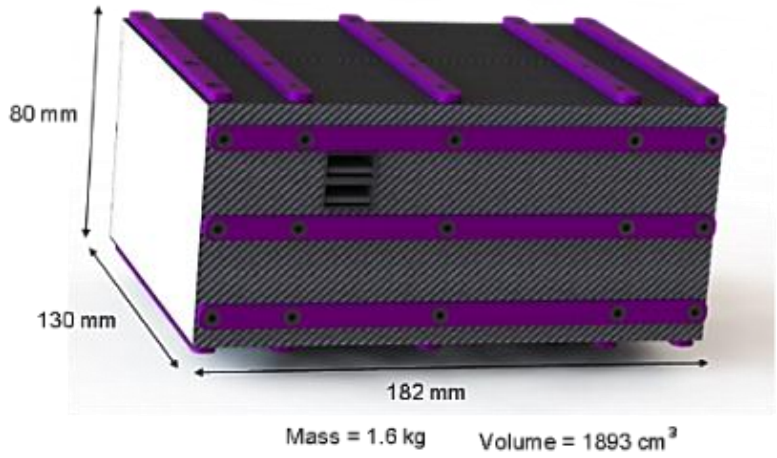

Figure 7-3 Future design of power unit for footfall energy harvesting

The future design of the main unit had to incorporate all previous components, but be reduced in size and weight whist remaining a strong and durable device. This future design gives a suggested weight of around 1.6 kg and is the same size as small lunchbox, (130x80x182mm). This would mean this harvester could be placed at the bottom of a backpack in which the wearer could carry their portable electronic devices. The volume of the device was reduced by 5077 cm^3, almost 73% and this future design has a weight reduction of 3.4 kg which equals a 68 % weight reduction.

The unit has been shrunk by changing the orientation of the components. In the improved design prototype tested in Chapter 5, the layout was kept in-line for ease of manufacturing and to gain better understanding of the system. By using carbon fibre for the casings for the future design the stiffness of the unit is upheld, but also remains lightweight.

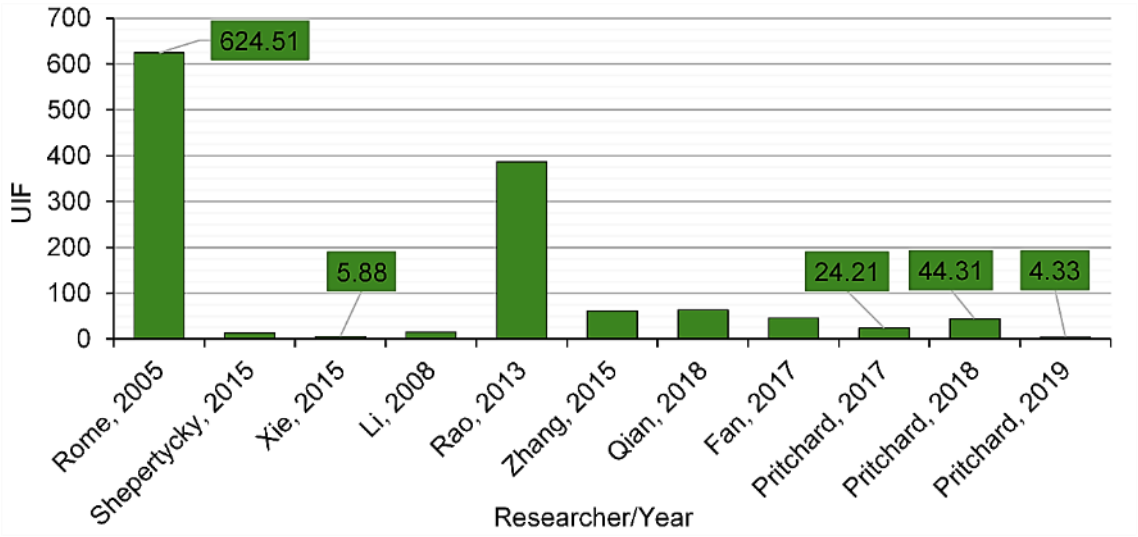

Figure 7-4 User impact factor including future design

The Graph shown in Figure 7-4 shows that if the harvester produces the same power as the improved design shown in Chapter 5, it would have the lowest UIF for a wearable footfall energy harvester to date.

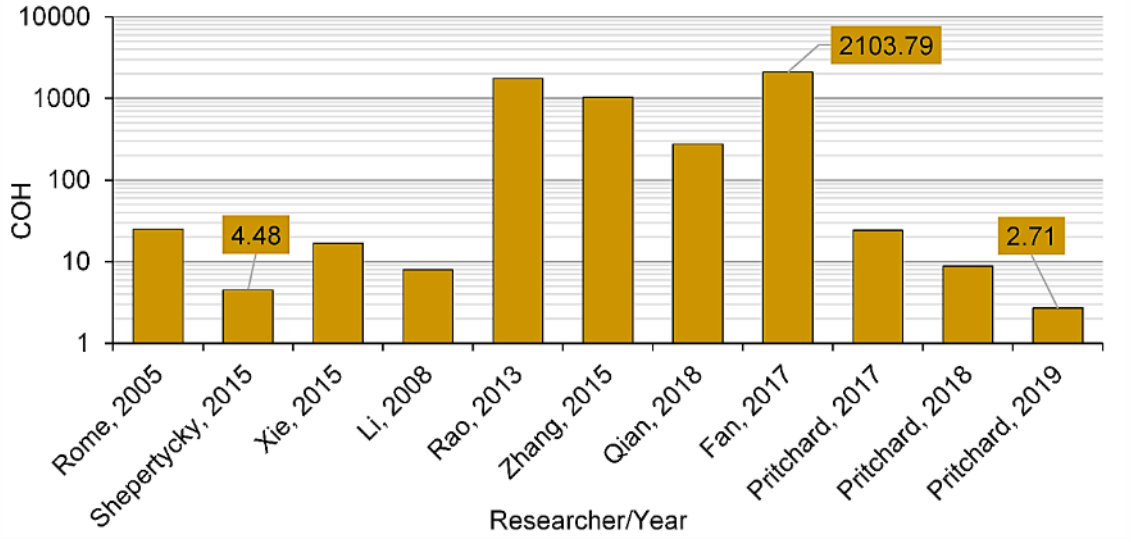

Figure 7-5 Cost Of Harvesting calculations including future design

If the future design is compared using the pre-existing approach called '*cost of harvesting*', then again it has the best results comparing it via this method. This is shown in Figure 7-5.

This design optimization for the future design also looked at improving the power transfer from the foot to the main harvester unit. The tension cables served their purpose, but also showed a very high wear rate. The second improvement required moving away from a tension cable to eliminate

the “flapping” of the cable running up the wearer’s leg to the unit. Each time the cable is pulled and released the cables had a tendency to move at will. In their normal application these types of cable are securely fixed to stop this and help improve power transfer. Attaching the cables to the trousers of the wearer would help the cable, but hinder the wearer’s comfort.

This is why the future design would use a hydraulic power transfer system. The input bar on the foot units will be used to compress a micro hydraulic ram that moves fluid through a 5 mm internal bore pipe up to another hydraulic ram in the main harvester unit. This ram will then move the input arm as the pull cable did.

This design change was a dramatic decision and time was spent on ensuring the harvester’s size and mass did not increase dramatically from adding the additional components required for the hydraulic transfer system.

The other advantage of changing to hydraulics was the idea that if this harvester is used for expeditions then carrying spare parts to overcome the tension cable failures would not be a preferred option. With hydraulics using a water based fluid as the hydraulic material, then any necessary refill could be from the water supplies the wearer would have to be carrying or finding in order to survive: Where there are humans, there is water.

7.2 Conclusion

In this section conclusions to the research will be presented. It will lead on to show that the work throughout this PhD has contributed to the research community and has developed novel wearable energy harvesters that have been proven to produce Watt-levels of power.

The initial design shown in Chapter 4, showed that a footfall energy harvester could be designed to produce enough electrical energy to charge portable electronic devices, but was held back from achieving this due to the requirement of a more efficient power management circuit. With a unique extraction area below the foot line and all of the components mounted on a retro-fit shoe cup, this conceptual design explored the idea of producing high enough power to charge modern portable electronic devices making it novel in aims and execution. This harvester with all attachments and covers weighed 1.2 kg, which is heavy, but not unusable. This would be the same as carrying a one litre bottle of water and a snack sized chocolate bar. The main drawback found was the fact the weight was on the foot, rather than the scale of the weight itself.

The improved design shown in Chapter 5, evolved the initial designs extraction method and transferred the power to a less noticeable location which in turn, reduced the metabolic energy consumption of the wearer. The improved design removed the electronic rectifier to smooth out the shape voltage spikes from footfall and replaced it with a mechanical version. This design also ensured any energy entered into the spring could only come out through the transducer and not be wasted. This design and the way in which it uses the reel spring has never been done before, making this design novel and a good contribution to the energy harvesting community.

This harvester produced an average of 2.6 W from normal walking, meeting the target power and not impacting the wearer. This design weighed 5 kg including bag, covers, and shoe units. This could easily be reduced now the concept has been tested and proved to be a success.

7.2.1 **Review of the Research Question and Research Aims**

- Was the research question answered?
- Were the research aims met?
- Was the hypothesis proved to be correct?

In this section the three questions listed above will be answered to help identify the successful completion of the research project. First, was the research question answered?

Can a footfall wearable energy harvester be shown to generate enough power to charge a smart phone currently available on the domestic market?

Yes!

The initial design confirmed the design idea and extraction method were going to produce a Watt-Level output, but also showed losses in efficiency due to the sharp spikes of voltage needing rectifying, smoothing and limiting, in order to be able to charge from a USB port and not output a voltage higher than 5-6 V. The improved design proved that the footfall harvester design was able to charge a modern smart phone (Samsung-Galaxy-S7, 2017) from normal walking conditions while not effecting the wearers walking pattern and only increasing the metabolic energy consumption of the wearer by carrying the device.

- *Research into available energy from humans for harvesting applications*

This was shown in Chapter 2 and a new diagram showing predicted energy levels available was created to show the latest research predictions Figure 2-13. This showed not all areas were going to be suitable for the application of charging a modern portable device. This led to footfall having the potential to provide the energy source for an innovative wearable energy harvester design.

- *Research current wearable harvesting approaches, designs and testing methods*

This was presented in Chapter 2 where a review of recent wearable energy harvesters was performed and presented. This showed that a wearable energy harvester, harvesting from footfall had not yet shown evidences of charging portable technologies. This helped confirm the uniqueness of the research and ensured time was not spent on a design or idea that had already been researched.

- *Research into modern portable technologies and their charging requirements*

The Table 3-2 shown in section 3.4, listed 10 portable devices sold in 2017. Hundreds of portable technologies were researched and the table represents the most popular devices sold. This ensured that the target powers and charging requirements were understood before attempting to charge one of these devices from a wearable energy harvester.

- *Design and develop a footfall wearable energy harvester for charging modern portable devices*

The initial design proved extraction method and the potential powers. The improved design completed this aim by charging a modern portable

technology device. This aim was by far the hardest to complete. Trying to design a bespoke wearable harvester that met the target, but was also lightweight, durable and was able to be tested 1000's of times took a lot of development. The improved design ended up being heavier than expected, but needed to be over engineered to ensure the harvester would survive hard testing sessions and the real world testing which was configured to find the limits of the harvester.

- *Investigate improving comparison methods of wearable energy harvesters, to aid design decisions of new innovations of harvester approaches or extraction methods*

The term "User-Impact-Factor" was created and shown to be a useful comparator of wearable energy harvesters. By combining previous method and including power to weight ratios as well as the location factor in the energy calculations, the user impact factor can now be used to compare wearable harvesters in terms of the weight, power output and location.

- *Document findings and confirm the hypothesis.*

After spending hours writing and reading this thesis, the intension of this is to communicate the thought and findings of this research project.

The hypothesis was;

> *If a wearable energy harvester is designed correctly, it should be able to produce a high enough average power from human footfall to charge a smart phone or tablet without effecting the users walking style and have as little effect on the wearers metabolic energy consumption as possible.*

This was proved by the improved design. The shoe units were lightweight, easy to fit and remove, and performed well at exacting the footfall forces from the desired area below the shoe line. Like any design it can always be improved, but as a first prototype used to prove the concept idea, and as research project test specimen, the design was fit for purpose. Lighter and smaller components can now be specified from the results and any design flaws could be worked on in future developments.

The improved design produced an average power output of 2.6 Watts from normal walking, higher than any other wearable energy harvester, harvesting from footfall found in published research from to date. The improved design was shown to charge a smart phone by 12% in 1 hour of normal walking. A novel way of extracting and transferring the footfall energy away from the foot area and up into a backpack, improving the impact to the wearer was also proven to be a success.

Overall, the research question was successfully answered and all aims were met.

7.2.2 Examination of Research Contribution and Justification

The simple justification to this research project is to benefit the future of our plant by reducing emissions and harmful waste products from traditional power sources such as power stations and non-rechargeable batteries. By having completed this research project, it is clear to see that the future of powering portable electronic technologies will be from energy harvesters. If the portable device is to be used and carried by a human, then it make sense the energy harvester is also a wearable energy harvester. Smart clothing that can help improve health conditions are being researched. Flexible and washable displays integrated into wearable items are also being developed. All of these state of the art technologies, will need a power source, again this is where wearable energy harvesters come into their own.

From this research and the conclusions drawn, it can be said that the harvester designs created and research throughout this projects were both bespoke and novel. Producing a Watt-Level average power from a wearable energy harvester that was driven by human footfall had not been shown to have the ability to charge modern portable electronic device, until now. This research proved charging today's technology is a real world possibility. It confirms the available energy from human footfall is high enough, and extractable to a level that can be used for wearable energy harvester applications aiming to charge portable electronics. This energy was converted into useable power for recharging a smart phone at a faster rate of charge than a standard computer USB port.

7.2.3 **Problems and Overcome Issue's**

This thesis investigated designs for footfall energy harvester with two key aims;

One size fits all

Every user produces useable power

This was found to have a number of awkward obstacles to overcome. Having a one-size-fit-all approach meant losses in energy extraction due to loose fitting. This was confirmed and seen during the treadmill test. When wearers wore the initial design with the carbon fibre shoe cup, wearers with smaller shoe sizes (less than UK male size 7) found it loose even on the clips tightest setting. Then wearers with larger shoe sizes (greater than UK male size 12) found it tight and restrictive. This ultimately led to lower power outputs than if the harvester had been permanently attached to one size and style of shoe.

The improved design had a different design for the shoe units, and included elastic strapping sown into the flexible strapping parts. This was done to increase strap tension and showed improvements on holding the harvester shoe unit tighter to the wearer's shoe. It also improved fitting on larger and smaller shoe sizes.

Feedback from wearers talking about the feel of both harvesters said the improved design felt nicer fitting than the initial design, but the look and style of the initial design was preferred.

The second key aim was useable power from all wearers. This meant that the harvester design had to work for light, little people and big, heavy people, even though the potential energy available from each wearer would be different. This meant having to optimize for both low energy inputs and

heavy shock loading situations. It was found in research that size and weight of a wear, had little effect on vertical footfall velocity. This was why the calculations were done concentrating on input velocities and not force. Vertical footfall velocities were effected by things such as stride and leg length, as well as terrain and walking effort. The input force was down to the wearers mass and this would change depending on wearer. This was optimized in the improved design with the installation of the reel spring.

When tests were performed on charging smart phones, it was found there were no trends of charging rates. It is well documented that energy delivered into a battery during charging will depend on multiple factors. Some of these factors include; current level of charge, drain on the battery at time of charge, battery age and past charging habits, and battery temperature. Because of these factors it has been in possible to make statements like

"The harvester will charge your phone by 8% in 30mins"

Or

"A flat to full charge will take 5 hours under normal walking conditions".

A more accurate statement would be:

"The harvester charge a well-used Samsung Galaxy
S7 by 12% in the endurance tests lasting one hour
walking at a normal rate."

It is still an impressive statement to make, and from research found, this is the first footfall wearable energy harvester, to document and prove this ability.

7.4 Closing summary

From this research project, a novel wearable energy harvester has been designed and proven to charge one of today's portable electronic devices currently available on the domestic market.

Two bespoke, novel, and useable wearable energy harvesters have been created. One showed a new and novel extraction method, and the second evolved the idea and incorporated a mechanical rectifier system like nothing seen before.

"The harvester incorporates a reel spring, which is winding up and unwinding at the same time, but at completely different rates".

This improved design showed an average power output of 2.6 Watts. This being higher than any other footfall harvester found to date. The harvester was also shown to produce this power at a wide range of walking rates. The retro-fit and one-size-fits-all proved challenging, but were both achieved via the foot units and the backpack. The novel designs and impressive results presented in this thesis give a strong contribution to the research community.

Overall this research project was a success and was completed in good time, on budget and all met the goals set.

References

[1] F. Qian, T. B. Xu, and L. Zuo, “Design, optimization, modeling and testing of a piezoelectric footwear energy harvester,” *Energy Convers. Manag.*, vol. 171, pp. 1352–1364, 2018.

[2] A. R. M. Siddique, S. Mahmud, and B. Van Heyst, “A review of the state of the science on wearable thermoelectric power generators (TEGs) and their existing challenges,” *Renew. Sustain. Energy Rev.*, vol. 73, pp. 730–744, 2017.

[3] E. Bonisoli, M. Repetto, N. Manca, and A. Gasparini, “Electromechanical and Electronic Integrated Harvester for Shoes Application,” *IEEE/ASME Trans. Mechatronics*, vol. 22, no. 5, pp. 1921–1932, 2017.

[4] S. Lee *et al.*, “Triboelectric energy harvester based on wearable textile platforms employing various surface morphologies,” *Nano Energy*, vol. 12, pp. 410–418, 2015.

[5] A. Delnavaz and J. Voix, “Flexible piezoelectric energy harvesting from jaw movements,” *Smart Mater. Struct.*, vol. 23, no. 10, 2014.

[6] J. Zhao and Z. You, “A shoe-embedded piezoelectric energy harvester for wearable sensors,” *Sensors (Switzerland)*, vol. 14, no. 7, pp. 12497–12510, 2014.

[7] Y. H. Lee *et al.*, “Wearable textile battery rechargeable by solar energy,” *Nano Lett.*, vol. 13, no. 11, pp. 5753–5761, 2013.

[8] L. Xie and M. Cai, “Increased energy harvesting and reduced accelerative load for backpacks via frequency tuning,” *Mech. Syst. Signal Process.*, vol. 58, pp. 399–415, 2015.

[9] Y. Yuan, M. Liu, W. C. Tai, and L. Zuo, “Design and Treadmill Test of a Broadband Energy Harvesting Backpack with a Mechanical Motion Rectifier,” *J. Mech. Des. Trans. ASME*, vol. 140, no. 8, pp. 1–8, 2018.

[10] Y. Yuan and L. Zuo, “Dynamics of energy harvesting backpack with human being interaction,” *Act. Passiv. Smart Struct. Integr. Syst. 2016*, vol. 9799, p. 97991K, 2016.

[11] Q. Li, V. Naing, and J. M. Donelan, “Development of a biomechanical energy harvester,” *J. Neuroeng. Rehabil.*, vol. 6, no. 1, p. 22, 2009.

[12] M. Shepertycky and Q. Li, “Generating electricity during walking with a lower limb-driven energy harvester: Targeting a minimum user effort,” *PLoS One*, vol. 10, no. 6, pp. 1–16, 2015.

[13] L. C. Rome, L. Flynn, E. M. Goldman, and T. D. Yoo, “Biophysics: Generating electricity while walking with loads,” *Science (80-.).*, vol. 309, no. 5741, pp. 1725–1728, 2005.

[14] L. B. Strang, “[Important physiological considerations in artificial respiration and reanimation of newborn infants].,” *Ann. Anesthesiol. Fr.*, vol. 16 Spec No 1, pp. 97–100, 1975.

[15] T. Starner, “Human-powered wearable computing,” *IBM Syst. J.*, vol. 35, no. 3–4, pp. 618–629, 1996.

[16] Q. Li, V. Naing, J. A. Hoffer, D. J. Weber, A. D. Kuo, and J. M. Donelan, “Biomechanical energy harvesting: Apparatus and method,” *Proc. - IEEE Int. Conf. Robot. Autom.*, vol. 48109, pp. 3672–3677, 2008.

[17] N. Terry and J. Palmer, “Trends in home computing and energy demand,” *Build. Res. Inf.*, vol. 44, no. 2, pp. 175–187, 2016.

[18] J. Lester, C. Hartung, L. Pina, R. Libby, G. Borriello, and G. Duncan, “Validated caloric expenditure estimation using a single body-worn sensor,” *ACM Int. Conf. Proceeding Ser.*, pp. 225–234, 2009.

[19] M. C. Chiu and M. J. Wang, “The effect of gait speed and gender on perceived exertion, muscle activity, joint motion of lower extremity, ground reaction force and heart rate during normal walking,” *Gait Posture*, vol. 25, no. 3, pp. 385–392, 2007.

[20] K. J. Chi and D. Schmitt, “Mechanical energy and effective foot mass during impact loading of walking and running,” *J. Biomech.*, vol. 38, no. 7, pp. 1387–1395, 2005.

[21] C. Divert, G. Mornieux, P. Freychat, L. Baly, F. Mayer, and A. Belli, “Barefoot-shod running differences: Shoe or mass effect?,” *Int. J. Sports Med.*, vol. 29, no. 6, pp. 512–518, 2008.

[22] R. Riemer and A. Shapiro, “Biomechanical energy harvesting from human motion: Theory, state of the art, design guidelines, and future directions,” *J. Neuroeng. Rehabil.*, vol. 8, no. 1, p. 22, 2011.

[23] V. Leonov, “Thermoelectric energy harvesting of human body heat for wearable sensors,” *IEEE Sens. J.*, vol. 13, no. 6, pp. 2284–2291, 2013.

[24] Z. Lu, H. Zhang, C. Mao, and C. M. Li, “Silk fabric-based wearable thermoelectric generator for energy harvesting from the human body,” *Appl. Energy*, vol. 164, pp. 57–63, 2016.

[25] Y. Wang, Y. Shi, D. Mei, and Z. Chen, “Wearable thermoelectric generator to harvest body heat for powering a miniaturized accelerometer,” *Appl. Energy*, vol. 215, pp. 690–698, 2018.

[26] M. K. Kim, M. S. Kim, S. Lee, C. Kim, and Y. J. Kim, “Wearable thermoelectric generator for harvesting human body heat energy,” *Smart Mater. Struct.*, vol. 23, no. 10, 2014.

[27] K. Y. Steve Beeby, John Tudor, Russel Torah, “Energy Harvesting for Wearable Applications Energy,” pp. 1–33, 2017.

[28] C. Tunca, N. Pehlivan, N. Ak, B. Arnrich, G. Salur, and C. Ersoy, “Inertial sensor-based robust gait analysis in non-hospital settings for neurological disorders,” *Sensors (Switzerland)*, vol. 17, no. 4, pp. 1–29, 2017.

[29] N. S. Shenck and J. A. Paradiso, “Energy scavenging with shoe-mounted piezoelectrics,” *IEEE Micro*, vol. 21, no. 3, pp. 30–42, 2001.

[30] J. Y. Hayashida, “Unobtrusive Integration of Magnetic Generator Systems into Common Footwear by,” *, BS thesis, Dept. Electr. Eng. MIT Media Lab. Massachusetts Inst. Technol.*, 2000.

[31] L. Xie, J. Li, S. Cai, and X. Li, “Design and experiments of a self-charged power bank by harvesting sustainable human motion,” *Adv. Mech. Eng.*, vol. 8, no. 5, pp. 1–10, 2016.

[32] L. Xie and M. Cai, “An In-Shoe Harvester with Motion Magnification for Scavenging Energy from Human Foot Strike,” *IEEE/ASME Trans. Mechatronics*, vol. 20, no. 6, pp. 3264–3268, Dec. 2015.

[33] Y. Liu, W. Fu, W. Li, and M. Sun, “Design and analysis of a shoe-embeded power

harvester based on magnetic gear," *IEEE Trans. Magn.*, vol. 52, no. 7, pp. 3–6, 2016.

[34] R. Baghebani and M. Ashoorirad, "A power generating system for mobile electronic devices using human walking motion," *2009 Int. Conf. Comput. Electr. Eng. ICCEE 2009*, vol. 2, pp. 385–388, 2009.

[35] D. F. Berdy, D. J. Valentino, and D. Peroulis, "Kinetic energy harvesting from human walking and running using a magnetic levitation energy harvester," *Sensors Actuators, A Phys.*, vol. 222, pp. 262–271, 2015.

[36] R. Cross, "Standing, walking, running, and jumping on a force plate," *Am. J. Phys.*, vol. 67, no. 4, pp. 304–309, 1999.

[37] J. M. Donelan, Q. Li, V. Naing, J. A. Hoffer, D. J. Weber, and A. D. Kuo, "Biomechanical energy harvesting: Generating electricity during walking with minimal user effort," *Science (80-.).*, vol. 319, no. 5864, pp. 807–810, 2008.

[38] Y. Kuang and M. Zhu, "Characterisation of a knee-joint energy harvester powering a wireless communication sensing node," *Smart Mater. Struct.*, vol. 25, no. 5, p. 5013, 2016.

[39] S. Wu, P. C. K. Luk, C. Li, X. Zhao, Z. Jiao, and Y. Shang, "An electromagnetic wearable 3-DoF resonance human body motion energy harvester using ferrofluid as a lubricant," *Appl. Energy*, vol. 197, pp. 364–374, 2017.

[40] Y. Rao, S. Cheng, and D. P. Arnold, "An energy harvesting system for passively generating power from human activities," *J. Micromechanics Microengineering*, vol. 23, no. 11, p. 114012, 2013.

[41] C. R. Saha, T. O'Donnell, N. Wang, and P. McCloskey, "Electromagnetic generator for harvesting energy from human motion," *Sensors Actuators, A Phys.*, vol. 147, no. 1, pp. 248–253, 2008.

[42] J. J. Wang, H. J. Su, C. I. Hsu, and Y. C. Su, "Composite piezoelectric rubber band for energy harvesting from breathing and limb motion," *J. Phys. Conf. Ser.*, vol. 557, no. 1, 2014.

[43] M. A. Karami and D. J. Inman, "Powering pacemakers from heartbeat vibrations using linear and nonlinear energy harvesters," *Appl. Phys. Lett.*, vol. 100, no. 4, 2012.

[44] M. H. Ansari and M. A. Karami, "Modeling and experimental verification of a fan-folded vibration energy harvester for leadless pacemakers," *J. Appl. Phys.*, vol. 119, no. 9, 2016.

[45] C. Dagdeviren *et al.*, "Conformal piezoelectric energy harvesting and storage from motions of the heart, lung, and diaphragm," *Proc. Natl. Acad. Sci. U. S. A.*, vol. 111, no. 5, pp. 1927–1932, 2014.

[46] N. Qunfeng, W. Li, D. Tao, and Y. Huijun, "Application of a MEMS-based energy harvester for artificial heart wireless energy transmission," *2009 Second ISECS Int. Colloq. Comput. Commun. Control. Manag. CCCM 2009*, vol. 1, pp. 38–41, 2009.

[47] M. Deterre, E. Lefeuvre, Y. Zhu, M. Woytasik, B. Boutaud, and R. D. Molin, "Micro blood pressure energy harvester for intracardiac pacemaker," *J. Microelectromechanical Syst.*, vol. 23, no. 3, pp. 651–660, 2014.

[48] A. Zurbuchen *et al.*, "Energy harvesting from the beating heart by a mass imbalance oscillation generator," *Ann. Biomed. Eng.*, vol. 41, no. 1, pp. 131–141, 2013.

[49] A. Pfenniger, M. Jonsson, A. Zurbuchen, V. M. Koch, and R. Vogel, “Energy harvesting from the cardiovascular system, or how to get a little help from yourself,” *Ann. Biomed. Eng.*, vol. 41, no. 11, pp. 2248–2263, 2013.

[50] B. Shi, Z. Li, and Y. Fan, “Implantable Energy-Harvesting Devices,” *Adv. Mater.*, vol. 30, no. 44, pp. 1–18, 2018.

[51] J. K. Gupta, C. H. Lin, and Q. Chen, “Characterizing exhaled airflow from breathing and talking,” *Indoor Air*, vol. 20, no. 1, pp. 31–39, 2010.

[52] H. Xue *et al.*, “A wearable pyroelectric nanogenerator and self-powered breathing sensor,” *Nano Energy*, vol. 38, pp. 147–154, 2017.

[53] E. Shahhaidar, O. Boric-Lubecke, R. Ghorbani, and M. Wolfe, “Electromagnetic generator: As respiratory effort energy harvester,” *2011 IEEE Power Energy Conf. Illinois, PECI 2011*, no. 1, pp. 1–4, 2011.

[54] Z. Wen *et al.*, “Blow-driven triboelectric nanogenerator as an active alcohol breath analyzer,” *Nano Energy*, vol. 16, pp. 38–46, 2015.

[55] X. Wang, S. Wang, Y. Yang, and Z. L. Wang, “Hybridized electromagnetic-triboelectric nanogenerator for scavenging air-flow energy to sustainably power temperature sensors,” *ACS Nano*, vol. 9, no. 4, pp. 4553–4562, 2015.

[56] A. Delnavaz and J. Voix, “Electromagnetic micro-power generator for energy harvesting from breathing,” *IECON Proc. (Industrial Electron. Conf.*, pp. 984–988, 2012.

[57] J. Mi, L. Xu, L. Zuo, Z. Zhu, and M. Liu, “Design, modeling and testing of a one-way energy harvesting backpack,” vol. 105, p. 71, 2018.

[58] Y. Yuan, M. Liu, W.-C. Tai, and L. Zuo, “Design and experimental studies of an energy harvesting backpack with mechanical motion rectification,” *Sensors Smart Struct. Technol. Civil, Mech. Aerosp. Syst. 2017*, vol. 10168, p. 1016825, 2017.

[59] Y. Cha, J. Hong, J. Lee, J. M. Park, and K. Kim, “Flexible piezoelectric energy harvesting from mouse click motions,” *Sensors (Switzerland)*, vol. 16, no. 7, pp. 1–10, 2016.

[60] R. Yang, Y. Qin, C. Li, G. Zhu, and Z. L. Wang, “Converting biomechanical energy into electricity by a muscle-movement- driven nanogenerator,” *Nano Lett.*, vol. 9, no. 3, pp. 1201–1205, 2009.

[61] J. Zhong *et al.*, “Finger typing driven triboelectric nanogenerator and its use for instantaneously lighting up LEDs,” *Nano Energy*, vol. 2, no. 4, pp. 491–497, 2013.

[62] Y. Yang *et al.*, “Human skin based triboelectric nanogenerators for harvesting biomechanical energy and as self-powered active tactile sensor system,” *ACS Nano*, vol. 7, no. 10, pp. 9213–9222, 2013.

[63] N. Ben Amor, O. Kanoun, A. Lay-Ekuakille, G. Specchia, G. Vendramin, and A. Trotta, “Energy harvesting from human body for biomedical autonomous systems,” *Proc. IEEE Sensors*, pp. 678–680, 2008.

[64] N. Exerting, “Mdxiimum Torque Exerted About the Elbow Joint,” vol. 7, pp. 393–398, 2019.

[65] B. Yang and K. S. Yun, “Piezoelectric shell structures as wearable energy harvesters

for effective power generation at low-frequency movement," *Sensors Actuators, A Phys.*, vol. 188, pp. 427–433, 2012.

[66] V. Linnamo, V. Strojnik, and P. V. Komi, "Maximal force during eccentric and isometric actions at different elbow angles," *Eur. J. Appl. Physiol.*, vol. 96, no. 6, pp. 672–678, 2006.

[67] L. Xie and M. Cai, "Human motion: Sustainable power for wearable electronics," *IEEE Pervasive Comput.*, vol. 13, no. 4, pp. 42–49, 2014.

[68] P. Maharjan, R. M. Toyabur, and J. Y. Park, "A human locomotion inspired hybrid nanogenerator for wrist-wearable electronic device and sensor applications," *Nano Energy*, vol. 46, pp. 383–395, 2018.

[69] Y. Guo *et al.*, "All-fiber hybrid piezoelectric-enhanced triboelectric nanogenerator for wearable gesture monitoring," *Nano Energy*, vol. 48, pp. 152–160, 2018.

[70] X. Ren *et al.*, "Magnetic force driven noncontact electromagnetic-triboelectric hybrid nanogenerator for scavenging biomechanical energy," *Nano Energy*, vol. 35, pp. 233–241, 2017.

[71] S. P. Beeby *et al.*, "A micro electromagnetic generator for vibration energy harvesting," *J. Micromechanics Microengineering*, vol. 17, no. 7, pp. 1257–1265, 2007.

[72] P. Pillatsch, E. M. Yeatman, and A. S. Holmes, "A piezoelectric frequency up-converting energy harvester with rotating proof mass for human body applications," *Sensors Actuators, A Phys.*, vol. 206, pp. 178–185, 2014.

[73] E. Goll, H. P. Zenner, and E. Dalhoff, "Upper bounds for energy harvesting in the region of the human head," *IEEE Trans. Biomed. Eng.*, vol. 58, no. 11, pp. 3097–3103, 2011.

[74] X. Xu and S. Yuan, "An examination of the force generated from incisor penetration into foods with different textural properties Part I: Experimental observation," *J. Texture Stud.*, vol. 42, no. 3, pp. 228–235, 2011.

[75] V. Leonov and R. J. M. Vullers, "Wearable electronics self-powered by using human body heat: The state of the art and the perspective," *J. Renew. Sustain. Energy*, vol. 1, no. 6, p. 062701, 2009.

[76] R. Yang, Y. Qin, C. Li, G. Zhu, and Z. L. Wang, "Converting biomechanical energy into electricity by a muscle-movement- driven nanogenerator," *Nano Lett.*, vol. 9, no. 3, pp. 1201–1205, 2009.

[77] Epson, "Seiko Quartz Astron 35SQ," no. December 1969, p. 1, 1969.

[78] C. A. Howells, "Piezoelectric energy harvesting," *Energy Convers. Manag.*, vol. 50, no. 7, pp. 1847–1850, 2009.

[79] S. Song and K. S. Yun, "Design and characterization of scalable woven piezoelectric energy harvester for wearable applications," *Smart Mater. Struct.*, vol. 24, no. 4, p. 045008, 2015.

[80] M. Leinonen, J. Juuti, H. Jantunen, and J. Palosaari, "Energy Harvesting with a Bimorph Type Piezoelectric Diaphragm Multilayer Structure and Mechanically Induced Pre-stress," *Energy Technol.*, vol. 4, no. 5, pp. 620–624, 2016.

[81] W. Wu, S. Bai, M. Yuan, Y. Qin, Z. L. Wang, and T. Jing, "Lead zirconate titanate

nanowire textile nanogenerator for wearable energy-harvesting and self-powered devices," *ACS Nano*, vol. 6, no. 7, pp. 6231–6235, 2012.

[82] J. Kymissis, C. Kendall, J. Paradiso, and N. Gershenfeld, "Parasitic power harvesting in shoes," *Int. Symp. Wearable Comput. Dig. Pap.*, vol. 1998-Octob, pp. 132–139, 1998.

[83] R. Meier, N. Kelly, O. Almog, and P. Chiang, "A piezoelectric energy-harvesting shoe system for podiatric sensing," *2014 36th Annu. Int. Conf. IEEE Eng. Med. Biol. Soc. EMBC 2014*, pp. 622–625, 2014.

[84] Y. Kuang and M. Zhu, "Characterisation of a knee-joint energy harvester powering a wireless communication sensing node," *Smart Mater. Struct.*, vol. 25, no. 5, 2016.

[85] X. Pu *et al.*, "Ultrastretchable, transparent triboelectric nanogenerator as electronic skin for biomechanical energy harvesting and tactile sensing," *Sci. Adv.*, vol. 3, no. 5, p. 1715, 2017.

[86] K. Fan, Z. Liu, H. Liu, L. Wang, Y. Zhu, and B. Yu, "Scavenging energy from human walking through a shoe-mounted piezoelectric harvester," *Appl. Phys. Lett.*, vol. 110, no. 14, 2017.

[87] L. Xie and M. Cai, "Increased piezoelectric energy harvesting from human footstep motion by using an amplification mechanism," *Appl. Phys. Lett.*, vol. 105, no. 14, pp. 1–5, 2014.

[88] P. Bai *et al.*, "Integrated multilayered triboelectric nanogenerator for harvesting biomechanical energy from human motions," *ACS Nano*, vol. 7, no. 4, pp. 3713–3719, 2013.

[89] F. R. Fan, Z. Q. Tian, and Z. Lin Wang, "Flexible triboelectric generator," *Nano Energy*, vol. 1, no. 2, pp. 328–334, 2012.

[90] D. W. Shin *et al.*, "A New Facile Route to Flexible and Semi-Transparent Electrodes Based on Water Exfoliated Graphene and their Single-Electrode Triboelectric Nanogenerator," *Adv. Mater.*, vol. 30, no. 39, pp. 1–7, 2018.

[91] K. Dong *et al.*, "3D Orthogonal Woven Triboelectric Nanogenerator for Effective Biomechanical Energy Harvesting and as Self-Powered Active Motion Sensors," *Adv. Mater.*, vol. 29, no. 38, pp. 1–11, 2017.

[92] D. Zhu, S. P. Beeby, M. J. Tudor, and N. R. Harris, "Electromagnetic Vibration Energy Harvesting Using an Improved Halbach Array," *PowerMEMS 2012*, no. 1, pp. 1–4, 2012.

[93] K. Ylli, D. Hoffmann, A. Willmann, P. Becker, B. Folkmer, and Y. Manoli, "Energy harvesting from human motion: Exploiting swing and shock excitations," *Smart Mater. Struct.*, vol. 24, no. 2, p. 25029, 2015.

[94] F. Sprei, S. Karlsson, and J. Holmberg, "Better performance or lower fuel consumption: Technological development in the Swedish new car fleet 1975-2002," *Transp. Res. Part D Transp. Environ.*, vol. 13, no. 2, pp. 75–85, 2008.

[95] J. De Mol, S. Vlassenroot, E. Zwerts, G. Allaert, and F. Witlox, "The evolution of car power, weight and top speed during the last twenty years in Belgium: a consideration for future policies," *3rd Transp. Res. Day*, vol. 2, no. Idm, pp. 607–620, 2009.

[96] I. Arsie, A. Di Domenico, M. Marotta, C. Pianese, G. Rizzo, and M. Sorrentino, "A Parametric Study of the Design Variables for a Hybrid Electric Car with Solar Cells," *Proc. METIME …*, no. Viking 23, 2005.

[97] P. D. Mitcheson, E. K. Reilly, T. Toh, P. K. Wright, and E. M. Yeatman, “Transduction Mechanisms and Power Density for MEMS Inertial Energy Scavengers,” vol. 278, pp. 275–278, 2006.

[98] Y. M. Choi, M. G. Lee, and Y. Jeon, “Wearable biomechanical energy harvesting technologies,” *Energies*, vol. 10, no. 10, p. 1483, 2017.

[99] P. M. Mills, R. S. Barrett, and S. Morrison, “Toe clearance variability during walking in young and elderly men,” *Gait Posture*, vol. 28, no. 1, pp. 101–107, 2008.

[100] W. Braune and O. Fischer, “The Human Gait,” *Hum. Gait*, vol. 1, pp. 105–114, 1987.

[101] D. McGrath, B. R. Greene, C. Walsh, and B. Caulfield, “Estimation of minimum ground clearance (MGC) using body-worn inertial sensors,” *J. Biomech.*, vol. 44, no. 6, pp. 1083–1088, 2011.

[102] B. Mariani, S. Rochat, C. J. Büla, and K. Aminian, “Heel and toe clearance estimation for gait analysis using wireless inertial sensors,” *IEEE Trans. Biomed. Eng.*, vol. 59, no. 12 PART2, pp. 3162–3168, 2012.

[103] S. C. Walpole, D. Prieto-Merino, P. Edwards, J. Cleland, G. Stevens, and I. Roberts, “The weight of nations: An estimation of adult human biomass,” *BMC Public Health*, vol. 12, no. 1, p. 1, 2012.

[104] A. I. T. Salo, I. N. Bezodis, A. M. Batterham, and D. G. Kerwin, “Elite sprinting: Are athletes individually step-frequency or step-length reliant?,” *Med. Sci. Sports Exerc.*, vol. 43, no. 6, pp. 1055–1062, 2011.

[105] M. A. Cavanagh and Lafortune, “GRF in distance running,” *J. Biomech.*, vol. 13, pp. 397–406, 1980.

[106] R. F. G. K. B. PANDOLF, B. GIVONI, “WHILE STANDING OR WALKiNG VER Y SLOWLY U S A R M Y RE SE A RCH IN STIT UTE OF ENVIR ONMENTAL ME DICINE Natick , Massachuse tts,” pp. 66–72, 1976.

[107] H. Russell, N. John, and R. Matt, “Battery technology charges ahead,” *McKinsey Q.*, vol. 1, 2012.

[108] Z. Luo *et al.*, “Energy harvesting study on single and multilayer ferroelectret foams under compressive force,” *IEEE Trans. Dielectr. Electr. Insul.*, vol. 22, no. 3, pp. 1360–1368, 2015.

[109] Y. Rao, S. Cheng, and D. P. Arnold, “An energy harvesting system for passively generating power from human activities,” *J. Micromechanics Microengineering*, vol. 23, no. 11, 2013.

[110] K. Zhang, X. Wang, Y. Yang, and Z. L. Wang, “Hybridized Electromagnetic-Triboelectric Nanogenerator for Scavenging Biomechanical Energy for Sustainably Powering Wearable Electronics,” *ACS Nano*, vol. 9, no. 4, pp. 3521–3529, 2015.

Thanks for Reading and I look forward

to hearing your responses.

Thanks, David Pritchard. ☺

Blank Page